Memoirs of the Faculty of Engineering, Nagoya University
Vol. 34, No. 2 (1982)

"ON THE UNSTABLE VIBRATIONS OF A SHAFT HAVING ASYMMETRICAL STIFFNESS AND / OR ASYMMETRICAL ROTOR"

HIROSHI ŌTA and KAZUKI MIZUTANI

Department of Electronic Mechanical Engineering

(Received October 29, 1982)

Abstract

In a rotating asymmetrical shaft having a keyway or a rectangular cross section, or in a rotating shaft with an asymmetrical rotor such as a two-pole generator or two-blade propeller, there occur two types of unstable vibrations. When bearing pedestals supporting a directional inequality in stiffness, each unstable region splits up into several regions. The position, width and number of the unstable regions and a dynamic behavior of the shaft are analytically obtained by approximation both for a rotating asymmetrical shaft and an asymmetrical rotor. The analytical results show a good coincidence with those obtained by an analog computer.

In order to understand the mechanism for the occurrence of these two types of unstable vibrations, the authors clarify the conditions under which the time average of a torque applied to the shaft end is positive, so that the whirling amplitudes of the shaft increase and unstable vibrations occur. Vibratory solutions in the unstable region obtained by an analog computer are found to satisfy this instability condition.

CONTENTS

General Introduction

With advance of machinery, high performance has been demanded for rotating machines, that is, electric motor, steam turbine, gas turbine, and turbo-compressor. In order to improve the performance, the rotating machinery must be operated at high rotational speed, and thus vibrations with even a small amplitude must be removed. In order to prevent vibrations, the cause of these vibrations must be clarified for the various vibrations which occur in a high speed region beyond the first critical speed.

There have been a large number of studies about the vibration of rotating shaft system since A. Stodola[1], S. Timoshenko[2], and J. P. Den Hartog[3] investigated the vibration of a rotating shaft at the major critical speed.

A rotating shaft which passes through the major critical speed[4~10], and the balancing[1, 2, 11] of a flexible shaft system at the major critical speed were studied. T. Yamamoto[12] reported a series of theoretical and experimental works upon various critical speeds but the major critical one with regard to a rotating shaft, both ends of which are supported by ball bearings. A synchronous backward precession[12~14] caused by directionally unequal flexibility of pedestals, secondary critical speed[15~19] caused in a horizontal shaft with asymmetrical stiffness, and vibration of shaft system with variable rotating speed[20~23] were studied. Moreover, upon a rotating asymmetrical shaft and an asymmetrical rotor, the study of forced vibration was related to the change of response curve with the angular position of rotor unbalance[16, 24~28], the vibration of a shaft passing through the major critical speed[29, 30], and the balancing of shaft system.

A directional inequality in stiffness of an asymmetrical shaft and different diametral moments of inertia of an asymmetrical rotor are examples of a rotating inequality system turning at the angular velocity of shaft ω. When the equations of motion of shaft system with rotating inequality are expressed by a stationary rectangular coordinate, the coefficient of those contains the periodic function such as $\sin 2\omega t$ and $\cos 2\omega t$. Therefore, unstable vibrations of the so-called "parametric excitation"[33, 34] take place in this shaft system.

In a rotor mounted on the middle of an asymmetrical shaft, the unstable vibration takes place near the major critical speed[1, 6, 10, 15~19, 35~39]. When the bearing pedestals supporting an asymmetrical shaft have different stiffness in x- and y-directions, coexistence of stational inequality in stiffness and rotating one makes each unstable region split into several parts, and the analysis of this shaft system is very complicated. Concerning the position, width and number of these unstable regions, although a lot of research have been reported[15, 19, 40~54], each paper of those has given a different result.

In shaft system carrying an asymmetrical rotor, L. Y. Banaf and F. M. Dimentberg[55], P. J. Brosens and S. H. Crandall[56], and T. Yamamoto and H. Ōta[57] have reported that the unstable vibration appears near the major critical speed. Furthermore, S. Aiba[58, 60], and T. Yamamoto and H. Ōta[59] have shown that unstable vibrations also take place near the rotating speed where the sum of two natural frequencies p_1 and p_2 is always equal to the twice rotating speed of shaft, that is, $p_i+p_j=2\omega$ $(i\neq j)$. When a shaft carrying an asymmetrical rotor is supported by flexible pedestals with directionally different stiffnesses[56, 61~63], each

unstable region splits up into several ones in the same way as an asymmetrical shaft.

In an asymmetrical shaft carrying an asymmetrical rotor, a few papers[25, 26, 48, 64~66] indicated that the width of unstable region changes with the orientation angle ζ between the inequality of shaft stiffness and that of rotor moment of inertia.

In this paper, the authors deal with the influence of unequal pedestal stiffness on the unstable regions of an asymmetrical shaft and an asymmetrical rotor, and the necessary condition for which unstable vibration occurs in the shaft system with rotating asymmetry.

Chapter 1 deals with lateral vibrations of an asymmetrical shaft supported by flexible pedestals with a directional inequality in stiffness. The approximate analyses regarding unstable regions are carried out by classifying three cases in which directional inequality of pedestal stiffness ε is much less than, much greater than, or nearly equal to asymmetry of shaft stiffness Δ, and the analytical results assuming that $\varepsilon \simeq \Delta$ can expand to other two cases that $\varepsilon \ll \Delta$ or $\varepsilon \gg \Delta$ is assumed. The width and number of unstable regions, and dynamical characteristics of the shaft system are solely determined by only one parameter λ which consists of mass ratio of pedestal to rotor σ and stiffness ratio of pedestal to shaft κ. Analytical results derived by the assumption that $\varepsilon \simeq \Delta$ were found to agree well with those obtained by an analog computer.

Chapter 2 analyses the conical mode of vibrations of a rotor in the same shaft system as Chapter 1. When coefficient of gyroscopic term i_p is small, a similar approximate analysis to Chapter 1 asumming that $\varepsilon \simeq \Delta$ can be adopted by considering i_p, ε and Δ to be small quantities of the same order, and it is shown how the unstable regions are changed by the gyroscopic effect. When i_p is larger than ε and Δ, same approximate analyses can be carried out by distinguishing whether the terms smaller than ε^2 are negligible or not. The approximation for the case that i_p is relatively large is compared with the solutions obtained by an analog computer, and they are found to show a good coincidence.

Chapter 3 clarifies the mechanism through which unstable vibrations occur in an asymmetrical shaft supported by flexible pedestals with unequal stiffness. Unstable vibrations occur just as input energy into the shaft system tends to increase the whirling amplitude of a rotor. The conditions which cause two types of unstable vibrations are obtained analytically, and unstable solutions obtained by an analog computer are found to satisfy these conditions for instability. Moreover, if the higher order of small quantities ε and Δ is taken into consideration, a number of very narrow unstable regions can occur.

Chapter 4 makes clear unstable vibrations of a shaft with an asymmetrical rotor, both ends of which are supported by flexible pedestals with directional inequality in stiffness. On conical vibrations of an asymmetrical rotor, the position, width and number of unstable regions are approximately obtained by the similar analysis to Chapter 2. These approximations coincide well with the solutions obtained by an analog computer. Moreover, the mechanism for occurrence of these unstable vibrations is explained, and the conditions necessary for instability are obtained. The solutions obtained by an analog computer are found just to satisfy these conditions.

Chapter 5 describes the condition under which unstable vibrations occur in a rotating asymmetrical shaft with an asymmetrical rotor. This condition necessary

for instability depends on the orientation angle ζ between inequality of shaft stiffness and that of rotor moment of inertia, and so the width of unstable region changes with the angle ζ. It is ascertained that the solutions of unstable vibration obtained by an analog computer satisfy the condition necessary for instability.

Chapter 6 obtains the increase in rate of total energy of the shaft system and the torque applied to shaft end in a rotating asymmetrical shaft with an asymmetrical rotor. This increase in rate of total energy and the shaft end torque change with the angular positions of static unbalance and dynamic one. On the parallel and conical motions of a rotor mounted on an asymmetrical shaft, the shaft end torque can be directly obtained from the equilibrium of forces and moments acting upon the shaft system. Furthermore, it is shown in an asymmetrical shaft and an asymmetrical rotor that the shaft end torque changes in the similar way to the response curve which also depends on the angular positions of rotor unbalances.

1. Influence of Unequal Pedestal Stiffness on the Unstable Regions of a Rotating Asymmetrical Shaft (Parallel Motion of a Rotor)[70]

1. 1. Introduction

In a rotating asymmetrical shaft[25, 26] which has a keyway or a rectangular cross section as well as in a shaft with an asymmetrical rotor[55~61], there occur two types of unstable vibrations. If the bearing pedestals supporting the shaft end have different stiffnesses in x- and y-directions, each unstable region splits up into several others. In respect to the position, width and number of these unstable regions, many analytical results have been reported [15, 19, 40~54]. In most papers, either a massless asymmetrical shaft with a rotor[15, 19, 40, 43, 46, 48], or an asymmetrical shaft with a uniformly distributed mass[42, 44, 49~52, 54] is considered, and the mass of bearing pedestals is disregarded. In a shaft system in practical use, the mass of flexible bearing pedestals cannot be neglected. A few studies[41, 45, 47, 53] have been reported in which the mass of bearing pedestals is taken into consideration, but the number and position of unstable regions differ in them.

This chapter deals with a simple vibratory system consisting of an asymmetrical shaft with a rotor mounted at its midpoint, both ends of the shaft are supported by the same flexible bearing pedestal possessing a directional inequality in stiffness and a concentrated mass. The analysis of this problem is carried out by an approximation method[59, 61, 63], which was found to be very useful for the unstable vibrations of an asymmetrical rotor having a similar dynamic property to an asymmetrical shaft. When the analyses regarding unstable regions are carried out by classifying three cases in which a directional inequality of bearing pedestal stiffness ε is much less than, much greater than, or nearly equal to asymmetry of shaft stiffness Δ, the analytical results assuming that $\varepsilon \simeq \Delta$ can include the other two cases that $\varepsilon \ll \Delta$ and $\varepsilon \gg \Delta$. Consequently, the position, width and number of unstable regions, and a dynamic behavior of shaft motion are solely determined by nothing but a parameter $\lambda = 0 \sim 1$ which consists of σ=ratio of bearing mass to rotor mass and κ=ratio of mean bearing stiffness to mean shaft stiffness. The analytical results by approximation in which ε and Δ are assumed to be a small quantity of the same order show a good coincidence with those obtained by an analog computer.

1. 2. Equations of Motion and Frequency Equation

1. 2. 1. Equations of motion

Upper and lower flexible bearing pedestals B, A shown in Fig. 1. 1 are exactly alike. Therefore, the two equivalent concentrated masses of bearing pedestal are equal, i. e., $m_a=m_b$, and also $k_a\mp\Delta k_a=k_b\mp\Delta k_b$. At the mounting point of rotor S, the asymmetrical shaft possesses directionally different stiffnesses $k-\Delta k$ and $k+\Delta k$ in x'- and y'-directions, respectively. Mass of the rotor, and polar moment of inertia are defined as m_0, I_p. Let us consider a rotating rectangular coordinate system O-$x'y'$ turning at an angular velocity ω. This system just coincides with a stationary rectangular coordinate system O-xy at the moment $t=0$. The rotor center S and the centers of the upper and lower bearings B, A may be assumed to move only in planes containing the equilibrium points O, O_b and O_a, respectively, and perpendicular to the z-axis, because the rotor is mounted at the middle of a shaft, and rotor inclination and lateral displacement are not interconnected. In this chapter the bearing pedestals A and B are assumed to move symmetrically to the xy- plane, that is,

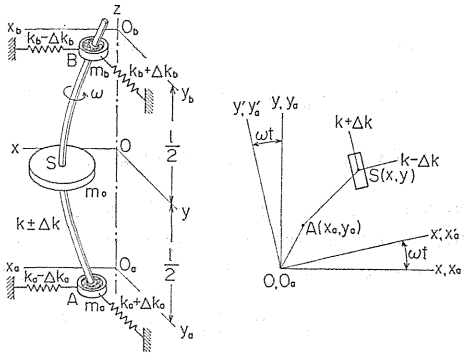

Fig. 1. 1 Asymmetrical shaft and asymmetrically flexible pedestals ($m_a=m_b$, $k_a=k_b$, $\Delta k_a=\Delta k_b$) for parallel motion of rotor ($x_a=x_b$, $y_a=y_b$).

$$x_a=x_b,\quad y_a=y_b \tag{1.1}$$

When equation (1. 1) is used, the kinetic energy of translation T and the potential energy V of this system are expressed as

$$2T=m_0(\dot{x}^2+\dot{y}^2)+2m_a(\dot{x}_a^2+\dot{y}_a^2)+I_p\omega^2 \tag{1.2}$$

$$2V=(k-\Delta k)(x'-x'_a)^2+(k+\Delta k)(y'-y'_a)^2 +2\{(k_a-\Delta k_a)x_a^2+(k_a+\Delta k_a)y_a^2\} \tag{1.3}$$

Since relative displacements of the rotor center S to lower bearing pedestal A, $x'-x'_a$ and $y'-y'_a$, as shown Fig. 1. 1, are represented by

$$\begin{bmatrix} x'-x'_a \\ y'-y'_a \end{bmatrix}=\begin{bmatrix} \cos\omega t & \sin\omega t \\ -\sin\omega t & \cos\omega t \end{bmatrix}\begin{bmatrix} x-x_a \\ y-y_a \end{bmatrix} \tag{1.4}$$

Substitution of equations (1. 2) ~ (1. 4) into the Lagrange's equation yields the equations of motion for stationary coordinates x, y, x_a and y_a:

$$m_0\ddot{x}+k(x-x_a)=\Delta k\{(x-x_a)\cos 2\omega t+(y-y_a)\sin 2\omega t\}$$

$$m_0\ddot{y}+k(y-y_a)=\Delta k\{(x-x_a)\sin 2\omega t-(y-y_a)\cos 2\omega t\}$$

$$2m_a\ddot{x}_a-k(x-x_a)+2(k_a-\Delta k_a)x_a=-\Delta k\{(x-x_a)\cos 2\omega t+(y-y_a)\sin 2\omega t\}$$
$$2m_a\ddot{y}_a-k(y-y_a)+2(k_a+\Delta k_a)y_a=-\Delta k\{(x-x_a)\sin 2\omega t-(y-y_a)\cos 2\omega t\} \tag{1.5}$$

For simplicity's sake, the following dimensionless quantities (1.6) are introduced:

$$\left.\begin{aligned} &2m_a/m_0=\sigma,\quad 2k_a/k=\kappa,\quad \Delta k/k=\Delta,\quad \Delta k_a/k_a=\varepsilon,\\ &t\sqrt{k/m_0}=t',\quad p/\sqrt{k/m_0}=p',\quad \omega/\sqrt{k/m_0}=\omega' \end{aligned}\right\} \tag{1.6}$$

Hereafter, the primes on the dimensionless quantities (1.6) are omitted and the dots over dimensionless quantities mean the differential coefficient with respect to t'. Using an imaginary unit i and complex variables

$$z=x+iy,\quad \bar{z}=x-iy,\quad z_a=x_a+iy_a,\quad \bar{z}_a=x_a-iy_a \tag{1.7}$$

and then adding the first equation of equation (1.5) to the second equation multiplied by i, and adding the third equation to the fourth equation multiplied by i, the equations of motion are rewritten as follows:

$$\left.\begin{aligned} &\ddot{z}+z-z_a=\Delta e^{2i\omega t}(\bar{z}-\bar{z}_a)\\ &\sigma\ddot{z}_a+(1+\kappa)z_a-z=\kappa\varepsilon\bar{z}_a-\Delta e^{2i\omega t}(\bar{z}-\bar{z}_a) \end{aligned}\right\} \tag{1.8}$$

1. 2. 2. Frequency equation

Both amplitudes A and A_a of free vibrations $z=Ae^{ipt}$ and $z_a=A_ae^{ipt}$ whirling at an angular velocity p are assumed to be the zero order of small quantities ε and Δ. Because of the existence of rotating asymmetry Δ, the whirling motion with a frequency $\hat{p}=2\omega-p$ is caused by an external force of the right hand side of equation (1.8) $\pm\Delta e^{2i\omega t}(\bar{z}-\bar{z}_a)=\pm\Delta(\bar{A}-\bar{A})e^{i\hat{p}t}$ and the excited amplitudes B and B_a are of the same order of Δ. Similarly, an external force $\kappa\varepsilon\bar{z}_a=\kappa\varepsilon\bar{A}_ae^{-ipt}$ on the right hand side of the second equation of equation (1.8) yields the whirling of bearing pedestal z_a, consisting not only of A_ae^{ipt} but also of a_ae^{-ipt} with a frequency $-p$ and amplitude of ε order. Furthermore, the vibrations with a frequency $-\hat{p}=p-2\omega$ are induced by the coexistence of ε and the vibration with frequency $\hat{p}$ and the amplitudes b and b_a are of $\varepsilon\Delta$ order. Next, the coexistence of Δ and the vibration with frequency $-p$ gives the vibrations with a frequency $2\omega+p$ and the amplitudes C and C_a are of $\varepsilon\Delta$ order. Successively, there occur many vibrations[61], the amplitudes of which are of a higher order of small quantities ε and Δ. Table 1. 1 shows the frequencies of vibrations, the amplitudes of which are larger than of ε^4 and Δ^4 order. In this table the vibrations in the right column, and in the lower row are induced by Δ and ε, respectively.

If amplitudes up to the second order of small quantities ε and Δ are counted, solutions of free vibration of equation (1.8) have the following five frequencies p, $-p$, $\hat{p}$, $-\hat{p}$ and $2\omega+p$:

$$\left.\begin{aligned} &z=Ae^{ipt}+ae^{-ipt}+Be^{i\hat{p}t}+be^{-i\hat{p}t}+Ce^{i(2\omega+p)t}\\ &z_a=A_ae^{ipt}+a_ae^{-ipt}+B_ae^{i\hat{p}t}+b_ae^{-i\hat{p}t}+C_ae^{i(2\omega+p)t} \end{aligned}\right\} \tag{1.9}$$

Table 1. 1 List of whirling frequencies, amplitudes with which are larger than of ε^4 and Δ^4 order.

Order of ε and Δ	Δ^0	Δ^1	Δ^2	Δ^3	Δ^4
ε^0	p	$\hat{p}=2\omega-p$			
ε^1	$-p$	$-\hat{p}=p-2\omega$ / $2\omega+p$	$4\omega-p$		
ε^2		$-2\omega-p$	$p-4\omega$ / $4\omega+p$	$6\omega-p$	
ε^3			$-4\omega-p$	$p-6\omega$ / $6\omega+p$	$8\omega-p$
ε^4				$-6\omega-p$	$p-8\omega$ / $8\omega+p$

where amplitudes A, a, B, b, C, A_a, a_a, B_a, b_a and C_a are all complex numbers. Further, for example, $\overline{B}$ means a conjugate complex number of B. When equation (1. 9) is substituted into equation (1. 8), the 10th square determinant which consists of the coefficients of the complex amplitudes A, A_a, $\bar{a}$, $\bar{a}_a$, $\overline{B}$, $\overline{B}_a$, b, b_a, C and C_a is obtained as

$$F=\begin{vmatrix} H(p) & -1 & 0 & 0 & -\Delta & \Delta & 0 & 0 & 0 & 0 \\ -1 & G(p) & 0 & -\kappa\varepsilon & \Delta & -\Delta & 0 & 0 & 0 & 0 \\ 0 & 0 & H(-p) & -1 & 0 & 0 & 0 & 0 & -\Delta & \Delta \\ 0 & -\kappa\varepsilon & -1 & G(-p) & 0 & 0 & 0 & 0 & \Delta & -\Delta \\ -\Delta & \Delta & 0 & 0 & H(\hat{p}) & -1 & 0 & 0 & 0 & 0 \\ \Delta & -\Delta & 0 & 0 & -1 & G(\hat{p}) & 0 & -\kappa\varepsilon & 0 & 0 \\ 0 & 0 & 0 & 0 & 0 & 0 & H(-\hat{p}) & -1 & 0 & 0 \\ 0 & 0 & 0 & 0 & 0 & -\kappa\varepsilon & -1 & G(-\hat{p}) & 0 & 0 \\ 0 & 0 & -\Delta & \Delta & 0 & 0 & 0 & 0 & H(2\omega+p) & -1 \\ 0 & 0 & \Delta & -\Delta & 0 & 0 & 0 & 0 & -1 & G(2\omega+p) \end{vmatrix}=0$$

Expansion of this determinant gives the following frequency equation:

$$F=f(2\omega+p)\Phi(p)\Phi(\hat{p})-\Delta^2\{f(2\omega+p)h(p)h(\hat{p})+g(2\omega+p)\Phi(\hat{p})h(-p)\}$$
$$+\Delta^4 g(2\omega+p)h(\hat{p})\{g(p)g(-p)-\kappa^2\varepsilon^2\}=0 \qquad (1.10)$$

where

$$\left.\begin{aligned} &H(p)=1-p^2,\quad G(p)=1+\kappa-\sigma p^2,\quad f(p)=H(p)G(p)-1,\\ &g(p)=H(p)+G(p)-2,\quad \Phi(p)=f(p)f(-p)-\kappa^2\varepsilon^2H(p)H(-p),\\ &h(p)=f(-p)g(p)-\kappa^2\varepsilon^2H(-p)\end{aligned}\right\}\quad(1.11)$$

The frequency equation of a circular shaft ($\Delta=0$) supported by equally flexible bearing pedestals ($\varepsilon=0$) is $f(p)=0$, and the frequency equation of a circular shaft ($\Delta=0$) supported in unequal stiffnesses ($\varepsilon\neq0$) is $\Phi(p)=0$ in equation (1.11).

1. 3. *Occurrence of Unstable Vibrations, and Position, Width and Number of Unstable Regions*

1. 3. 1. *When directional inequality of pedestal stiffness is smaller than asymmetry of shaft stiffness*[61]

Neglecting the ε^2 order terms in equation (1.10), a frequency equation is derived as follows:

$$F=f(-\hat{p})\{f(p)f(\hat{p})-\Delta^2g(p)g(\hat{p})\}\{f(-p)f(2\omega+p)$$
$$-\Delta^2g(-p)g(2\omega+p)\}=0\quad(1.12)$$

The terms $f(-\hat{p})$ in equation (1.12) has no relation to the occurrence of unstable vibrations, because this term does not contain Δ. The relations

$$F_1=f(p)f(\hat{p})-\Delta^2g(p)g(\hat{p})=0\quad(1.13)$$

and $F_1(-p)=f(-p)f(2\omega+p)-\Delta^2g(-p)g(2\omega+p)=0$ have symmetrical roots with respect to the abscissa ($p=0$), and so the equation (1.13) is only considered. By defining four real roots derived by $f(p)=0$ in equation (1.13) as $p_{i,0}$ ($i=1, 2, 3, 4$) and using equation (1.11), we obtain $p_{i,0}$ as follows:

$$p_{i,0}^2=\{\sigma+\kappa+1\pm\sqrt{(\sigma+\kappa+1)^2-4\sigma\kappa}\}/2\sigma\quad(1.14)$$

where the upper and lower signs correspond to $i=1$, 4 and $i=2$, 3, respectively. The following relation holds regarding $p_{i,0}$:

$$p_{4,0}<-1<p_{3,0}<0<p_{2,0}<1<p_{1,0}$$

The roots of $f(\hat{p})=0$ are $\hat{p}=p_{i,0}$, i. e., $p=2\omega-p_{i,0}=\hat{p}_{i,0}$. For example, the roots $p_{i,0}$ derived from $f(p)=0$ and the roots $\hat{p}_{i,0}$ from $f(\hat{p})=0$ are shown by solid and dotted lines in Fig. 1.2, respectively. Both roots of $g(p)=\kappa-(1+\sigma)p^2=0$ defined by equation (1.11) are

$$p_{gi}=\pm\sqrt{\kappa/(1+\sigma)}\quad(i=1,\ 2)\quad(1.15)$$

and $\hat{p}_{gi}=2\omega-p_{gi}$, roots of $g(\hat{p})=0$ are also shown by the fine lines in Fig. 1.2. A real root p, derived from equation (1.13) in the unhatched parts on the p, ω plane of Fig. 1.2, may exist in the limited area in which the sign of the function $f(p)f(\hat{p})g(p)g(\hat{p})$ is positive. Generally speaking, if ε is small, unstable regions

are restricted to the neighbourhood of four intersecting points C_1, C_2, D_1 and D_2 shown by indication ○ where curves of $f(p)=0$ and curves of $f(\hat{p})=0$ cross each other[59]. Let the abscissas of the four intersecting points C_1, C_2, D_1 and D_2 in Fig. 1.2 be $\omega_{ij,0}$:

$$\omega_{ij,0}=(p_{i,0}+p_{j,0})/2=\omega_{ji,0}$$

because the relation $p_{i,0}=\hat{p}_{j,0}=2\omega-p_{j,0}$ holds at the intersecting points $(\omega=\omega_{ij,0})$. In Fig. 1.2 for $\sigma=1$ and $\kappa=1$, $\omega_{11,0}=1.618$, $\omega_{12,0}=\omega_{21,0}=1.118$, and $\omega_{22,0}=0.618$. The coordinates near the intersecting points on the $p-\omega$ diagram are set as

$$\omega=\omega_{ij,0}+\xi, \quad p=p_{i,0}+\eta_i \qquad (1.16)$$

and the frequency equation (1.12) is expanded into Taylor's series at this point. By adopting up to the second power of small quantities ξ, η_i and Δ, the frequency equation is expanded into Taylor's series [61], that is,

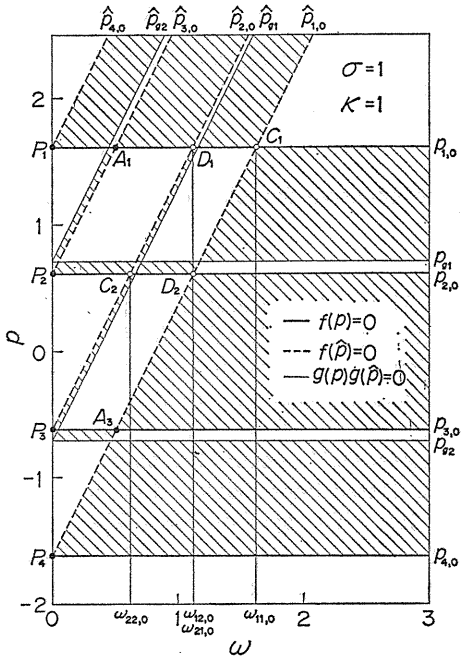

Fig. 1. 2 $p-\omega$ diagram and four intersecting points C_1, C_2, D_1, D_2 ($\sigma=1$, $\kappa=1$, $\varepsilon=0$).

$$F_1\simeq\{(\partial f/\partial p)_i\eta_i+(\partial f/\partial\omega)_i\xi\}\{(\partial\hat{f}/\partial p)_i\eta_i+(\partial\hat{f}/\partial\omega)_i\xi\}-\Delta^2(g\hat{g})_i=0 \qquad (1.17)$$

where simpler symbols f, $\hat{f}$, g and $\hat{g}$ are used instead of symbols $f(p)$, $f(\hat{p})$, $g(p)$ and $g(\hat{p})$. Lower subscripts i and j in equation (1.17) indicate the values at the intersecting points $(\omega_{ij,0}, p_{i,0})$ and $(\omega_{ij,0}, p_{j,0})$ in Fig. 1.2, respectively. The following relations hold with respect to f and g defined by equation (1.11):

$$\left.\begin{aligned}&(\partial f/\partial\omega)_i=0,\ (\partial\hat{f}/\partial p)_i=-(\partial f/\partial p)_j,\ (\partial\hat{f}/\partial\omega)_i=2(\partial f/\partial p)_j,\\&(\hat{g})_i=(g)_j\end{aligned}\right\} \qquad (1.18)$$

A quadratic equation for η_i which is obtained by substituting equation (1.18) into equation (1.17) has a solution as

$$\eta_i=\xi\pm\sqrt{\xi^2-\Delta^2(g)_i(g)_j/(\partial f/\partial p)_i(\partial f/\partial p)_j} \qquad (1.19)$$

Unstable regions are restricted to the neighbourhood of the four intersecting points C_1, C_2, D_1 and D_2 in Fig. 1.2 where the second term in the square root of equation (1.19) is negative, that is, the relation

$$(g)_i(g)_j(\partial f/\partial p)_i(\partial f/\partial p)_j>0 \qquad (1.20)$$

holds. The unstable region is $-|\xi_0|<\xi<|\xi_0|$ within which there exists imaginary solution η_i, and $|\xi_0|$ is obtained as follows:

$$|\xi_0| = \Delta\sqrt{(g)_i(g)_j/(\partial f/\partial p)_i(\partial f/\partial p)_j} = m_{\max} = 2\Delta' \tag{1.21}$$

In the unstable region, the whirling frequency p in epuation (1.16) takes imaginary number:

$$p = p_{i,0} + \eta_i = \omega + (p_{i,0} - p_{j,0})/2 \pm im \tag{1.22}$$

The negative damping coefficient m is obtained from equation (1.19):

$$m = m_{\max}\sqrt{1-(\xi/\xi_0)^2} \tag{1.23}$$

Near the intersecting points C_1 $(ij=11)$ and C_2 $(ij=22)$, there occurs a statically unstable vibration[25, 26, 57] with the whirling speed ω, the amplitude of which increases with time in the form e^{mt}. Near the intersecting points D_1 $(ij=12)$ and D_2 $(ij=21)$, there occur simultaneously two unstable vibrations with frequencies P_1, $P_2 = \omega \pm (p_{1,0} - p_{2,0})/2$, in other words, dynamically unstable vibrations[25, 26, 59] occur, the amplitude of which increases exponentially as e^{mt}. In Fig. 1.4, dotted lines indicate the width of unstable region $2|\xi_0|$ calculated from equation (1.21). The symbol $\varepsilon' = \sqrt{\varepsilon_i'\varepsilon_j'}$ in Fig. 1.4 is to be defined by equation (1.29). At the intersecting points C_1 and C_2, ε' and Δ'/ε' are determined by four parameters σ, κ, ε and Δ:

$$\left.\begin{aligned} \varepsilon' &= \frac{\kappa\varepsilon\{1 \pm (1+\kappa-\sigma)/\sqrt{(\sigma+\kappa+1)^2-4\sigma\kappa}\}}{2\sqrt{2\sigma\{\sigma+\kappa+1 \pm \sqrt{(\sigma+\kappa+1)^2-4\sigma\kappa}\}}} \\ \frac{\Delta'}{\varepsilon'} &= \frac{\Delta}{2\kappa\varepsilon}\left\{1+\sigma+\frac{2\sigma(1+\sigma-\kappa)}{1+\kappa-\sigma \pm \sqrt{(\sigma+\kappa+1)^2-4\sigma\kappa}}\right\} \end{aligned}\right\} \tag{1.24}$$

where the upper and lower signs, $\pm$, correspond to the intersecting points C_1 $(i=j=1)$ and C_2 $(i=j=2)$, respectively. At the intersecting points D_1 and D_2 $(i \neq j)$,

$$\left.\begin{aligned} \varepsilon' &= \kappa\varepsilon/2\sqrt[4]{\sigma\kappa}\sqrt{(\sigma+\kappa+1)^2-4\sigma\kappa} \\ \Delta'/\varepsilon' &= \Delta/2\varepsilon \end{aligned}\right\} \tag{1.25}$$

1. 3. 2. When directional inequality of pedestal stiffness is larger than asymmetry of shaft stiffness[63]

When $\varepsilon \gg \Delta$, we must discuss the unstable vibrations near the intersections of $\Phi(p)=0$ and $\Phi(\hat{p})=0$, that is, the frequency equations for $\varepsilon \neq 0$ and $\Delta=0$, on the $p-\omega$ diagram. When the terms including $\Delta^2\Phi(\hat{p})$ and Δ^4 in equation (1.10) are neglected, the frequency equation (1.10) becomes $F = f(2\omega+p)F_2 = 0$, and so unstable vibrations may be discussed by the following equation:

$$F_2 = \Phi(p)\Phi(\hat{p}) - \Delta^2 h(p)h(\hat{p}) = 0 \tag{1.26}$$

Equation (1.26) is nothing but the frequency equation obtained by substitution of the solution of free vibration (1.9) excepting the fifth term in the right hand side. The same analytical method as Section 1.3.1 may be also applied to this section. Eight real roots p_{i0} $(i=1\sim8)$ of equation $\Phi(p)=0$ show the following relation:

$$p_{80}<p_{4,0}<p_{70}<-1<p_{60}<p_{3,0}<p_{50}<0<p_{40}<p_{2,0}<p_{30}$$
$$<1<p_{20}<p_{1,0}<p_{10}$$

The roots p_{i0} are obtained by using $\Phi(p)=(f+\kappa\varepsilon H)(f-\kappa\varepsilon H)=0$ in equation (1.11):

$$\left.\begin{aligned} p_{10}^2,\ p_{20}^2&=\{\sigma+\kappa+1\pm\kappa\varepsilon+\sqrt{(\sigma+\kappa+1\pm\kappa\varepsilon)^2-4\sigma\kappa(1\pm\varepsilon)}\}/2\sigma \\ p_{30}^2,\ p_{40}^2&=\{\sigma+\kappa+1\pm\kappa\varepsilon-\sqrt{(\sigma+\kappa+1\pm\kappa\varepsilon)^2-4\sigma\kappa(1\pm\varepsilon)}\}/2\sigma \end{aligned}\right\} \quad (1.27)$$

The roots p_{i0} of $\Phi(p)=0$ and the roots $\hat{p}_{j0}=2\omega-p_{j0}$ of $\Phi(\hat{p})=0$ are indicated by solid and dotted lines, respectively, as in Fig. 1.3 for $\sigma=1$, $\kappa=1$ and $\varepsilon=0.4$. The roots p_{hi0} of $h(p)=0$ and the roots $\hat{p}_{hj0}=2\omega-p_{hj0}$ of $h(\hat{p})=0$ are also indicated by fine lines in Fig. 1.3. In this case, $p_{10}=-p_{80}=1.709$, $p_{20}=-p_{70}=1.531$, $p_{30}=-p_{60}=0.692$, $p_{40}=-p_{50}=0.506$, $p_{h10}=-p_{h60}=1.626$, $p_{h20}=-p_{h50}=0.763$, and $p_{h30}=-p_{h40}=0.522$. Unstable vibrations occur near the sixteen points as shown by ○ indications in Fig. 1.3 where roots p_{i0} of $\Phi(p)=0$ cross roots $\hat{p}_{j0}=2\omega-p_{j0}$ of $\Phi(\hat{p})=0$. The abscissas ω_{ij} of these intersecting points are represented as

$$\omega_{ij}=(p_{i0}+p_{j0})/2=\omega_{ji}$$

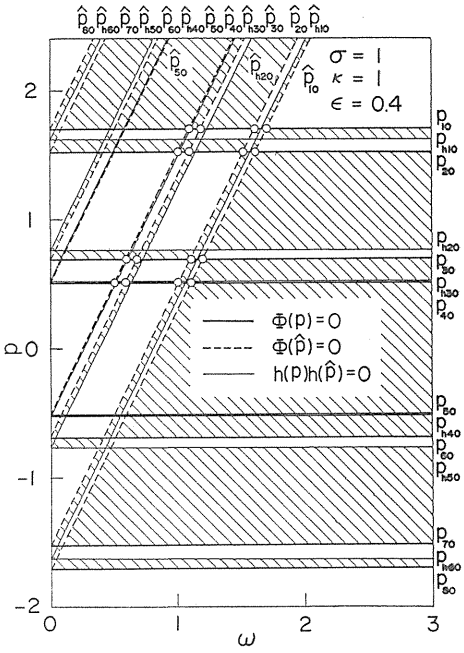

Fig. 1.3 $p-\omega$ diagram ($\sigma=1$, $\kappa=1$, $\varepsilon=0.4$).

Near the intersecting point C_1 of Fig. 1.2, statically unstable vibrations occur at the two rotating speeds $\omega=\omega_{11}$ and ω_{22}, and a dynamically unstable vibration at a rotating speed $\omega=\omega_{12}=\omega_{21}$. Near the intersecting point C_2, statically unstable vibrations occur at two rotating speeds $\omega=\omega_{33}$ and ω_{44}, and dynamically one at a rotating speed $\omega=\omega_{34}=\omega_{43}$. Near the intersecting points D_1 and D_2, on the other hand, dynamically unstable vibrations occur at four rotating speed $\omega=\omega_{13}$, ω_{23}, ω_{14} and ω_{24}.

When symbols ω_{ij}, p_{i0}, $\Phi=\Phi(p)$, $\hat{\Phi}=\Phi(\hat{p})$, $h=h(p)$ and $\hat{h}=h(\hat{p})$ are adopted instead of symbols $\omega_{ij,0}$, $p_{i,0}$, f, $\hat{f}$, g and $\hat{g}$ in equations (1.16) ~ (1.22), the values ξ_0 and m near the rotating speed ω_{ij} are calculated by equations (1.21) and (1.23), respectively.

1. 3. 3. When both inequality of pedestal stiffness and asymmetry of shaft stiffness are small quantities of same order

Expansion of frequency equation (1.10) is made into Taylor's series by using equation (1.16) near any one intersecting point among four points C_1, C_2, D_1 and

D_2 in Fig. 1.2. By adopting up to the fourth power of small quantities ξ, η_i, ε and Δ, equation (1.10) yields

$$F \simeq \left[\left\{\left(\frac{\partial f}{\partial p}\right)_i \eta_i + \left(\frac{\partial f}{\partial \omega}\right)_i \xi\right\}^2 - \kappa^2 \varepsilon^2 (H)_i^2\right]\left[\left\{\left(\frac{\partial \hat{f}}{\partial p}\right)_i \eta_i + \left(\frac{\partial \hat{f}}{\partial \omega}\right)_i \xi\right\}^2 - \kappa^2 \varepsilon^2 (\hat{H})_i^2\right]$$

$$-\Delta^2 (g\hat{g})_i \left\{\left(\frac{\partial f}{\partial p}\right)_i \eta_i + \left(\frac{\partial f}{\partial \omega}\right)_i \xi\right\}\left\{\left(\frac{\partial \hat{f}}{\partial p}\right)_i \eta_i + \left(\frac{\partial \hat{f}}{\partial \omega}\right)_i \xi\right\} = 0 \tag{1.28}$$

When following new symbols

$$\varepsilon_i' = \kappa\varepsilon\left(H \Big/ \frac{\partial h}{\partial p}\right)_i, \quad \varepsilon' = \sqrt{\varepsilon_i' \varepsilon_j'}, \quad \lambda = \frac{\varepsilon_i'}{\varepsilon_j'}, \quad \eta = \eta_i - \xi \tag{1.29}$$

are adopted, and relations (1.18) are used, equation (1.28) is reduced to a biquadratic equation for η:

$$\eta^4 + a_2\eta^2 + a_1\eta + a_0 = 0 \tag{1.30}$$

Coefficients and discriminant of the foregoing equation are given as follows:

$$\left.\begin{aligned} a_2 &= -2\xi^2 + 4\Delta'^2 - (\lambda + 1/\lambda)\varepsilon'^2 \\ a_1 &= 2(\lambda - 1/\lambda)\varepsilon'^2\xi \\ a_0 &= \xi^4 - \{4\Delta'^2 + (\lambda + 1/\lambda)\varepsilon'^2\}\xi^2 + \varepsilon'^4 \\ 27D &= 4(a_2^2 + 12a_0)^3 - (2a_2^3 - 72a_2a_0 + 27a_1^2)^2 \end{aligned}\right\} \tag{1.31}$$

where the symbol Δ' is already defined by equation (1.21).

As seen from equations (1.30) and (1.31), the root η/ε' of equation (1.30) is determined by three parameters Δ'/ε', ξ/ε' and λ. The unstable regions where the root η/ε' is not real but complex are given by only one parameter λ on the plane $(\xi/\varepsilon', \Delta'/\varepsilon')$ as Fig. 1.4. Since the relations $ij=11$ and $ij=22$ hold at the intersecting points C_1 and C_2 in Fig. 1.2, the parameter $\lambda = \varepsilon_i'/\varepsilon_j'$ is equal to one.

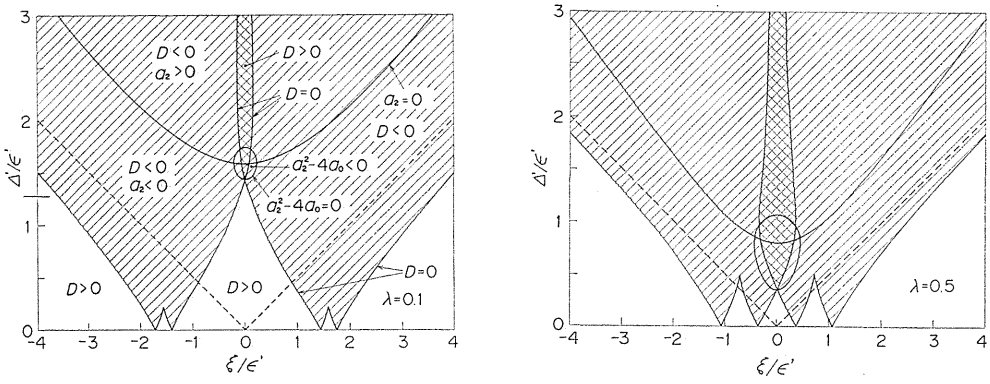

(a) (b)

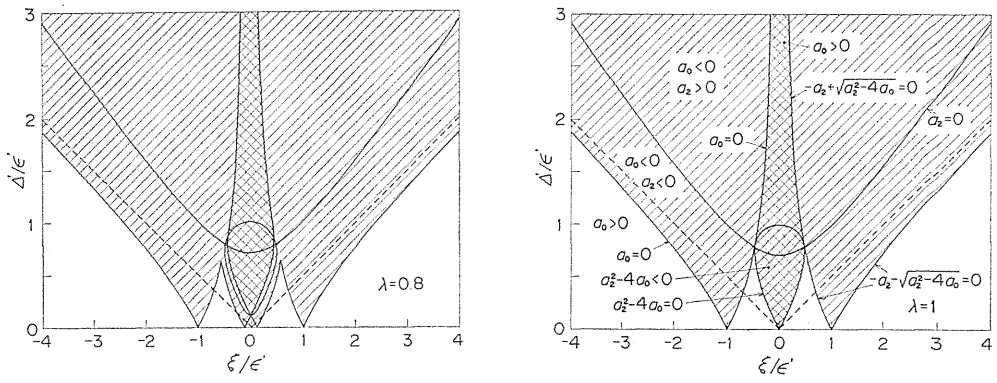

Fig. 1. 4 Unstable regions for $\varepsilon \simeq \Delta$ (λ=0.1, 0.5, 0.8, 1).

The parameter λ for $ij=12$, 21 at the point D_i is expressed by

$$\lambda(\sigma,\ \kappa)=\frac{(\sigma-\kappa)^2+(\sigma+\kappa)+(\kappa-\sigma)\sqrt{(\sigma+\kappa+1)^2-4\sigma\kappa}}{2\sqrt{\sigma\kappa}}=\frac{1}{\lambda(\kappa,\ \sigma)} \qquad (1.32)$$

which only includes σ and κ. When σ and κ are interchanged, $\lambda(\kappa,\ \sigma)$ takes a reciprocal of $\lambda(\sigma,\ \kappa)$. The particular case that $\sigma=\kappa$ gives $\lambda=1$.

The relation between roots and coefficients of the biquadratic equation (1. 30) is given as follows[6 7]:

(i) Granted that $D>0$, $a_2<0$ and $a_2^2-4a_0>0$, equation (1. 30) has four real roots.

(ii) Granted that $D<0$, equation (1. 30) has two real roots, and the other two roots are a pair of conjugate complex numbers.

(iii) Granted that $D>0$ and that $a_2>0$ or $a_2^2-4a_0<0$, equation (1. 30) has four complex roots.

Thus, unstable regions expressed on the plane (ξ/ε', Δ'/ε') satisfy either case (ii) or case (iii). Unstable regions are symmetrically shown with respect to the ordinate $\xi=0$, and unstable regions show no change even for the reciprocal parameter $1/\lambda$, because ξ and λ are included in the form of ξ^2, $(\lambda+1/\lambda)$ and $(\lambda-1/\lambda)^2$ in the stability criterion that $D=0$, $a_2=0$ and $a_2^2-4a_0=0$.

At first let us consider the dynamically unstable regions near the intersecting point D_1 (D_2). The unstable regions on the plane (ξ/ε', Δ'/ε') in Fig. 1. 4 have no dependence either upon D_1 or D_2, because the parameter $\lambda=\varepsilon_1'/\varepsilon_2'$ referring to the intersecting point D_1 is nothing but a reciprocal of $\lambda=\varepsilon_2'/\varepsilon_1'$ referring to another intersecting point D_2. The unstable regions which satisfy requirements (ii) and (iii) are shown in Figs. 1. 4(a) ~ (d) for given parameters λ=0. 1, 0. 5, 0. 8 and 1. The hatched part in Fig. 1. 4 corresponds to the unstable region which satisfies requirement (ii), that is, $D<0$. If we let Re[η] be a real part of complex roots η, and also let Im[η]$=\pm m$ ($m>0$) be an imaginary part of η, two vibrations with frequencies $p=p_{i,0}+\xi+$Re[η], (i=1, 2) occur simultaneously in the hatched part, and the amplitude of unstable vibration increases exponentially with the form of e^{mt}.

Even outside the hatched part ($D>0$), either the inside of a closed curve ($a_2^2-4a_0<0$) or the upside of the concaved curve ($a_2>0$) satisfies the instability requirement (iii) shown by the crosshatched part in Fig. 1. 4. The roots η become two

pairs of conjugate complex numbers in the crosshatched part. Letting $\mathrm{Im}[\eta]=\pm m_1$, $\pm m_2$ (m_1, $m_2>0$), there occur simultaneously two unstable vibrations with increasing amplitude of the form $e^{m_1 t}$, and also two other vibrations with increasing amplitude of the form $e^{m_2 t}$.

Regarding unstable regions near two intersecting points C_1 and C_2, the relation $\lambda=1$ is derived due to the relation $i=j$. The discriminant in equation (1.31) is changed by using the relation $a_1=0$:

$$D=16a_0(a_2^2-4a_0)^2 \tag{1.33}$$

Thus, the closed curve in Fig. 1.4(d) represents an equal root of the relations $a_2^2-4a_0=0$ and $D=0$. By putting $a_1=0$, equation (1.30) becomes a compound quadratic equation; solving for η^2, we find that

$$\eta=\pm\sqrt{(-a_2\pm\sqrt{a_2^2-4a_0})/2}$$

gives the dynamically unstable vibrations[59] which have two frequencies $\omega+\mathrm{Re}[\eta]$ within a closed curve ($a_2^2-4a_0<0$) [cf. Fig. 1.9(a)]. When $a_2^2-4a_0>0$ outside of a closed curve and simultaneously $-a_2\pm\sqrt{a_2^2-4a_0}<0$, the root η is purely imaginary and the statically unstable vibrations occur[57]. In the crosshatched part besides a closed curve ($a_2>0$ and $a_0>0$) in Fig. 1.4 (d), both relations $-a_2+\sqrt{a_2^2-4a_0}<0$ and $-a_2-\sqrt{a_2^2-4a_0}<0$ hold simultaneously, and so equation (1.34) has two pairs of purely imaginary roots, $\eta=\pm im_1$, $\pm im_2$. There occur two vibrations of statical instability which whirl with the same angular velocity of shaft ω and increase their amplitudes with time in the form $e^{m_1 t}$ and $e^{m_2 t}$ [cf. Fig. 1.9(b)].

When the ratio $\Delta'/\varepsilon'=0\sim2$ is given, the number of unstable regions is indicated upon the plane (λ, Δ'/ε') as shown in Fig. 1.5 where symbols 1, 2, 3 and 4 indicate the number of unstable regions. The number of unstable regions changes from four to one with a combination of Δ'/ε' and λ. Two curves $\Delta'/\varepsilon'=(1/2)\times\sqrt{(\lambda+1/\lambda)\pm2}$ which decrease with λ in Fig. 1.5 represent the height Δ'/ε' of two intersections of the closed curve $a_2^2-4a_0=0$ and the ordinate $\xi=0$ in Fig. 1.4. When $\lambda=0.5$, and $\Delta'/\varepsilon'=0.18$, 0.42, 0.8 and 1.5, η_i/ε', $m/\varepsilon'-\xi/\varepsilon'$ diagrams are shown in Figs. 1.6 (a) ~ (d). The values of $\eta_i=\xi+\mathrm{Re}[\eta]$ and $m=\mathrm{Im}[\eta]$ obtained from the root of equation (1.30) are plotted against ξ in the upper and the lower figures in Fig. 1.6, respectively. Near the intersecting point C_1 for $\lambda=1$ and $\Delta'/\varepsilon'=0.327$ and 1.309, p, $m-\omega$ diagrams are indicated by solid lines in Figs. 1.9 (a) and (b).

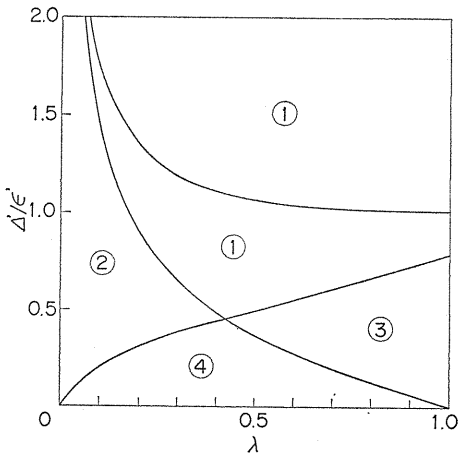

Fig. 1. 5 Number of unstable regions for $\Delta'/\varepsilon'=0\sim2$ and $\lambda=0\sim1$.

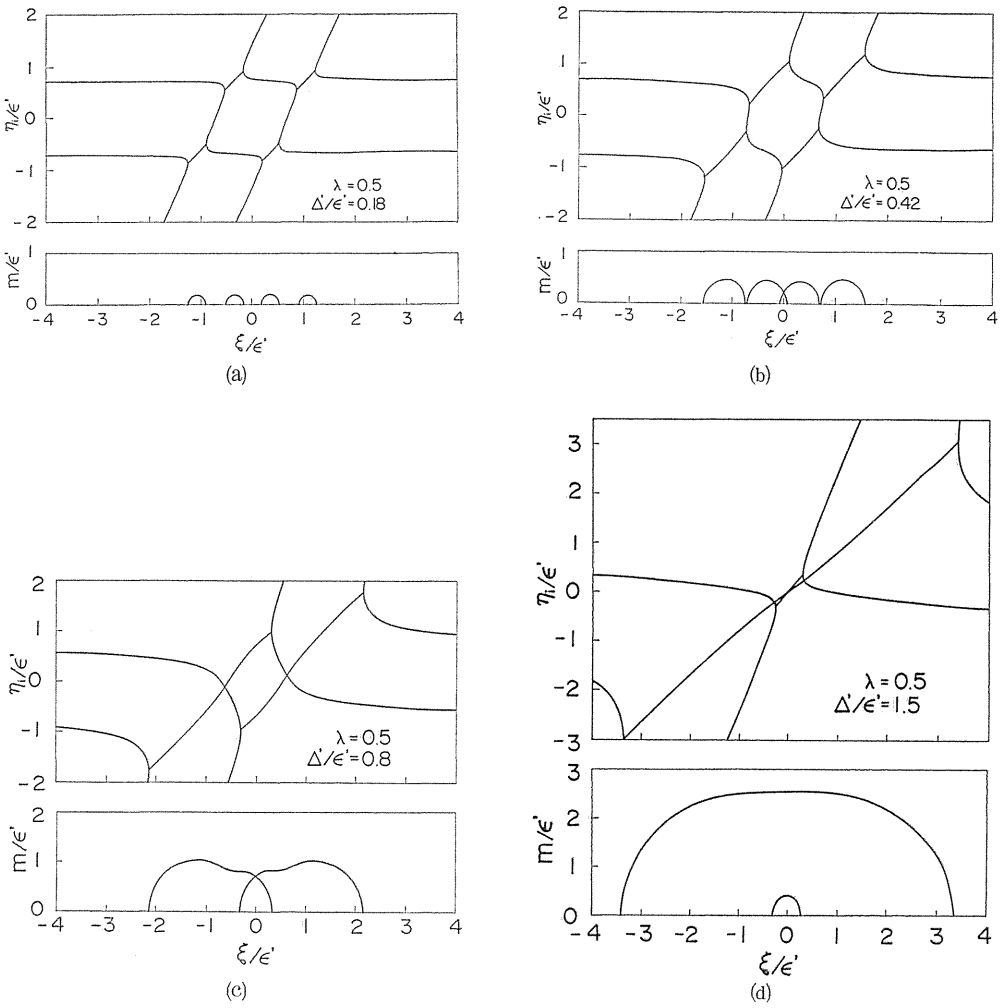

Fig. 1. 6 $\eta_i, m-\xi$ diagram near points D_1, D_2.

1. 3. 4. Special case in which mass of bearing pedestal is negligible

In a special case in which the mass of the bearing pedestal is not considered[15, 19, 40, 43, 46, 48], letting $\sigma \to 0$ in equation (1. 14) gives $p_{1,0}=\infty$ and $p_{2,0}=\sqrt{\kappa/(1+\kappa)}$. An unstable vibration is able to occur only near the intersecting point C_2, where convergent values of ε' and Δ' for $\sigma \to 0$:

$$\varepsilon'=\frac{\varepsilon}{2}\sqrt{\frac{\kappa}{(1+\kappa)^3}}, \qquad \frac{\Delta'}{\varepsilon'}=\frac{\kappa\Delta}{2\varepsilon} \tag{1. 35}$$

can be used, and unstable region coincides with Fig. 1. 4 (d) for $\lambda=1$.

1. 4. Comparison with Results Obtained by Analog Computer

The real and imaginary parts of equations of motion (1. 8) become

$$\left.\begin{aligned}
\ddot{x}&=-x+x_a+\varDelta\{(x-x_a)\cos 2\omega t+(y-y_a)\sin 2\omega t\}\\
\ddot{y}&=-y+y_a+\varDelta\{(x-x_a)\sin 2\omega t-(y-y_a)\cos 2\omega t\}\\
\ddot{x}_a&=[x-x_a-\kappa(1-\varepsilon)x_a-\varDelta\{(x-x_a)\cos 2\omega t+(y-y_a)\sin 2\omega t\}]/\sigma\\
\ddot{y}_a&=[y-y_a-\kappa(1+\varepsilon)y_a-\varDelta\{(x-x_a)\sin 2\omega t-(y-y_a)\cos 2\omega t\}]/\sigma
\end{aligned}\right\}\quad(1.36)$$

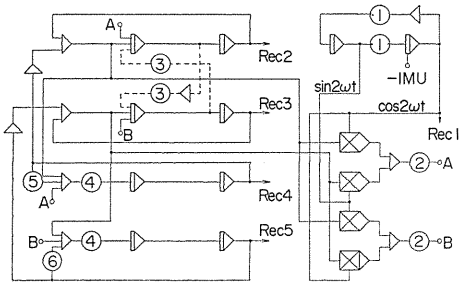

Fig. 1. 7 Simulation circuit for analog computer
Rec 1: cos $2\omega t$, Rec 2: x, Rec 3: y,
Rec 4: x_a, Rec 5: y_a
Potentiometers ①: 2ω, ②: $\varDelta$,
③: $i_p\omega$, ④: $1/\sigma$,
⑤: $\kappa(1-\varepsilon)$,
⑥: $\kappa(1+\varepsilon)$.

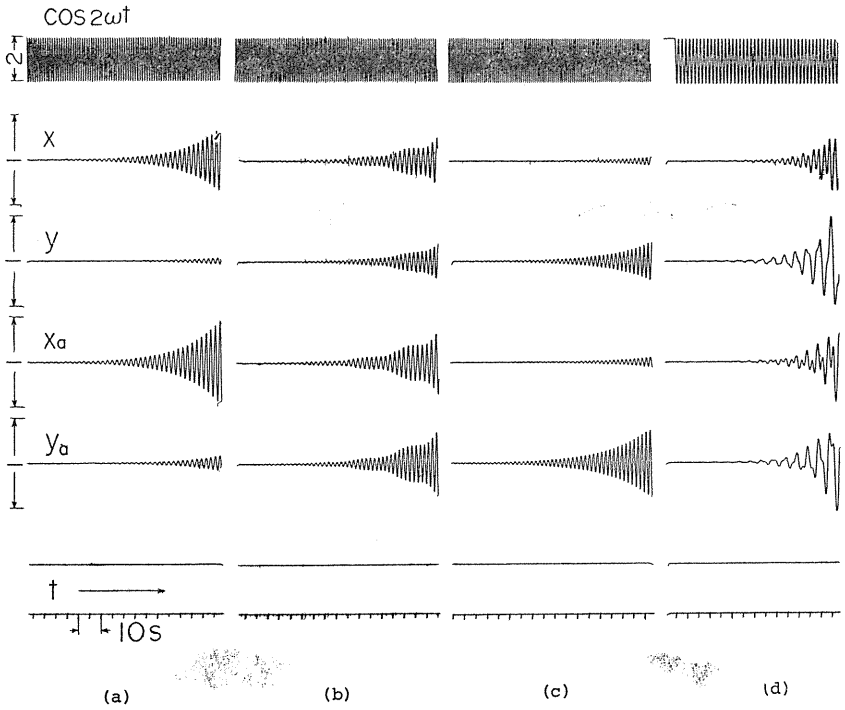

Fig. 1. 8 Examples of vibratory waves in unstable regions
(a), (b), (c) for cross point C_1 and $\sigma=1$, $\kappa=1$, $\varDelta=0.1$, $\varepsilon=0.4$, $\varDelta'/\varepsilon'=0.327$
(d) for cross points D_1, D_2 and $\sigma=1.5$, $\kappa=0.825$, $\varDelta=0.4$, $\varepsilon=0.2$, $\varDelta'/\varepsilon'=1$
(a) $\omega=1.52$, $m=0.030$, (b) $\omega=1.62$, $m=0.029$, $\omega+\mathrm{Re}[\eta]=1.705$, 1.535,
(c) $\omega=1.72$, $m=0.026$, (d) $\omega=0.96$, $m=0.053$, $P_1=1.336$, $P_2=0.584$.

Solid lines in Fig. 1.7 show the simulation circuit for an analog computer ALS-200X which satisfies equation (1.36). Vibratory waves cos $2\omega t$, x, y, x_a and y_a are given by recorders 1, 2, 3, 4 and 5, respectively. The added circuit shown by dotted lines has gyroscopic coefficient i_p and it satisfies the real and imaginary parts of equation (2.8) for a conical motion dealed with Chapter 2. In this case, recorders 2, 3, 4 and 5 describe vibratory waves θ_x, θ_y, θ_{ax} and θ_{ay}.

In order to show statically and dynamically unstable vibrations, three types of vibratory waves near the intersecting point C_1 are indicated by an analog computer in Figs. 1.8 (a), (b) and (c). Figures 1.8 (a) and (c) show statically unstable vibrations[57], the circular frequency of which coincides with ω. Dynamically unstable vibrations[59] are shown in Fig. 1.8 (b), where two frequencies P_1, $P_2=\omega+\mathrm{Re}[\eta]$, and the relation $P_1+P_2=2\omega$ always holds. Dynamically unstable vibrations occur in the neighbourhood of the intersecting point D_1 as shown in Fig. 1.8(d).

p, $m-\omega$ diagram in Fig. 1.6 is compared with the solutions obtained by an analog computer [cf. Fig. 1.7] which satisfies equation (1.8). Figures 1.9 (a) and (b) show the frequency p and the negative damping coefficient m for $\sigma=1$ and $\kappa=1$ near the intersecting point C_1 ($\omega=\omega_{11,0}=1.618$). The case in which $\varepsilon=0.4$ and $\Delta=0.1$ ($\Delta'/\varepsilon'=0.327$) is shown in Fig. 1.9 (a), wherein statically unstable vibrations occur at the right side and the left side, and dynamically unstable ones are in the center, and with three unstable regions. The case of $\varepsilon=0.2$ and $\Delta=0.2$ ($\Delta'/\varepsilon'=1.309$) is shown in Fig. 1.9 (b) wherein statically unstable two vibrations overlap in the middle of the unstable region. The circles in Fig. 1.9 are solutions

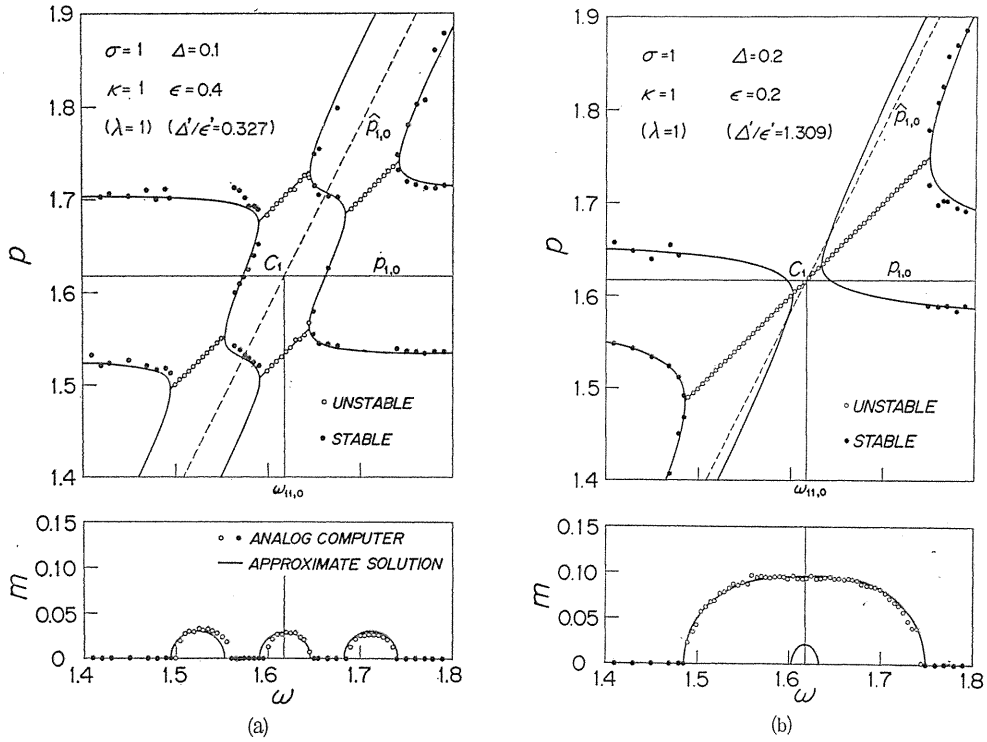

Fig. 1.9 $p,m-\omega$ diagram near point C_1.

obtained by an analog computer. Blank and solid circles indicate unstable solution and stable solution, respectively. The results obtained by an analog computer agree well with the solid line curves derived by numerical solution of approximate equation (1. 30).

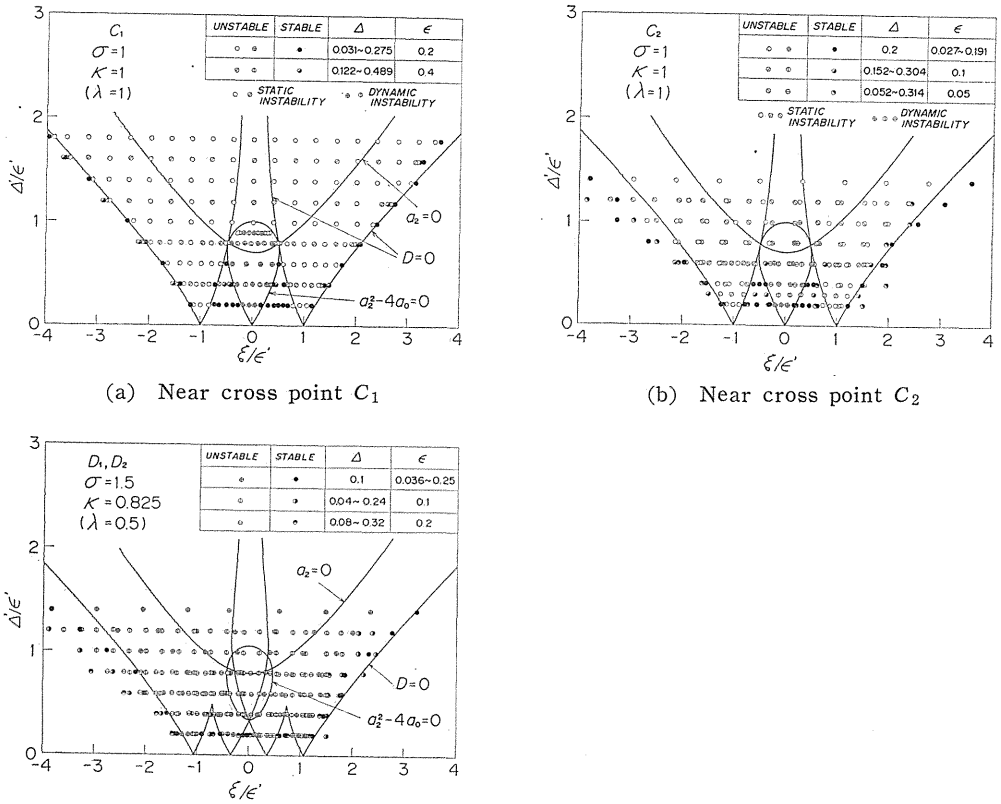

(a) Near cross point C_1

(b) Near cross point C_2

(c) Near cross points D_1, D_2

Fig. 1. 10 Approximate solutions for unstable regions and solutions derived by analog computer.

In Fig. 1. 10, unstable regions on the plane $(\xi/\varepsilon', \Delta'/\varepsilon')$ are compared with solutions by analog computer. Figures 1. 10 (a) and (b) show unstable regions at the intersecting points C_1 and C_2, respectively, and the vibrations x, y, x_a and y_a for $\sigma=1$, $\kappa=1$ determine whether the solutions are stable or not. The indications ○ ⊘ ⊗ mean statically unstable vibrations[57], while ⊕ ⦶ ⊖ mean dynamically unstable vibrations[59]. Figure 1. 10 (c) shows dynamically unstable regions for $\sigma=1.5$, $\kappa=0.825$ $(\lambda=0.5)$ regarding the intersecting point D_1 (D_2). When both values ε and Δ are smaller than 0. 3, the numerical results by approximate equation (1. 30) in Section *1. 3. 3* show good agreement with the analog computer solution.

1. 5. Conclusions

Conclusions obtained in this chapter may be summarized as follows:

(1) When the bearing pedestals supporting a rotating asymmetrical shaft have different stiffnesses, one unstable region near $\omega=\omega_{ij,0}=(p_{i,0}+p_{j,0})/2$ splits up into four parts, depending upon the ratio Δ/ε.

(2) When the analyses regarding unstable regions are carried out by classifying three cases in which $\varepsilon \ll \Delta$, $\varepsilon \gg \Delta$ and $\varepsilon \simeq \Delta$, the approximate solutions assuming that $\varepsilon \simeq \Delta$ can include the other two cases that $\varepsilon \ll \Delta$ and $\varepsilon \gg \Delta$.

(3) When both ε and Δ are assumed to be small quantities of the same order, the approximate solution for unstable regions is derived and it also includes the special case in which $\varepsilon \ll \Delta$.

(4) When a parameter $\lambda=0\sim1$ consisting of σ and κ is given, the width, number of cross sections of unstable regions and behavior of shaft motion are fully determined.

(5) The numerical solution of approximate equation coincides well with analog computer solution when both ε and Δ are assumed to be small of the same order.

(6) The unstable regions for a special case in which mass of bearing pedestal is neglected are the same as with the unstable regions for $\lambda=1$ by using convergent values ε' and Δ' for $\sigma\to0$.

2. Influence of Unequal Pedestal Stiffness on the Unstable Regions of a Rotating Asymmetrical Shaft (Conical Motion of a Rotor with Gyroscopic Effect)[71]

2. 1. Introduction

In this chapter, conical motions of a rotor with gyroscopic effect are treated. When gyroscopic coefficient i_p is small, a similar approximate analysis to Section *1. 3. 3* assuming that $\varepsilon \simeq \Delta$ can be done by considering i_p, ε and Δ to be small quantities of the same order, and it is shown how the unstable regions are changed by the gyroscopic effect. When i_p is larger than ε and Δ, the same approximate analyses can be carried out by distinguishing whether or not the terms smaller than ε^2 are negligible. The approximation regarding unstable regions for the case in which i_p is relatively large is compared with the solutions obtained by an analog computer, and they are found to show a good coincidence.

2. 2. Equations of Motion and Frequency Equation

2. 2. 1. Equations of motion

A rotating shaft system shown in Fig. 2. 1 is discussed. Pedestals A and B are exactly alike, that is, $m_a=m_b$, and $k_a\mp\Delta k_a=k_b\mp\Delta k_b$, in which the negative sign corresponds to x_a- and x_b-directions, and the positive one to y_a- and y_b-directions. Mass of rotor, polar moment of inertia, and diametral moment of inertia are defined as m_0, I_p and I, respectively. The rotor center S mounted at the midpoint of the asymmetrical shaft coincides with the origin O in the equilibrium state. We consider a stationary rectangular coordinate system O-xy, the z-axis of which coincides with a bearing center line AOB in equilibrium. A rectangular coordinate system O-$x'y'$ turning at an angular velocity ω just coincides with O-xy at the moment $t=0$. When the principal axis of inertia SZ is projected to $x'z$- or $y'z$-plane, each unit deflection angle yields the restoring moment of shaft $\delta-\Delta\delta$ or

$\delta+\delta\Delta$. This chapter deals with only the conical motion which is not interconnected with the parallel motion in this vibratory system. The rotor center S always coincides with the origin O, and the lower and upper pedestals A and B move symmetrically to the origin O, that is,

$$x_a=-x_b, \quad y_a=-y_b \tag{2.1}$$

The inclination angle θ_a of the bearing center line has the components θ_{ax} and θ_{ay} in x- and y-directions:

$$\left.\begin{aligned}\theta_{ax}&=(x_b-x_a)/l=-2x_a/l\\ \theta_{ay}&=(y_b-y_a)/l=-2y_a/l\end{aligned}\right\} \tag{2.2}$$

Let the inclination angle θ of the principal axis SZ have the components θ_x and θ_y in x- and y-directions, θ'_x and θ'_{ax} be the components of θ and θ_a in x'-direction, and θ'_y and θ'_{ay} the ones in y'-direction, respectively. The kinetic energy T and the potential energy V of this system are expressed[57] by using equations (2.1) and (2.2):

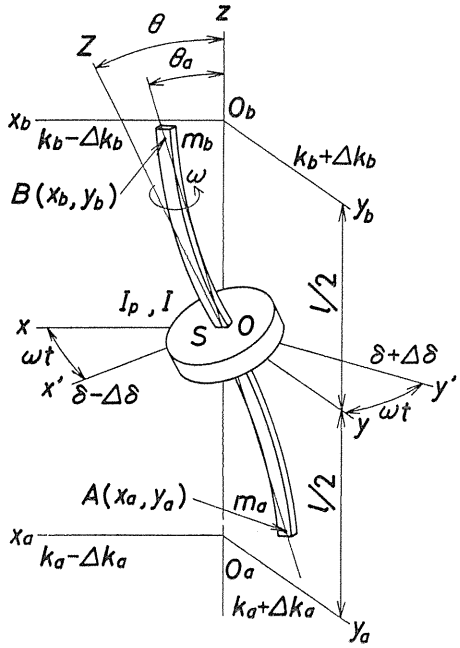

Fig. 2.1 Asymmetrical shaft and asymmetrically flexible pedestals ($m_a=m_b$, $k_a=k_b$, $\Delta k_a=\Delta k_b$) for conical motion of rotor ($x_a=-x_b$, $y_a=-y_b$).

$$\left.\begin{aligned}2T&=I_p\{\omega^2+\omega(\dot\theta_x\theta_y-\dot\theta_y\theta_x)\}+I(\dot\theta_x^2+\dot\theta_y^2)+2m_a(\dot x_a^2+\dot y_a^2)\\ 2V&=(\delta-\Delta\delta)(\theta'_x-\theta'_{ax})^2+(\delta+\Delta\delta)(\theta'_y-\theta'_{ay})^2\\ &\qquad+2\{(k_a-\Delta k_a)x_a^2+(k_a+\Delta k_a)y_a^2\}\end{aligned}\right\} \tag{2.3}$$

The following relationship exists between the stationary coordinate and the rotating one:

$$\begin{bmatrix}\theta'_x-\theta'_{ax}\\ \theta'_y-\theta'_{ay}\end{bmatrix}=\begin{bmatrix}\cos\omega t & \sin\omega t\\ -\sin\omega t & \cos\omega t\end{bmatrix}\begin{bmatrix}\theta_x-\theta_{ax}\\ \theta_y-\theta_{ay}\end{bmatrix} \tag{2.4}$$

Substitution of equations (2.2) ~ (2.4) into Lagrange's equation yields four equations of motion regarding θ_x, θ_y, θ_{ax} and θ_{ay}:

$$\left.\begin{aligned}&I\ddot\theta_x+I_p\omega\dot\theta_y+\delta(\theta_x-\theta_{ax})=\Delta\delta\{(\theta_x-\theta_{ax})\cos 2\omega t+(\theta_y-\theta_{ay})\sin 2\omega t\}\\ &I\ddot\theta_y-I_p\omega\dot\theta_x+\delta(\theta_y-\theta_{ay})=\Delta\delta\{(\theta_x-\theta_{ax})\sin 2\omega t-(\theta_y-\theta_{ay})\cos 2\omega t\}\\ &m_al^2\ddot\theta_{ax}-2\delta(\theta_x-\theta_{ax})+(k_a-\Delta k_a)l^2\theta_{ax}\\ &\qquad=-2\Delta\delta\{(\theta_x-\theta_{ax})\cos 2\omega t+(\theta_y-\theta_{ay})\sin 2\omega t\}\end{aligned}\right\} \tag{2.5}$$

$$\left.\begin{aligned} & m_a l^2 \ddot{\theta}_{ay} - 2\delta(\theta_y - \theta_{ay}) + (k_a + \Delta k_a) l^2 \theta_{ay} \\ & \quad = -2\Delta\delta\{(\theta_x - \theta_{ax}) \sin 2\omega t - (\theta_y - \theta_{ay}) \cos 2\omega t\} \end{aligned}\right\}$$

Now, complex variables

$$\theta_z = \theta_x + i\theta_y, \quad \bar{\theta}_z = \theta_x - i\theta_y, \quad \theta_{az} = \theta_{ax} + i\theta_{ay}, \quad \bar{\theta}_{az} = \theta_{ax} - i\theta_{ay} \tag{2.6}$$

are introduced, and ε in equation (1.6) and the following dimensionless quantities are used for simplicity's sake:

$$\left.\begin{aligned} & m_a l^2/2I = \sigma, \quad k_a l^2/2\delta = \kappa, \quad \Delta\delta/\delta = \Delta, \quad t\sqrt{\delta/I} = t', \\ & p/\sqrt{\delta/I} = p', \quad \omega/\sqrt{\delta/I} = \omega', \quad I_p/I = i_p \end{aligned}\right\} \tag{2.7}$$

Hereafter, the primes on the dimensionless quantities (2.7) are omitted, and the dots over dimensionless quantities mean the differential coefficient with respect to t'. By using equation (1.6) and (2.7), the equations of motion (2.5) are rewritten as

$$\left.\begin{aligned} & \ddot{\theta}_z - i i_p \omega \dot{\theta}_z + \theta_z - \theta_{az} = \Delta e^{2i\omega t}(\bar{\theta}_z - \bar{\theta}_{az}) \\ & \sigma\ddot{\theta}_{az} + (1+\kappa)\theta_{az} - \theta_z = \kappa\varepsilon\bar{\theta}_{az} - \Delta e^{2i\omega t}(\bar{\theta}_z - \bar{\theta}_{az}) \end{aligned}\right\} \tag{2.8}$$

If the gyroscopic term $-ii_p\omega\dot{\theta}_z$ is excluded from the first equation in equation (2.8), and θ_z and θ_{az} are replaced by complex numbers z and z_a, respectively, equation (2.8) coincides with equations of motion (1.8) regarding the parallel motion of a rotor mounted on an asymmetrical shaft.

2. 2. 2. *Frequency equation*

In amplitudes up to the second order of small quantities ε and Δ are considered with respect to conical motions of a rotor, solutions of free vibration satisfying equation (2.8) are expressed in the following forms:

$$\left.\begin{aligned} & \theta_z = Ae^{ipt} + ae^{-ipt} + Be^{i\hat{p}t} + be^{-i\hat{p}t} + Ce^{i(2\omega+p)t} \\ & \theta_{az} = A_a e^{ipt} + a_a e^{-ipt} + B_a e^{i\hat{p}t} + b_a e^{-i\hat{p}t} + C_a e^{i(2\omega+p)t} \end{aligned}\right\} \tag{2.9}$$

where amplitudes A, a, B, b, C, A_a, a_a, B_a, b_a and C_a are complex numbers. When equation (2.9) is substituted into the equations of motion (2.8), the 10 th-order determinant which consists of the coefficient of complex amplitudes is obtained as

$$F=\begin{vmatrix} H_1(p) & -1 & 0 & 0 & -\Delta & \Delta & 0 & 0 & 0 & 0 \\ -1 & G(p) & 0 & -\kappa\varepsilon & \Delta & -\Delta & 0 & 0 & 0 & 0 \\ 0 & 0 & H_1(-p) & -1 & 0 & 0 & 0 & 0 & -\Delta & \Delta \\ 0 & -\kappa\varepsilon & -1 & G(-p) & 0 & 0 & 0 & 0 & \Delta & -\Delta \\ -\Delta & \Delta & 0 & 0 & H_1(\hat{p}) & -1 & 0 & 0 & 0 & 0 \\ \Delta & -\Delta & 0 & 0 & -1 & G(\hat{p}) & 0 & -\kappa\varepsilon & 0 & 0 \\ 0 & 0 & 0 & 0 & 0 & 0 & H_1(-\hat{p}) & -1 & 0 & 0 \\ 0 & 0 & 0 & 0 & 0 & -\kappa\varepsilon & -1 & G(-\hat{p}) & 0 & 0 \\ 0 & 0 & -\Delta & \Delta & 0 & 0 & 0 & 0 & H_1(2\omega+p) & -1 \\ 0 & 0 & \Delta & -\Delta & 0 & 0 & 0 & 0 & -1 & G(2\omega+p) \end{vmatrix}=0 \tag{2.10}$$

where $G(p)$ has been defined by equation (1.11), and

$$H_1(p)=1+i_p\omega p-p^2 \tag{2.11}$$

The following frequency equation is obtained by expanding the determinant (2.10):

$$F=f_1(2\omega+p)\Phi_1(p)\Phi_1(\hat{p})-\Delta^2\{f_1(2\omega+p)h_1(p)h_1(\hat{p})$$
$$+g_1(2\omega+p)\Phi_1(\hat{p})h_1(-p)\}+\Delta^4 g_1(2\omega+p)h_1(\hat{p})\{g_1(p)g_1(-p)-\kappa^2\varepsilon^2\}=0 \tag{2.12}$$

where

$$\left.\begin{aligned} &f_1(p)=H_1(p)G(p)-1, \quad g_1(p)=H_1(p)+G(p)-2, \\ &h_1(p)=f_1(-p)g_1(p)-\kappa^2\varepsilon^2 H_1(-p), \\ &\Phi_1(p)=f_1(p)f_1(-p)-\kappa^2\varepsilon^2 H_1(p)H_1(-p) \end{aligned}\right\} \tag{2.13}$$

2. 3. *Occurrence of Uustable Vibrations, and Position, Width and Number of Unstable Regions*

2. 3. 1. *When gyroscopic effect is small*

In the vibratory system shown in Fig. 2. 1, the unstable vibration is caused by shaft asymmetry Δ[25,26]. When both pedestal inequality ε and gyroscopic coefficient i_p are smaller than Δ, and all terms including i_p and ε^2 in equations (2.12) and (2.13) are neglected, frequency equation (2.12) coincides with equation (1.12) given in Chapter 1, and so equation (1.13) is also considered as a frequency equation. In this case, unstable vibrations only occur near four intersecting points C_1, C_2, D_1 and D_2 in Fig. 1. 2.

In order to investigate how unstable regions come under the gyroscopic effect, an analysis is carried out by assuming that i_p is of the same order as ε and Δ. Because unstable regions are considered to have the extent of the same order as ε, Δ and i_p in the neighbourhood of intersecting points C_1, C_2, D_1 and D_2 in Fig. 1. 2, the coordinates near the intersecting point are set as equation (1.16). Frequency equation (2.12) is expanded into Taylor's series. If the small quantities ξ,

η_i, i_p, ε and Δ are adopted up to the fourth power, equation (2. 12) becomes

$$F=[\{(\partial f/\partial p)_i\eta_i+(\partial f/\partial\omega)_i\xi\}^2-\kappa^2\varepsilon^2(H)_i^2-i_p^2(\omega pG)_i^2][\{(\partial\hat{f}/\partial p)_i\eta_i$$
$$+(\partial\hat{f}/\partial\omega)_i\xi\}^2-\kappa^2\varepsilon^2(\hat{H})_i^2-i_p^2(\omega\hat{p}\hat{G})_i^2]-\Delta^2(g\hat{g})_i\{(\partial f/\partial p)_i\eta_i+(\partial f/\partial\omega)_i\xi$$
$$-i_p(\omega pG)_i\}\{(\partial\hat{f}/\partial p)_i\eta_i+(\partial\hat{f}/\partial\omega)_i\xi-i_p(\omega\hat{p}\hat{G})_i\}=0 \tag{2. 14}$$

where simpler symbols G, $\hat{G}$, H and $\hat{H}$ are used instead of symbols $G(p)$, $G(\hat{p})$, $H(p)$ and $H(\hat{p})$, respectively. The following relations regarding G and H

$$(\hat{G})_i=(G)_j,\quad (\hat{H})_i=(H)_j \tag{2. 15}$$

hold, and new symbols defined by

$$\mu_i=i_p\left(\omega pG/\frac{\partial f}{\partial p}\right)_i,\quad \mu=\sqrt{\mu_i\mu_j}/\varepsilon',\quad \nu=\sqrt{\mu_i/\mu_j} \tag{2. 16}$$

are adopted. By using equations (1. 18), (1. 21), (1. 29), (2. 15) and (2. 16), and noting that the sings of μ_i and μ_j are both negative, equation (2. 14) is reduced to a biquadratic equation for η:

$$\eta^4+a_2\eta^2+a_1\eta+a_0=0 \tag{2. 17}$$

The discriminant D in equation (2. 17) is given by equation (1. 31) and the coefficients are given as follows:

$$\left.\begin{aligned}
a_2&=-2\xi^2+4\Delta'^2-\left(\lambda+\mu^2\nu^2+\frac{1}{\lambda}+\frac{\mu^2}{\nu^2}\right)\varepsilon'^2\\
a_1&=2\{(\lambda+\mu^2\nu^2)-\left(\frac{1}{\lambda}+\frac{\mu^2}{\nu^2}\right)\}\varepsilon'^2\xi+4\left(\mu\nu-\frac{\mu}{\nu}\right)\Delta'^2\varepsilon'\\
a_0&=\xi^4-\{4\Delta'^2+\left(\lambda+\mu^2\nu^2+\frac{1}{\lambda}+\frac{\mu^2}{\nu^2}\right)\varepsilon'^2\}\xi^2-4\left(\mu\nu+\frac{\mu}{\nu}\right)\Delta'^2\varepsilon'\xi\\
&\quad+\{(\lambda+\mu^2\nu^2)\left(\frac{1}{\lambda}+\frac{\mu^2}{\nu^2}\right)\varepsilon'^4-4\mu^2\Delta'^2\varepsilon'^2\}
\end{aligned}\right\} \tag{2. 18}$$

At the intersecting points C_1 ($ij=11$) and C_2 ($ij=22$) in Fig. 1. 2, the relations $\lambda=1$ and $\nu=1$ hold from equations (1. 29) and (2. 16), and μ is expressed by

$$\mu=\frac{i_p\sigma}{\varepsilon\kappa}\cdot\frac{\sqrt{(\sigma+\kappa+1)^2-4\sigma\kappa}\pm(\sigma-\kappa+1)}{\sqrt{(\sigma+\kappa+1)^2-4\sigma\kappa}\pm(\kappa-\sigma+1)} \tag{2. 19}$$

where the upper and lower signs correspond to $ij=11$ and $ij=22$, respectively. In the special case in which the pedestal mass is negligible ($\sigma\to 0$), the convergent value of the lower sign in equation (2. 19) may be used, i. e., $\mu=i_p(1+\kappa)/\varepsilon$.

At the intersecting points D_1 and D_2 ($i\neq j$) in Fig. 1. 2,

$$\mu=i_p\sqrt{2\sigma\kappa+(\sigma+\kappa+1)\sqrt{\sigma\kappa}}/(2\varepsilon\kappa) \tag{2. 20}$$

At the intersecting point D_1 ($ij=12$), λ is given by equation (1.32), and also ν is expressed by

$$\nu=\sqrt{\frac{\sqrt{(\sigma+\kappa+1)^2-4\sigma\kappa}-(\kappa-\sigma+1)}{\sqrt{(\sigma+\kappa+1)^2-4\sigma\kappa}+(\kappa-\sigma+1)}} \tag{2.21}$$

The parameters λ and ν at the intersecting point D_2 ($ij=21$) coincide with reciprocals of each parameter at point D_1. Parameter μ only expresses the gyroscopic effect, because μ includes i_p as seen from equations (2.19) and (2.20), and other parameters λ and ν do not include i_p.

As seen from equation (2.18), the root η/ε' of equation (2.17) is determined by five values Δ/ε', ξ/ε', λ, μ and ν. Thus the unstable regions in which the root η/ε' of equation (2.17) is not real but complex can be indicated on the plane (ξ/ε', Δ'/ε') for three other parameters λ, μ and ν. Unstable regions satisfy either case (ii) or (iii) among three requirements (i), (ii) and (iii) in Section *1. 3. 3*, and the bound of the unstable region expressed on the plane (ξ/ε', Δ'/ε') are given by three curves $D=0$, $a_2=0$ and $a_2^2-4a_0=0$. In Figs. 2. 2 and 2. 3, the unstable region belonging to the case (ii) is hatched, and the unstable one belonging to the case (iii) is crosshatched.

At first, let us consider the unstable regions near two intersecting points C_1 and C_2. Since the relations $ij=11$ and $ij=22$ hold in this case, the parameters $\lambda=1$ and $\nu=1$ hold, and then $a_1=0$ always holds from equation (2.18). That is, equation (2.17) is expressed by a compound quadratic equation, and the root η and the discriminant D are the same form as equations (1.33) and (1.34). Unstable regions near the intersecting points C_1 and C_2 are shown in Figs. 2. 2 (a) and (b) for $\mu=0.5$ and 1.5. Let $\mathrm{Re}[\eta]$ be a real part of the complex root η, and also let $\mathrm{Im}[\eta]=\pm m$ ($m>0$) be an imaginary part of η, there simultaneously occur two vibrations with frequencies $p=\omega+\mathrm{Re}[\eta]$ within a closed curve ($a_2^2-4a_0<0$) of Fig. 2. 2; in

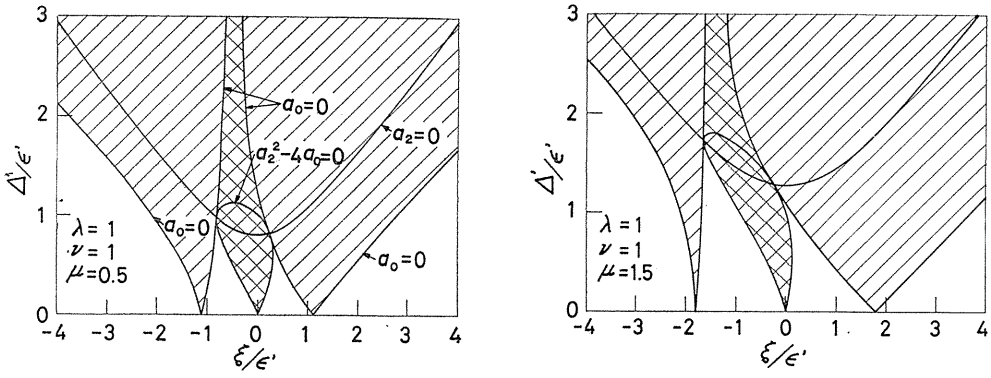

Fig. 2. 2 Unstable regions for small i_p near cross points C_1 and C_2.

other words, the dynamically unstable vibration[59] occur, the amplitude of which increases exponentially with the form e^{mt}. In the crosshatched part and outside of a closed curve ($a_2^2-4a_0>0$, $a_0>0$), the relations $D=16a_a(a_2^2-4a_0)^2>0$ and $a_2>0$ hold, and so $\eta=\pm\sqrt{(-a_2\pm\sqrt{a_2^2-4a_0})/2}$ has two pairs of purely imaginary

roots $\eta=\pm im_1$, $\pm im_2$. There occur two vibrations of static instability[57] which whirl with the same angular velocity of shaft ω, and increase their amplitudes with time in the form $e^{m_1 t}$ and $e^{m_2 t}$. In the hatched part ($a_0<0$) of Fig. 2. 2, the relation $\eta^2=-a_2-\sqrt{a_2^2-4a_0}<0$ always holds regardless of the sign of a_2, and then a statically unstable vibration occurs. When μ increases from $\mu=0.5$ [Fig. 2. 2 (a)] to $\mu=1.5$ [Fig. 2. 2 (b)], separation of unstable regions into three parts by the effect of pedestal inequality ε becomes larger, and the higher unstable region becomes much wider than the lower one.

Next, the unstable vibrations near the intersecting points D_1 and D_2 are considered. All vibrations near the intersecting points D_1 and D_2 are dynamically unstable, because equation (2. 17) has no purely imaginary roots η. When μ increases but other parameters $\lambda=0.5$ and $\nu=1.4$ remain fixed, the unstable regions are indicated as shown in Figs. 2. 3 (a) ($\mu=0.5$) and (b) ($\mu=1.5$). There occur vibrations with two frequencies $p=p_{i,0}+\xi+\mathrm{Re}[\eta]$, ($i=1, 2$) in the hatched part of Fig. 2. 3, and the amplitude increases in the form e^{mt}. The roots η become

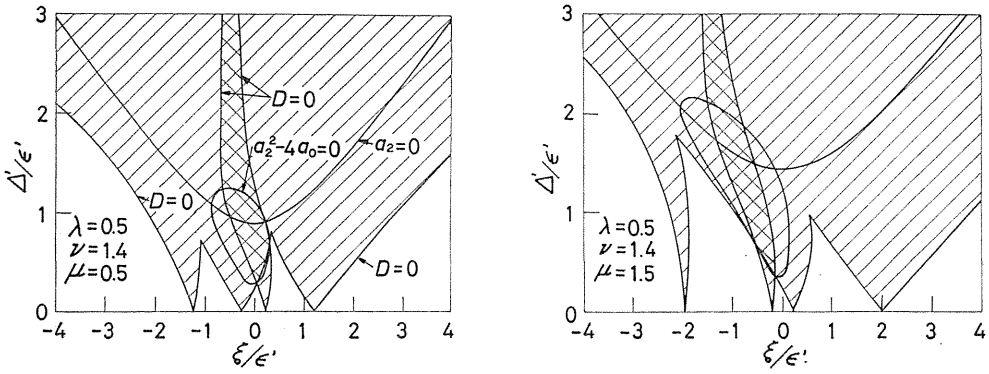

Fig. 2. 3 Unstable regions for small i_p near cross points D_1 and D_2.

two pairs of conjugate complex numbers in the crosshatched part. Let $\mathrm{Im}[\eta]$ be $\pm m_1$ and $\pm m_2$ (m_1, $m_2>0$), there occur two unstable vibrations increasing in the form $e^{m_1 t}$, and two other vibrations also increasing in the form $e^{m_2 t}$. The effect of μ separates further the unstable regions split by ε. The number of unstable regions remains four, but the higher unstable region becomes wider than the lower one.

2. 3. 2. *When gyroscopic effect is large*

2. 3. 2. 1. *Case in which a directional inequality of pedestal stiffness is small*

It is assumed that the gyroscopic coefficient i_p is large, and pedestal inequality ε is fairly small. Since the value ε is much smaller than i_p and Δ, neglecting the term ε^2 yields frequency equation (2. 12) :

$$F=f_1(-\hat{p})F_2(p)F_2(-p)=0 \tag{2. 22}$$

$F_2(p)$ and $F_2(-p)$ in equation (2. 22) have roots symmetrical to the abscissa ($p=$

0). Thus we may consider only the solution of the following equation:

$$F_2(p)=f_1(p)f_1(\hat{p})-\Delta^2 g_1(p)g_1(\hat{p})=0 \tag{2.23}$$

Let us define four real roots derived by $f_1(p)=0$ in equation (2.13) as p_i ($i=1$, 2, 3, 4), and two real roots derived by $g_1(p)=0$ as p_{gi} ($i=1$, 2). The roots p_i and $\hat{p}_i$ are indicated by solid lines, and the roots p_{gi} and $\hat{p}_{gi}$ by dotted lines in Fig. 2.4 (a) for $\sigma=1$, $\kappa=1$, $i_p=0.8$ and $\varepsilon=0$. The real root p of equation (2.23) may

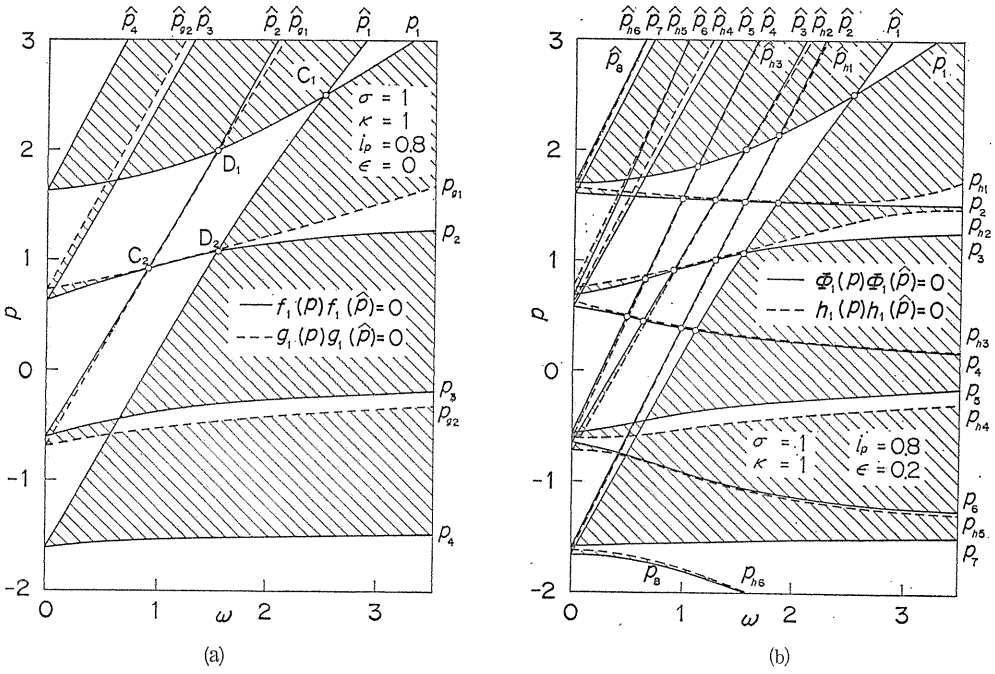

Fig. 2. 4 $p-\omega$ diagram for large i_p ($i_p=0.8$).

exist only in the unhatched area where $f_1(p)f_1(\hat{p})g_1(p)g_1(\hat{p})$ is positive. Unstable regions are restricted to the neighbourhood of four intersecting points C_1, C_2, D_1 and D_2, where curves $f_1(p)=0$ and $f_1(\hat{p})=0$ cross each other. Let the abscissa of these four intersecting points be ω_{ij},

$$p_i=\hat{p}_j=2\omega_{ij}-p_j \tag{2.24}$$

always holds, and the following relation is obtained:

$$\omega_{ij}=(p_i+p_j)/2=\omega_{ji} \tag{2.25}$$

The abscissas ω_{11} and ω_{22} of intersecting points C_1 and C_2 are given as follows:

$$\begin{matrix}\omega_{22}\\ \omega_{11}\end{matrix}=\sqrt{\frac{(\kappa+1)(i_p-1)-\sigma\pm\sqrt{\{(\kappa+1)(i_p-1)-\sigma\}^2+4\sigma\kappa(i_p-1)}}{2\sigma(i_p-1)}} \tag{2.26}$$

The abscissas ω_{12} and ω_{21}, and the ordinates p_1 and p_2 of intersecting points D_1

and D_2 are given in a way similar to the rotating shaft with an asymmetrical rotor[59] as follows:

$$\omega_{12}=\omega_{21}=\sqrt{\frac{(\kappa+1)i_p^2+4(\sigma+\kappa+1)(2-i_p)+(4-i_p)\sqrt{(\kappa+1)^2 i_p^2+8\sigma\kappa(2-i_p)}}{8\sigma(2-i_p)^2}} \tag{2.27}$$

$$\begin{matrix} p_1 \\ p_2 \end{matrix}=\omega_{12}\pm\sqrt{\frac{\sigma(3i_p-4)\omega_{12}^2+2(\sigma+\kappa+1)-(\kappa+1)i_p}{\sigma(4-i_p)}} \tag{2.28}$$

The intersecting points in Fig. 2.4 (a) are given by C_1 ($\omega_{11}=2.488$), C_2 ($\omega_{22}=0.899$), and D_1 and D_2 ($\omega_{12}=\omega_{21}=1.526$, $p_1=1.985$, $p_2=1.068$). Equation (2.23) is expanded into Taylor's series at the intersecting point (ω_{ij}, p_i). When small quantities Δ, η_i and ξ are adopted up to the second power, equation (2.23) becomes

$$F_2=\left\{\left(\frac{\partial f_1}{\partial p}\right)_i\eta_i+\left(\frac{\partial f_1}{\partial \omega}\right)_i\xi\right\}\left\{\left(\frac{\partial \hat{f}_1}{\partial p}\right)_i\eta_i+\left(\frac{\partial \hat{f}_1}{\partial \omega}\right)_i\xi\right\}-\Delta^2(g_1\hat{g}_1)_i=0 \tag{2.29}$$

A quadratic equation (2.29) for η_i has a solution

$$\eta_i=\frac{1}{2}\left[-\left\{\frac{(\partial f_1/\partial\omega)_i}{(\partial f_1/\partial p)_i}+\frac{(\partial \hat{f}_1/\partial\omega)_i}{(\partial \hat{f}_1/\partial p)_i}\right\}\xi \right.$$
$$\left.\pm\sqrt{\left\{\frac{(\partial f_1/\partial\omega)_i}{(\partial f_1/\partial p)_i}-\frac{(\partial \hat{f}_1/\partial\omega)_i}{(\partial \hat{f}_1/\partial p)_i}\right\}^2\xi^2+\frac{4\Delta^2(g_1)_i(\hat{g}_1)_i}{(\partial f_1/\partial p)_i(\partial \hat{f}_1/\partial p)_i}}\right] \tag{2.30}$$

When a square root in equation (2.30) becomes imaginary, root η_i becomes a complex number, and there occur unstable vibrations. Symbols used in equations (2.29) and (2.30) have the relations

$$\left.\begin{aligned} &(\partial f_1/\partial\omega)_i=i_p(pG)_i\neq 0, \quad (\partial \hat{f}_1/\partial p)_i=-(\partial f_1/\partial p)_j, \\ &(\partial \hat{f}_1/\partial\omega)_i=(\partial f_1/\partial\omega)_j+2(\partial f_1/\partial p)_j, \quad (\hat{g}_1)_i=(g_1)_j \end{aligned}\right\} \tag{2.31}$$

The unstable region has the width $-|\xi_0|<\xi<|\xi_0|$, and ξ_0 is obtained as follows:

$$\xi_0=\frac{\pm 2\Delta\sqrt{-(g_1)_i(\hat{g}_1)_i/(\partial f_1/\partial p)_i(\partial \hat{f}_1/\partial p)_i}}{|\{(\partial f_1/\partial\omega)_i/(\partial f_1/\partial p)_i\}-\{(\partial \hat{f}_1/\partial\omega)_i/(\partial \hat{f}_1/\partial p)_i\}|} \tag{2.32}$$

The negative damping coefficient m and its maximum value $m_{\max}$ become

$$\left.\begin{aligned} &m=m_{\max}\sqrt{1-(\xi/\xi_0)^2} \\ &m_{\max}=\Delta\sqrt{-(g_1)_i(\hat{g}_1)_i/(\partial f_1/\partial p)_i(\partial \hat{f}_1/\partial p)_i} \end{aligned}\right\} \tag{2.33}$$

2. 3. 2. 2. Case in which a directional inequality of pedestal stiffness cannot be neglected

When ε is not negligible, we must discuss the unstable vibrations at the intersecting points where curves $\Phi_1(p)=0$ and $\Phi_1(\hat{p})=0$ derived from equation (2. 12) cross each other on the $p-\omega$ diagram as in Fig. 2. 4(b). When the terms smaller than or equal to Δ^3 order are neglected in frequency equation (2. 12), the following equation is obtained:

$$F=f_1(2\omega+p)\{\Phi_1(p)\Phi_1(\hat{p})-\Delta^2 h_1(p)h_1(\hat{p})\}=0 \tag{2. 34}$$

Because $f_1(2\omega+p)$ does not have Δ, we may consider only the following equation:

$$F_3=\Phi_1(p)\Phi_1(\hat{p})-\Delta^2 h_1(p)h_1(\hat{p})=0 \tag{2. 35}$$

The roots of $\Phi_1(p)=0$ and $h_1(p)=0$ in equation (2. 13) are defined as p_i $(i=1\sim8)$ and p_{hi} $(i=1\sim6)$, respectively. Roots p_i and $\hat{p}_i=2\omega-p_i$ are indicated by solid lines, and roots p_{hi} and $\hat{p}_{hi}=2\omega-p_{hi}$ by dotted lines in Fig. 2. 4 (b) for $\sigma=1$, $\kappa=1$, $i_p=0.8$ and $\varepsilon=0.2$. The real root p derived from equation (2. 35) may exist in the unhatched part in Fig. 2. 4(b) where $\Phi_1(p)\Phi_1(\hat{p})h_1(p)h_1(\hat{p})$ is positive. In the same manner as Section *2. 3. 2. 1*, unstable regions occur near sixteen intersecting points shown by the ○ indication in Fig. 2. 4(b) where the roots p_i of $\Phi_1(p)=0$ crosses the root $\hat{p}_j$ of $\Phi_1(\hat{p})=0$. The values ξ_0 and $m_{\max}$ are calculated by adopting $\Phi_1(p)$ and $h_1(p)$ instead of $f_1(p)$ and $g_1(p)$, respectively, in equation (2. 32) and (2. 33). Thus:

$$\xi_0=\frac{\pm 2\Delta\sqrt{-(h_1)_i(\hat{h}_1)_i/(\partial\Phi_1/\partial p)_i(\partial\hat{\Phi}_1/\partial p)_i}}{|\{(\partial\Phi_1/\partial\omega)_i/(\partial\Phi_1/\partial p)_i\}-\{(\partial\hat{\Phi}_1/\partial\omega)_i/(\partial\hat{\Phi}_1/\partial p)_i\}|} \tag{2. 36}$$

$$m_{\max}=\Delta\sqrt{-(h_1)_i(\hat{h}_1)_i/(\partial\Phi_1/\partial p)_i(\partial\hat{\Phi}_1/\partial p)_i} \tag{2. 37}$$

2. 3. 2. 3. The change of position and number of unstable regions, and the negative damping coefficient by the gyroscopic effect

In order to show the gyroscopic effect on unstable regions, Figs. 2. 5 (a) and

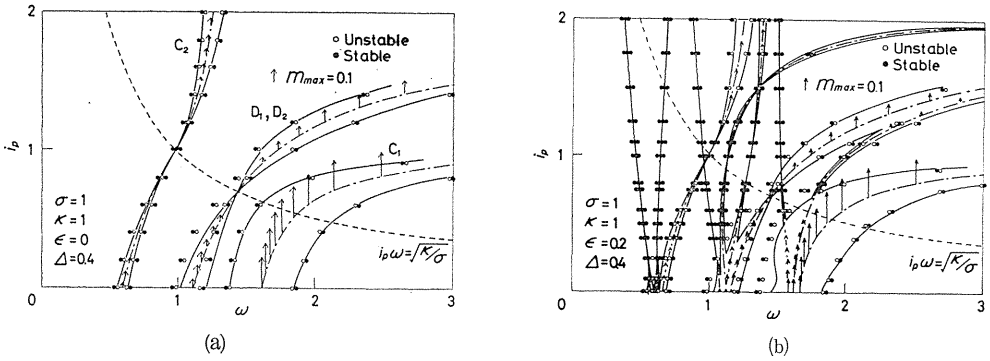

(a) (b)

Fig. 2. 5 Unstable regions by approximate solution ($i_p=0\sim2$)
Dot-dash lines; $\omega_{ij,0}$ and ω_{ij}
Solid lines; Limit of stable solution by equations (2. 32) and (2. 36)
○, ●; Unstable and stable solutions by analog computer.

(b) for $\sigma=1$, $\kappa=1$ and $\Delta=0.4$ are derived from equations (2.32), (2.33), (2.36) and (2.37), and an analog computer ALS-200X [cf. Fig. 1.7] indicates whether or not the solution of equation (2.5) is stable by the ●, ○ indications. Dot-dash lines in Fig. 2.5 (b) show the abscissa ω_{ij} at the intersection of p_i and $\hat{p}_j$, and solid lines are the bounds of unstable regions obtained by equations (2.32) and (2.36), respectively. The arrow length of upward direction is in propotion to the magnitude of $m_{\max}$. The rotating speed between the two ○ indications shows the unstable region for a certain value of i_p.

Figure 2.5 (a) shows how unstable regions change with the parameter i_p, and approximate solutions by equations (2.32) and (2.33) agree well with the results by an analog computer.

At the intersection of dot-dash lines and a hyperbola

$$i_p\omega=\sqrt{\kappa/\sigma} \tag{2.38}$$

shown by a dotted line in Fig. 2.5 (a), the width of the unstable regions near the intersecting points C_2, D_1 and D_2 is zero. If the two relations $G=1$ $(p=\pm\sqrt{\kappa/\sigma})$ and $H_1=1$ $(p=0,\ i_p\omega)$ hold simultaneously, and the following two equations, namely,

$$g_1=(H_1-1)+(G-1)=0,\quad f_1-g_1=(H_1-1)(G-1)=0 \tag{2.39}$$

also hold, this is nothing but equation (2.38).

Next, let us show that only a root p_2 among four roots of $f_1=0$ is in contact with one root p_{g1} between two roots of $g_1=0$ at the one point. When $i_p\omega<\sqrt{\kappa/\sigma}$, the following relation holds with regard to four roots $p=0$, $i_p\omega$, $\pm\sqrt{\kappa/\sigma}$ of equation $f_1-g_1=0$ given by equation (2.39):

$$p_4<-\sqrt{\kappa/\sigma}<p_{g2}<p_3<0<i_p\omega<p_2<p_{g1}<\sqrt{\kappa/\sigma}<p_1 \tag{2.40}$$

When $i_p\omega>\sqrt{\kappa/\sigma}$, on the other hand, the following relation holds:

$$p_4<-\sqrt{\kappa/\sigma}<p_{g2}<p_3<0<\sqrt{\kappa/\sigma}<p_2<p_{g1}<i_p\omega<p_1 \tag{2.41}$$

As shown from equations (2.40) and (2.41), the roots p_i and p_{gi} never intersect as far as the relation $i_p\omega\neq\sqrt{\kappa/\sigma}$ holds. When equation (2.38) is satisfied, the relation $p_{g1}=p_2=\sqrt{\kappa/\sigma}$ holds, and thus the curve $f_1=0$ is in contact with the curve $g_1=0$. When the contacting point between two curves $f_1=0$ and $g_1=0$ coincides with the intersecting points C_2 and D_2, unstable regions near the intersecting points C_2 and D_2 disappear whether Δ is large or not. Even if equation (2.38) is satisfied, the unstable region near the point C_1 appears as shown in Fig. 2.5 (a), because the relation $p_1>p_{g1}$ always holds. In Fig. 2.4(a) for $i_p=0.8$, the curve $f_1=0$ is in contact with the curve $g_1=0$ at the midpoint $(\omega=1.25)$ between C_2 and D_2, and the relation $p_{g1}>p_2$ always holds except the contact point.

Figure 2.5 (b) indicates solutions of approximate equations (2.36) and (2.37). The ●, ○ indications show stable and unstable solutions obtained by an analog computer for $\varepsilon=0.2$. Comparison of Figs. 2.5 (a) and (b) reveals fairly large unstable regions in Fig. 2.5 (b) near the intersecting points C_1, C_2, D_1 and D_2 of Fig. 2.5 (a); other narrow unstable regions which are split up into three or four parts by pedestal inequality appear near the above-mentioned unstable regions. This may be explained as follows; since $\Phi_1(p)$ and $h_1(p)$ in equation (2.13) include

only ε^2, and they can be approximated as $\Phi_1(p)\simeq f_1(p)f_1(-p)$ and $h_1(p)\simeq f_1(-p)g_1(p)$, equation (2.35) becomes

$$F_3\simeq f_1(-p)f_1(-\hat{p})F_2(p)=0$$

Solutions of equation (2.23) in Fig. 2.5 (a) near the intersecting points C_1, C_2, D_1 and D_2 differ little from ones of equation (2.35) in Fig. 2.5 (b). Two unstable regions to the left hand side than the intersecting points C_1 and C_2, and three unstable ones to the left hand side than the points D_1 and D_2 occur near the intersecting points where $f_1(-p)=0$ crosses $f_1(\hat{p})=0$ or $f_1(2\omega+p)=0$. Because $h_1\propto f_1(-p)\simeq 0$, the values ξ_0 and $m_{\max}$ become nearly zero from equations (2.36) and (2.37).

Next, the negative damping coefficient m is considered. In Fig. 2.6, the value m calculated from equation (2.37) is compared with the one in solutions of an analog computer for the same parameters σ, κ, ε and Δ in Fig. 2.5(b), and for $i_p=0$, 0.25, 0.75, 1.25 and 1.75. Solid lines in Fig. 2.6 indicate the value m calculated by equation (2.37), and the indications ● (stable) and ○ (unstable) show analog computer values. Vertical dot-dash lines indicate the abscissa ω_{ij} corresponding to the dot-dash lines in Fig. 2.5 (b). Dotted lines for $i_p=0$ and 0.25 in Fig. 2.6 indicate the imaginary part of root η calculated from equation (2.17). Solid lines agree well with the solutions obtained by an analog computer as i_p becomes large, but do not as i_p is small, and not at all with a special case in which $i_p=0$, since equation (2.37) is obtained by assuming that i_p is larger than ε and Δ. Because dotted lines for $i_p=0$ and 0.25 are obtained by equation (2.17), in which i_p, ε and Δ are assumed to be small quantities of the same order, the dotted line for $i_p=0$ shows a good coincidence with the solutions from an analog computer. The dotted line of equation (2.17) is not shown for $i_p=0.75$ or more in Fig. 2.6, because the dotted line is calculated according to the equation expanded near the intersecting points C_1, C_2, D_1 and D_2 for $i_p=0$ (Fig. 1.2), and the positions of the unstable region for $i_p=0.75$ or more differ entirely.

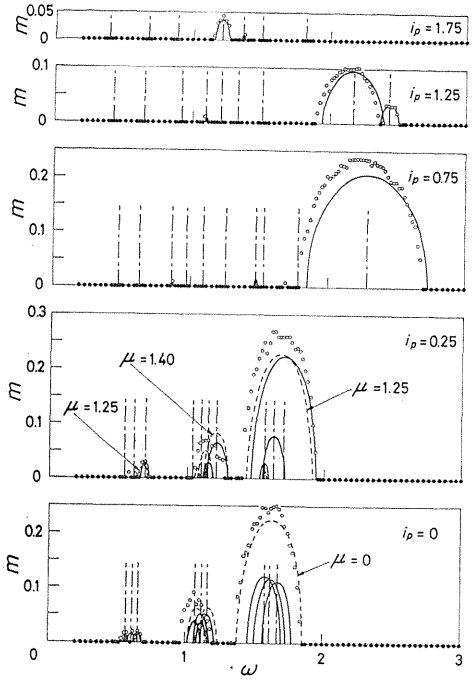

Fig. 2.6 $m-\omega$ diagram
Dot-dash lines; ω_{ij}
Solid lines; Approximate solution (2.37)
Dotted lines; Imaginary part of roots for equation (2.17).

2.4. *Conclusions*

Conclusions obtained in this chapter may be summarized as follows:

(1) An approximate analysis of a conical motion similar to a parallel motion

in Chapter 1 can be done for the two separate cases in which gyroscopic coefficient i_p is large or small.

(2) When the gyroscopic effect is small, the width and number of unstable regions can be determined by parameters λ and ν including σ and κ, and the parameter μ expressing the magnitude of gyroscopic effect.

(3) The number of unstable regions does not change due to the gyroscopic effect. When the gyroscopic effect increases, the unstable region at the higher rotating side becomes larger, and the unstable one at the lower rotating side splits up further and becomes smaller.

(4) When the gyroscopic effect is relatively large, the approximate analysis can be carried out for the two separate cases in which ε^2 is assumed to be negligible or not. The approximate results coincide well with the analog computer solution.

(5) If the angular velocity $\omega=\sqrt{\kappa/\sigma}/i_p$ coincides with the abscissa ω_{ij} of intersecting points C_2, D_1 and D_2, it is confirmed by the use of an analog computer that the unstable region may disappear.

3. Mechanism for Occurrence of Unstable Vibrations of a Rotating Asymmetrical Shaft Supported by Unequally Flexible Pedestals[72, 73]

3. 1. *Introduction*

When bearing pedestals supporting the shaft ends have a directional inequality in stiffness, each unstable region[25, 26, 70, 71] in which two types of unstable vibrations occur splits up into several regions. In this chapter, the mechanism by which these two types of unstable vibrations occur is clearly explained, and the condition is obtained in which unstable vibrations occur so that input energy into the rotating shaft system tends to increase the whirling amplitudes of the shaft. The condition is also explained from the fact that a counter-torque to a moment exerted by a restoring force about a bearing center line (or a component of a restoring moment caused by inclination of the shaft in the direction of the bearing center line) must be applied to the shaft end. Vibratory solutions in the unstable region obtained by an analog computer are found to satisfy this instability condition. Moreover, if the higher order of small quantities, that is, inequality of pedestal stiffness ε and asymmetrical shaft stiffness Δ are taken into consideration, a number of very narrow unstable regions can occur.

3. 2. *When a Rotor Moves in Parallel with the Upper and Lower Pedestals Motion*

A rotating shaft system[70] as shown in Fig. 1. 1 is also discussed. When kinetic energy (1. 2) and potential energy (1. 3) of this vibratory system are rewritten by use of the following complex variables and equation (1. 7),

$$\left.\begin{aligned} z'&=x'+iy'=z\mathrm{e}^{-i\omega t}, \quad \bar{z}'=x'-iy'=\bar{z}\mathrm{e}^{i\omega t} \\ z'_a&=x'_a+iy'_a=z_a\mathrm{e}^{-i\omega t}, \quad \bar{z}'_a=x'_a-iy'_a=\bar{z}_a\mathrm{e}^{i\omega t} \end{aligned}\right\} \quad (3.1)$$

differentiation with respect to time t yields the increase in rate of energy $\dot{T}$ and $\dot{V}$:

$$\left.\begin{aligned}\dot{T}&=m_0\mathrm{Re}[\dot{\bar{z}}\ddot{z}]+2m_a\mathrm{Re}[\dot{\bar{z}}_a\ddot{z}_a]\\ \dot{V}&=k\mathrm{Re}[(z'-z'_a)(\dot{\bar{z}}'-\dot{\bar{z}}'_a)]-\Delta k\mathrm{Re}[(z'-z'_a)(\dot{z}'-\dot{z}'_a)]\\ &\quad+2k_a\mathrm{Re}[z_a\dot{\bar{z}}_a]-2\Delta k_a\mathrm{Re}[z_a\dot{z}_a]\end{aligned}\right\}\quad(3.2)$$

where symbols Re[$\cdots$] and Im[$\cdots$] mean the real and imaginary parts of a complex number [$\cdots$]. Using equation (1.7), equations of motion (1.5) are rewritten as follows:

$$\left.\begin{aligned}&m_0\ddot{z}+k(z-z_a)=\Delta k e^{2i\omega t}(\bar{z}-\bar{z}_a)\\ &2m_a\ddot{z}_a-k(z-z_a)+2k_az_a=2\Delta k_a\bar{z}_a-\Delta k e^{2i\omega t}(\bar{z}-\bar{z}_a)\end{aligned}\right\}\quad(3.3)$$

When the first equation from equation (3.3) is multiplied by $\dot{\bar{z}}$, the second equation by $\dot{\bar{z}}_a$, and then these two equations are added together, the following equation is obtained:

$$\begin{aligned}&m_0[\dot{\bar{z}}\ddot{z}]+2m_a[\dot{\bar{z}}_a\ddot{z}_a]+k[(z-z_a)(\dot{\bar{z}}-\dot{\bar{z}}_a)]+2k_a[z_a\dot{\bar{z}}_a]\\ &\quad=2\Delta k_a[\bar{z}_a\dot{\bar{z}}_a]+\Delta k[e^{2i\omega t}(\bar{z}-\bar{z}_a)(\dot{\bar{z}}-\dot{\bar{z}}_a)]\end{aligned}\quad(3.4)$$

Substituting the real part in equation (3.4) and equation (3.1) into equation (3.2), the increase in rate of total energy $\dot{T}+\dot{V}$ is simply given as,

$$\dot{T}+\dot{V}=-2\Delta k\omega(x'-x'_a)(y'-y'_a)=-\Delta k\omega\mathrm{Im}[(z'-z'_a)^2]\quad(3.5)$$

It is obvious that the increase in rate of total energy (3.5) is equal to the time rate of work done by torque applied to the shaft end in Fig. 1. 1. In order to keep the points S and A on $x'y'$- and $x'_ay'_a$-planes, respectively, in such positions as shown in Fig. 3. 1, and also to rotate an asymmetrical shaft at a constant

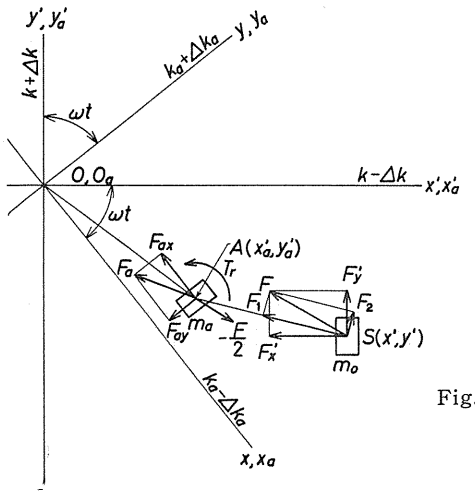

Fig. 3. 1 Shaft end torque T_r and components of restoring forces F and F_a.

angular velocity ω, torque T_r must be applied to the shaft end in the arrow direction. Torque T_r is obtained at first, and then the time rate of work applied to the shaft end ωT_r is compared with equation (3.5).

Due to shaft asymmetry $\Delta=\Delta k/k$, a restoring force vector F acting upon the rotor center S does not exist in the ABS-plane containing a deflected shaft. Two components F'_x and F'_y of the vector F in x'- and y'-directions are given as

$$F'_x=-(k-\Delta k)(x'-x'_a),\quad F'_y=-(k+\Delta k)(y'-y'_a) \tag{3.6}$$

This restoring force F is in balance with an inertial force $-F$. When a moment is produced by $-F$ about the bearing center line AB, a counter-torque T_r to this moment must be applied to the shaft end in order to turn the shaft at a constant angular velocity ω:

$$\begin{aligned} T_r&=-F'_x(y'-y'_a)+F'_y(x'-x'_a)\\ &=-2\Delta k(x'-x'_a)(y'-y'_a)=-\Delta k\mathrm{Im}[(z'-z'_a)^2] \end{aligned} \tag{3.7}$$

Equations (3.5) and (3.7) give the time rate of work applied to the shaft end:

$$\omega T_r=-\Delta k\omega\mathrm{Im}[(z'-z'_a)^2]=\dot{T}+\dot{V} \tag{3.8}$$

Equation (3.8) agrees precisely with the increase rate of total energy. Moreover, because of the directional inequality of the pedestal rigidity $\varepsilon=\Delta k_a/k_a$, a restoring force vector F_a acting upon pedestal A differs in its direction from that of a displacement vector z'_a as shown in Fig. 3. 1. Hence, the produced moment about Oz axis acts upon the foundation (the hatched parts in Fig. 1. 1). Pedestal inequality ε has no connection with the increase or decrease of total energy applied to an asymmetrical shaft system, because the foundation does not rotate.

3. 2. 1. *Statically unstable vibration*

In statically unstable regions in which a natural whirling frequency p coincides with an angular velocity of shaft ω, solutions of free vibration in respect to z and z_a are expressed in the following form which is obtained by putting $p=\omega$ in Table 1. 1.

$$\left.\begin{aligned} z&=Ae^{i\omega t}+ae^{-i\omega t}+Ce^{3i\omega t}+ce^{-3i\omega t}+Fe^{5i\omega t}+fe^{-5i\omega t}+He^{7i\omega t}+\cdots\\ z_a&=A_ae^{i\omega t}+a_ae^{-i\omega t}+C_ae^{3i\omega t}+c_ae^{-3i\omega t}+F_ae^{5i\omega t}+f_ae^{-5i\omega t}+H_ae^{7i\omega t}+\cdots \end{aligned}\right\} \tag{3.9}$$

By using equations (3.1) and (3.9), the term $(z'-z'_a)^2$ is expressed as

$$\begin{aligned} (z'-z'_a)^2&=\{(z-z_a)e^{-i\omega t}\}^2=\{(A-A_a)+(a-a_a)e^{-2i\omega t}+(C-C_a)e^{2i\omega t}\\ &+(c-c_a)e^{-4i\omega t}+(F-F_a)e^{4i\omega t}+(f-f_a)e^{-6i\omega t}+(H-H_a)e^{6i\omega t}+\cdots\}^2 \end{aligned} \tag{3.10}$$

When arithmetical means in the expanded equation (3.10) are calculated during a cycle $2\pi/\omega$, all time-varying terms $e^{2Ni\omega t}$ ($N=$ integers except zero) become zero, and they have no effect on the condition necessary for the occurrence of static instability. Therefore, the following constant terms may be taken into consideration as for the increase or decrease of total energy:

$$K = \text{Constant terms of } (z'-z'_a)^2$$
$$= (A-A_a)^2 + 2(a-a_a)(C-C_a) + 2(c-c_a)(F-F_a) + 2(f-f_a)(H-H_a) + \cdots \tag{3.11}$$

The first term in equation (3.11) solely affects the sign of equation (3.5), because all other terms except the first one are real numbers as seen from the right hand sides of equation (3.3). Equations (3.5) and (3.11) show the condition under which the mean value of total energy increases with time:

$$\mathrm{Im}[K] = \mathrm{Im}[(A-A_a)^2] < 0 \tag{3.12}$$

When a symbol arg (i. e., an argument of a complex number) is used, equation (3.12) is rewritten as

$$(2N-1)\pi < 2\arg(A-A_a) < 2N\pi \quad (N\text{: integer}) \tag{3.13}$$

The condition necessary for the occurrence of statically unstable vibration indicates that the constant term $(A-A_a)$ of $z'-z'_a$ in equation (3.10) must exist in the second or the fourth quadrant of a complex plane $z'-z'_a$.

3. 2. 2. *Dynamically unstable vibration*

Let natural whirling frequencies of the shaft be p_1 and p_2 $(0<p_2<\omega<p_1)$. In dynamically unstable regions, both amplitudes of frequencies p_1 and p_2 increase, and the following relation always holds:

$$\hat{p}_1 = 2\omega - p_1 = p_2, \quad p_1 + p_2 = 2\omega \tag{3.14}$$

Solutions of free vibration in respect to z and z_a are expressed in the following form:

$$\left.\begin{aligned} z &= \sum_{j=1}^{2} \{A_j e^{ip_j t} + a_j e^{-ip_j t} + C_j e^{i(2\omega+p_j)t} + c_j e^{-i(2\omega+p_j)t} + F_j e^{i(4\omega+p_j)t} \\ &\quad + f_j e^{-i(4\omega+p_j)t} + H_j e^{i(6\omega+p_j)t} + \cdots\} \\ z_a &= \sum_{i=1}^{2} \{A_{aj} e^{ip_j t} + a_{aj} e^{-ip_j t} + C_{aj} e^{i(2\omega+p_j)t} + c_{aj} e^{-i(2\omega+p_j)t} \\ &\quad + F_{aj} e^{i(4\omega+p_j)t} + f_{aj} e^{-i(4\omega+p_j)t} + H_{aj} e^{i(6\omega+p_j)t} + \cdots\} \end{aligned}\right\} \tag{3.15}$$

Using equations (3.1) and (3.15), $(z-z_a)^2$ is expressed as follows:

$$\begin{aligned} (z'-z'_a)^2 = [\sum_{j=1}^{2} \{&(A-A_a)_j e^{-i(\omega-p_j)t} + (a-a_a)_j e^{-i(\omega+p_j)t} + (C-C_a)_j e^{i(\omega+p_j)t} \\ &+ (c-c_a)_j e^{-i(3\omega+p_j)t} + (F-F_a)_j e^{i(3\omega+p_j)t} + (f-f_a)_j e^{-i(5\omega+p_j)t} \\ &+ (H-H_a)_j e^{i(5\omega+p_j)t} + \cdots\}]^2 \end{aligned} \tag{3.16}$$

When equation (3.16) is expanded by use of the relation (3.14), the terms including an exponential function do not affect the occurrence of dynamically unstable vibration, but only cause the torque T_r in equation (3.7) to change with time. Constant terms in equation (3.16) are calculated as follows:

$$K=\text{Constant terms of } (z'-z'_a)^2$$
$$=2(A-A_a)_1(A-A_a)_2+2(a-a_a)_1(C-C_a)_1+2(a-a_a)_2(C-C_a)_2$$
$$+2(c-c_a)_1(F-F_a)_1+2(c-c_a)_2(F-F_a)_2+2(f-f_a)_1(H-H_a)_1$$
$$+2(f-f_a)_2(H-H_a)_2+\cdots \tag{3.17}$$

All terms except the first one in equation (3.17) are real numbers, and they do not affect the sign of equation (3.5). Examining equations (3.5) and (3.17), the condition for the occurrence of dynamically unstable vibration is given by

$$\mathrm{Im}[K]=\mathrm{Im}[(A-A_a)_1(A-A_a)_2]<0 \tag{3.18}$$

Equation (3.18) indicates that the imaginary part of the complex product $(A-A_a)_1$ $(A-A_a)_2$ becomes negative. Thus:

$$(2N-1)\pi<\arg(A-A_a)_1+\arg(A-A_a)_2<2N\pi \tag{3.19}$$

The condition (3.19) means that an arithmetical mean β of the arguments of complex amplitudes $(A-A_a)_1$ and $(A-A_a)_2$ must exist in the second or the fourth quadrant of a complex plane.

Either when bearing pedestals A and B have no directional inequality ($\varepsilon=0$), or when ε is much less than Δ, the solutions of free vibration in regard to z and z_a can be represented only by the first term in the right hand side of equation (3.15). In view of the rotating coordinate systems O-$x'y'$ and O_a-$x'_a y'_a$ turning at an angular velocity ω, relative displacement $z'-z'_a$ between S and A is written as

$$z'-z'_a=\sum_{j=1}^{2}(A-A_a)_j e^{-i(\omega-p_j)t}=(A-A_a)_1 e^{i(p_1-\omega)t}+(A-A_a)_2 e^{-i(p_1-\omega)t} \tag{3.20}$$

Relative displacement $z'-z'_a$ is a vector sum of $(A-A_a)_1$ and $(A-A_a)_2$, each of which turns clockwise and counterclockwise as shown in Fig. 3. 2, and it describes an elliptic locus on a complex plane $z'-z'_a$. When the two rotating vectors meet as seen from equation (3.20), vector $z'-z'_a=\overrightarrow{OP}$ exists on the major axis of an ellipse, the length of which $|(A-A_a)_1|+|(A-A_a)|_2$. When the two rotating vector come in an opposite direction, vector $z'-z'_a=\overrightarrow{OQ}$ exists on the minor axis of an ellipse, the length of which is $|(A-A_a)_1|\sim|(A-A_a)_2|$ (Figure 3. 2 indicates the case in which $|(A-A_a)_1|>|(A-A_a)_2|$, and the elliptic locus moves in the arrow direction). The angle β between the major principal axis OP and the real axis $x'-x'_a$ is given by $\beta=\{\arg(A-A_a)_1+\arg(A-A_a)_2\}/2$. The condition (3.19) necessary for the occurrence of dynamically unstable vibration is that the major axis of the

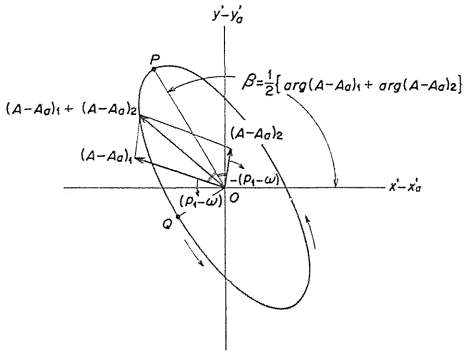

Fig. 3. 2 Elliptic locus described by relative displacement $z'-z_a'$, and vectors $(A-A_a)_1$ and $(A-A_a)_2$ just when $t=0$ for case of $|(A-A_a)_1|>|(A-A_a)_2|$.

ellipse must exist in the second or the fourth quadrant.

When the magnitude of pedestal inequality ε is not negligible, the vibrations with small amplitudes caused by both ε and Δ are added to the ellipse, and thus a locus $z'-z'_a$ expressed on a complex plane is very complicated [see Figs 3. 6(b) and 3. 8 (b)].

3. 3. *Conical Motion of a Rotor*

When the complex variables (2. 6) are used, the equations of motion (2. 5) for the rotating shaft[71] as shown in Fig. 2. 1 are expressed as follows:

$$\left.\begin{aligned} &I\ddot{\theta}_z-iI_p\omega\dot{\theta}_z+\delta(\theta_z-\theta_{az})=\Delta\delta e^{2i\omega t}(\bar{\theta}_z-\bar{\theta}_{az}) \\ &2m_a\ddot{z}_a+2\delta(\theta_z-\theta_{az})/l+2k_az_a=2\Delta k_a\bar{z}_a+2\Delta\delta e^{2i\omega t}(\bar{\theta}_z-\bar{\theta}_{az})/l \end{aligned}\right\} \tag{3. 21}$$

Equation (2. 2) is rewritten by the complex number, that is,

$$\theta_{az}=\theta_{ax}+i\theta_{ay}=-2z_a/l \tag{3. 22}$$

When the first and the second equations in equation (3. 21) are multiplied by $\dot{\bar{\theta}}_z$ and $\dot{\bar{z}}_a$, these two equations are added to each other, and equation (3. 22) is used, the following equation is obtained:

$$\begin{aligned} &I[\dot{\bar{\theta}}_z\ddot{\theta}_z]-I_p\omega[i\dot{\theta}_z\dot{\bar{\theta}}_z]+2m_a[\dot{\bar{z}}_a\ddot{z}_a]+\delta[(\theta_z-\theta_{az})(\dot{\bar{\theta}}_z-\dot{\bar{\theta}}_{az})]+2k_a[z_a\dot{\bar{z}}_a] \\ &=2\Delta k_a[\bar{z}_a\dot{\bar{z}}_a]+\Delta\delta[e^{2i\omega t}(\bar{\theta}_z-\bar{\theta}_{az})(\dot{\bar{\theta}}_z-\dot{\bar{\theta}}_{az})] \end{aligned} \tag{3. 23}$$

The kinetic energy T and the potential energy V in equation (2. 2) which are rewritten by using equation (2. 6) and the following complex variables

$$\left.\begin{aligned} &\theta'_z=\theta'_x+i\theta'_y=\theta_z e^{-i\omega t}, \quad \bar{\theta}'_z=\theta'_x-i\theta'_y=\bar{\theta}_z e^{i\omega t} \\ &\theta'_{az}=\theta'_{ax}+i\theta'_{ay}=\theta_{az}e^{-i\omega t}, \quad \bar{\theta}'_{az}=\theta'_{ax}-i\theta'_{ay}=\bar{\theta}_{az}e^{i\omega t} \end{aligned}\right\} \tag{3. 24}$$

are differentiated with respect to time t as follows:

$$\left.\begin{aligned} &\dot{T}=I\mathrm{Re}[\dot{\bar{\theta}}_z\ddot{\theta}_z]+(1/2)I_p\omega\mathrm{Im}[\theta_z\ddot{\bar{\theta}}_z]+2m_a\mathrm{Re}[\dot{\bar{z}}_a\ddot{z}_a] \\ &\dot{V}=\delta\mathrm{Re}[(\theta'_z-\theta'_{az})(\dot{\bar{\theta}}'_z-\dot{\bar{\theta}}'_{az})]-\Delta\delta\mathrm{Re}[(\theta'_z-\theta'_{az})(\dot{\theta}'_z-\dot{\theta}'_{az})] \\ &\qquad+2k_a\mathrm{Re}[z_a\dot{\bar{z}}_a]-2\Delta k_a\mathrm{Re}[z_a\dot{z}_a] \end{aligned}\right\} \tag{3. 25}$$

When relation (3. 24) is used, and the real part of equation (3. 23) is substituted into equation (3. 25), the increase in rate of total energy $\dot{T}+\dot{V}$ is derived as the following simplified relation similar to equation (3. 8):

$$\omega T_r=\dot{T}+\dot{V}=-\Delta\delta\omega\mathrm{Im}[(\theta'_z-\theta'_{az})^2]-\frac{1}{2}I_p\omega\mathrm{Im}[\bar{\theta}_z\ddot{\theta}_z] \tag{3. 26}$$

Torque T_r applied to the shaft end about the bearing center line AB is obtained from the equilibrium of moments in Fig. 3. 3 (a). Let us consider two parallel planes which make a small distance $z=\pm h/2$ from xy-plane as shown in Fig. 3. 3(a). Let the intersections of these two planes and the bearing center line AB be C and C', and let the intersections of these two planes and the tangent line

TT' to an asymmetrical shaft at the origin O be T and T'. The deflection angle of a shaft $\angle TOC = \angle TOC'$ is equal to $|\theta_z - \theta_{az}|$. Because of shaft asymmetry, a restoring moment M_t is expressed by a vector sum of a moment M_{t1} perpendicular to the TOC plane and a moment M_{t2} which is at right angle to tangent OT and exists in the TOC-plane. Strictly speaking, a vector M_t exists on the plane including the origin O and perpendicular to tangent OT as shown in Fig. 3. 3 (a). The same symbol M_t as Fig. 3. 3(a) is used in respect to the projectional vector of a vector M_t to the xy-plane in Fig. 3. 3 (b), because the inclination angle $\theta = |\theta_z|$ of tangent OT is a small quantity, the second order of which can be negligible. Components M'_{tx} and M'_{ty} of a restoring moment in x'- and y'-directions are expressed as follows:

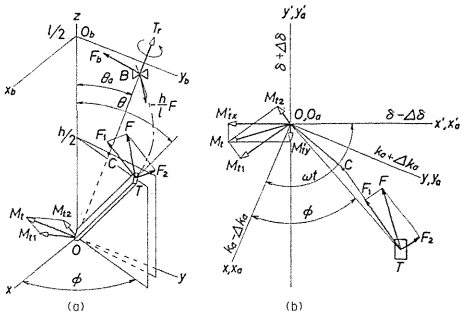

Fig. 3. 3 Shaft end torque T_r and restoring moment M_t.

$$M'_{tx} = (\delta + \Delta\delta)(\theta'_y - \theta'_{ay}), \quad M'_{ty} = -(\delta - \Delta\delta)(\theta'_x - \theta'_{ax}) \tag{3. 27}$$

Component M_{t1} of restoring moment M_t tends to decrease the deflection angle $|\theta_z - \theta_{az}|$ and, on the other hand, component M_{t2} encourages the whirling motion of a rotor. A restoring moment M_t in Fig. 3. 3(a) can be replaced by the equivalent restoring forces F and $-F$, which are at right angles to the tangent OT, and act on the two points T and T', respectively. Let F_2 and $-F_2$ be the perpendicular components of F and $-F$ to the $TOC(T'OC')$ plane, respectively. To maintain a constant angular velocity against the inertial couple balancing to a couple of F_2 and $-F_2$, torque T_r has to be applied to the shaft end. This torque T_r about AB line is equal to the OB component of a moment M_{t2}, and T_r is obtained from equation (3. 27) as follows:

$$T_r = -M'_{tx}(\theta'_x - \theta'_{ax}) - M'_{ty}(\theta'_y - \theta'_{ay}) = -\Delta\delta \mathrm{Im}[(\theta'_z - \theta'_{az})^2] \tag{3. 28}$$

Equation (3. 28) multiplied by ω becomes the first term on the right hand side of equation (3. 26). Take a time average of the second term $-I_p\omega \mathrm{Im}[\bar{\theta}_z\ddot{\theta}_z]/2$ of equation (3. 26);

$$-\frac{1}{2t_0} I_p\omega \int_t^{t+t_0} \mathrm{Im}[\bar{\theta}_z\ddot{\theta}_z]dt = -\frac{1}{2t_0} I_p\omega \Big[\mathrm{Im}(\bar{\theta}_z\dot{\theta}_z)\Big]_t^{t+t_0} \tag{3. 29}$$

When θ_z and θ_{az} are expressed by solutions of steady state free vibrations, an inclinational motion of the rotor returns to its original position after a certain time t_0, and thus term (3. 29) becomes zero. In the case of unstable vibration, since the inclination angle of the rotor θ_z gradually increases, and term (3. 29) does not become zero, a torque T_r applied at the shaft end is smaller than a torque given in equation (3. 28). Thus, the second term in equation (3. 26) has an effect on torque T_r in the unstable region, yet has no connection with the condition for the occurrence of unstable vibration. From the first term in the right hand side of equation (3. 26), the condition under which unstable vibration occurs

is obtained as:

$$-\Delta\delta\omega\mathrm{Im}[\text{Constant terms of } (\theta'_z-\theta'_{az})^2]>0 \tag{3.30}$$

If θ'_z, θ'_{az} and $\Delta\delta$ are replaced by z', z'_a and Δk, respectively, then the condition (3.30) for instability of the conical motion coincides with the condition for instability of the parallel motion. When similar solutions of free vibration to equation (3.9) are considered in respect to statically unstable vibration, and to equation (3.15) in respect to dynamically unstable one, the discussion of Section *3. 2* still holds. Equation (3.13) can be used as the condition in which the statically unstable vibration occurs, and equation (3.19) as the one in which the dynamically unstable one occurs.

3. 4. Solutions Obtained by Analog Computer and Condition Necessary for the Occurrence of Unstable Vibration

When the equations of motion (2.8) are rewritten by using equation (3.24), the real and imaginary parts of the equations of motion with respect to rotating coordinates θ'_z and θ'_{az} are obtained as follows:

$$\left.\begin{aligned}
\ddot{\theta}'_x&=(2-i_p)\omega\dot{\theta}'_y+(1-i_p)\omega^2\theta'_x-(1-\Delta)(\theta'_x-\theta'_{ax})\\
\ddot{\theta}'_y&=-(2-i_p)\omega\dot{\theta}'_x+(1-i_p)\omega^2\theta'_y-(1+\Delta)(\theta'_y-\theta'_{ay})\\
\ddot{\theta}'_{ax}&=2\omega\dot{\theta}'_{ay}+\omega^2\theta'_{ax}+(1/\sigma)\{-\kappa\theta'_{ax}+(1-\Delta)(\theta'_x-\theta'_{ax})\\
&\qquad+\kappa\varepsilon(\theta'_{ax}\cos 2\omega t-\theta'_{ay}\sin 2\omega t)\}\\
\ddot{\theta}'_{ay}&=-2\omega\dot{\theta}'_{ax}+\omega^2\theta'_{ay}+(1/\sigma)\{-\kappa\theta'_{ay}+(1+\Delta)(\theta'_y-\theta'_{ay})\\
&\qquad-\kappa\varepsilon(\theta'_{ax}\sin 2\omega t+\theta'_{ay}\cos 2\omega t)\}
\end{aligned}\right\} \tag{3.31}$$

Figure 3. 4 shows a simulation circuit from an analog computer which satisfies equation (3.31). Vibratory waves θ'_x, θ'_y, θ'_{ax}, θ'_{ay}, $\theta'_x-\theta'_{ax}$ and $\theta'_y-\theta'_{ay}$ are given by recorders 1, 2, 3, 4, 5 and 6. When i_p is adjusted to zoro in four potentiometers regarding i_p, vibratory waves x', y', x'_a, y'_a, $x'-x'_a$ and $y'-y'_a$ in Section *3. 2* are given by recorders 1~6. In order to investigate whether the conditions necessary for instability (3.13) and (3.19) are satisfied, output $\theta'_x-\theta'_{ax}$ and $\theta'_y-\theta'_{ay}$

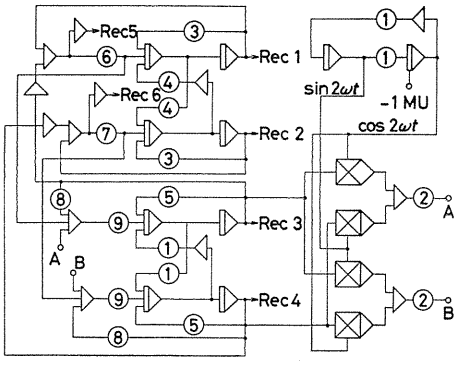

Fig. 3. 4 Simulation circuit for analog computer
Rec 1: θ'_x, Rec 2: θ'_y, Rec 3: θ'_{ax},
Rec 4: θ'_{ay}, Rec 5: $\theta'_x-\theta'_{ax}$,
Rec 6: $\theta'_y-\theta'_{ay}$
Potentiometers ①: 2ω, ②: $\kappa\varepsilon$,
③: $(1-i_p)\omega^2$, ④: $(2-i_p)\omega$, ⑤: ω^2,
⑥: $1-\Delta$, ⑦: $1+\Delta$, ⑧: κ, ⑨: $1/\sigma$.

should be put in the abscissa and the ordinate of an X–Y recorder.

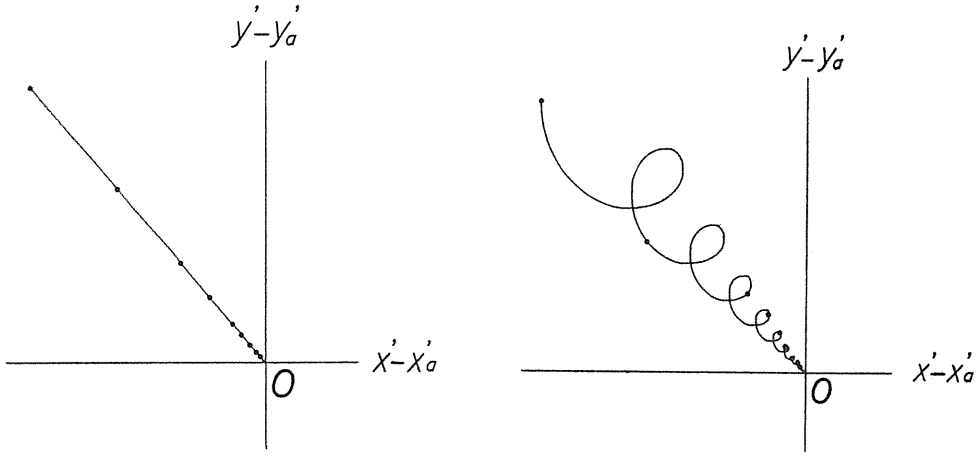

(a) $\varepsilon=0$ (b) $\varepsilon=0.2$

Fig. 3. 5 $\sigma=1$, $\kappa=1$, $i_p=0$, $\Delta=0.4$, $\omega=1.66$.

Figures 3. 5 (a) and (b) for $\varepsilon=0$ and 0. 2, respectively, show statically unstable examples of parallel motions, the parameters of which are $\sigma=1$, $\kappa=1$, $i_p=0$, $\Delta=0.4$ and $\omega=1.66$. The solid circles on the vibratory loci indicate a dimensionless time interval ($\Delta t=2$). In view of the rotating coordinate system, loci $z'-z'_a$ exists always in the second quadrant, and then the necessary condition (3. 13) for statical instability is satisfied. Because of $\varepsilon=0.2$, Fig. 3. 5 (b) shows that the terms with frequencies $\pm 2\omega$, $\pm 4\omega$, $\cdots$ are added to the straight motion resulting from the first term $(A-A_a)$ in equation (3. 10). Figures 3. 6 (a) and (b) show dynamically

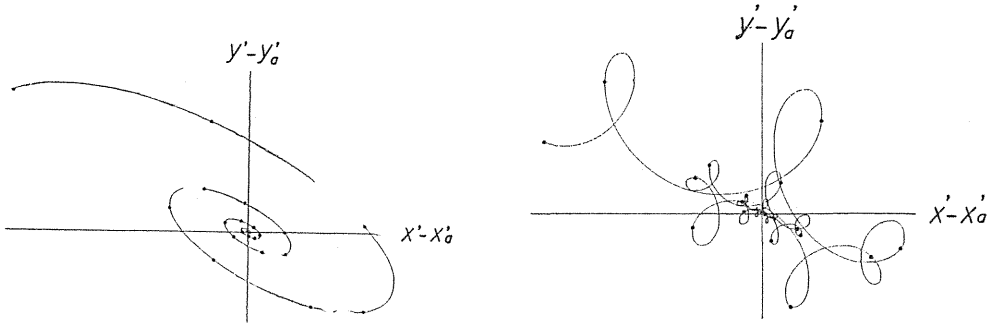

(a) $\varepsilon=0$ (b) $\varepsilon=0.2$

Fig. 3. 6 $\sigma=1$, $\kappa=1$, $i_p=0$, $\Delta=0.4$, $\omega=1.10$.

unstable examples in parallel motions for the same parameters as Fig. 3. 5 except that $\omega=1.10$. The locus of dynamically unstable vibration in Fig. 3. 6 (a) describes an ellipse which is composed of two rotating vectors, that is, one whirls at counterclockwise velocity $(p_1-\omega)>0$ with amplitude $|(A-A_a)_1|$ and the other

whirls at clockwise velocity $-(p_1-\omega)<0$ with amplitude $|(A-A_a)_2|$. Major and minor axes of this ellipse increase with time. The major axis of the ellipse always exists in the second and the fourth quadrants, and the remaining time at the second or the fourth quadrant is much longer than the one at the first or the third quadrant as seen by time marks ● on the locus. Thus the condition (3.19) necessary for the increase of the total energy $T+V$ is always satisfied. Figure 3. 6 (b) shows a complicated locus, since the waves of small amplitude with frequencies $\pm(\omega+p_1)$, $\pm(\omega+p_2)$, $\pm(3\omega+p_1)$, $\cdots$ overlap an elliptic locus of Fig. 3. 6 (a). In this case, the major axis of an ellipse composed of two rotating vectors moving in opposite directions with frequencies $\pm(p_1-\omega)$ exists in the second and the fourth quadrants, and the condition for instability is satisfied.

Figures. 3. 7 (a) and (b) for $\varepsilon=0$ and $\varepsilon=0.2$, respectively, show the loci for statical instability of conical motions, the parameters of which are $\sigma=1$, $\kappa=1$, $i_p=1.5$, $\Delta=0.4$ and $\omega=1.16$. Figures 3. 8 (a) and (b) show the loci of dynamically unstable vibration for the same parameters as Fig. 3. 7 except that $\omega=3.00$. Comparison of Fig. 3. 7 with Fig. 3. 5, or of Fig. 3. 8 with Fig. 3. 6, shows that the loci of conical motion on the $\theta'_z-\theta'_{az}$ plane have shapes very similar to the loci of parallel motion on the $z'-z'_a$ plane. This means that only the position and width of unstable regions change as the factor i_p changes remarkably from 0 to 2.

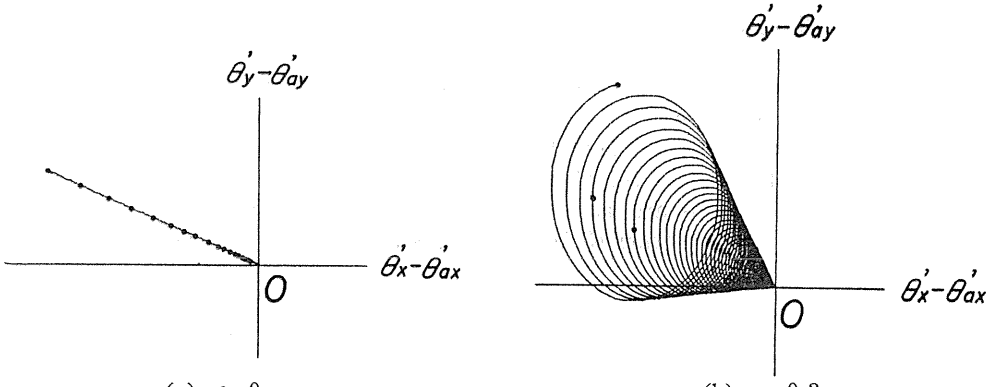

(a) $\varepsilon=0$ (b) $\varepsilon=0.2$

Fig. 3. 7 $\sigma=1$, $\kappa=1$, $i_p=1.5$, $\Delta=0.4$, $\omega=1.16$.

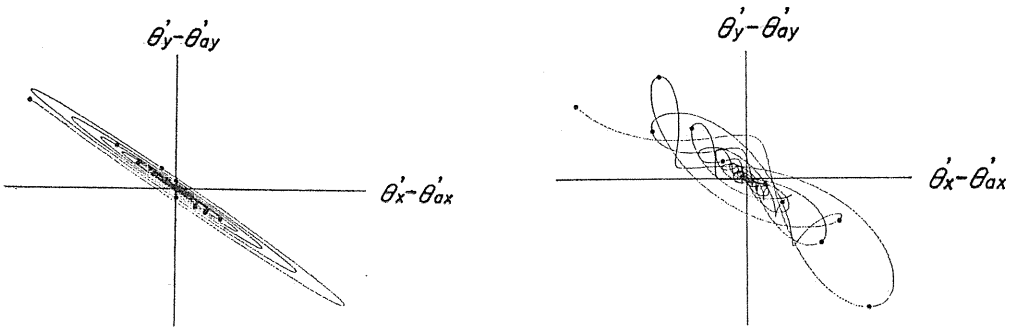

(a) $\varepsilon=0$ (b) $\varepsilon=0.2$

Fig. 3. 8 $\sigma=1$, $\kappa=1$, $i_p=1.5$, $\Delta=0.4$, $\omega=3.00$.

3. 5. *The Occurrence of Uustable Vibrations of Higher Order*

Solutions of free vibrations whirling at two natural frequencies p_1 and p_2, and whirling at many other natural frequencies caused by p_1 and p_2 vibrations are generally expressed as follows[70]:

$$
\begin{aligned}
z=\sum_{j=1}^{2}\{&A_j e^{ip_jt}+a_j e^{-ip_jt}+B_j e^{i(2\omega-p_j)t}+b_j e^{-i(2\omega-p_j)t}+C_j e^{i(2\omega+p_j)t}\\
&+c_j e^{-i(2\omega+p_j)t}+D_j e^{i(4\omega-p_j)t}+d_j e^{-i(4\omega-p_j)t}+F_j e^{i(4\omega+p_j)t}\\
&+f_j e^{-i(4\omega+p_j)t}+\cdots\}\\
z_a=\sum_{j=1}^{2}\{&A_{aj} e^{ip_jt}+a_{aj} e^{-ip_jt}+B_{aj} e^{i(2\omega-p_j)t}+b_{aj} e^{-i(2\omega-p_j)t}\\
&+C_{aj} e^{i(2\omega+p_j)t}+c_{aj} e^{-i(2\omega+p_j)t}+D_{aj} e^{i(4\omega-p_j)t}+d_{aj} e^{-i(4\omega-p_j)t}\\
&+F_{aj} e^{i(4\omega+p_j)t}+f_{aj} e^{-i(4\omega+p_j)t}+\cdots\}
\end{aligned}
\tag{3.32}
$$

A relative displacement $z'-z'_a$

$$
\begin{aligned}
z'-z'_a=\sum_{j=1}^{2}\{&(A-A_a)_j e^{-i(\omega-p_j)t}+(a-a_a)_j e^{-i(\omega+p_j)t}+(B-B_a)_j e^{i(\omega-p_j)t}\\
&+(b-b_a)_j e^{-i(3\omega-p_j)t}+(C-C_a)_j e^{i(\omega+p_j)t}+(c-c_a)_j e^{-i(3\omega+p_j)t}\\
&+(D-D_a)_j e^{i(3\omega-p_j)t}+(d-d_a)_j e^{-i(5\omega-p_j)t}+(F-F_a)_j e^{i(3\omega+p_j)t}\\
&+(f-f_a)_j e^{-i(5\omega+p_j)t}+\cdots\}
\end{aligned}
\tag{3.33}
$$

Table 3. 1 The terms of relative displacement $z'-z_a'$ in view of the rotating coordinate system and magnitudes of amplitudes.

Order of ε and Δ	Δ^0	Δ^1	Δ^2
ε^0	$(A-A_a)\exp\{-i(\omega-p)t\}$	$(B-B_a)\exp\{i(\omega-p)t\}$	
ε^1	$(a-a_a)\exp\{-i(\omega+p)t\}$	$(b-b_a)\exp\{-i(3\omega-p)t\}$ $(C-C_a)\exp\{i(\omega+p)t\}$	$(D-D_a)\exp\{i(3\omega-p)t\}$
ε^2		$(c-c_a)\exp\{-i(3\omega+p)t\}$	$(d-d_a)\exp\{-i(5\omega-p)t\}$ $(F-F_a)\exp\{i(3\omega+p)t\}$

is derived from equation (3. 32). Table. 3. 1 shows the order of magnitude for each amplitude of equation (3. 33). When term $(z'-z'_a)^2$ is calculated from equation (3. 33), and terms including up to the fourth order of ε and Δ are considered, there are 87 terms. Constant terms $2(A-A_a)_1(B-B_a)_1$, $2(A-A_a)_2(B-B_a)_2$, $2(a-a_a)_1(C-C_a)_1$ and $2(a-a_a)_2(C-C_a)_2$ are primarily included in these terms. However, these constant terms are always real numbers, and do not affect the sign of

$\mathrm{Im}[(z'-z_a')^2]$ of equation (3.7). Some terms in $(z'-z_a')^2$ may be constant in accordance with a combination of frequencies p_1, p_2 and ω. Table 3. 2 shows some

Table 3. 2 Examples of frequency combination which results a constant term of $(z'-z_a')^2$

Order of term	Term of $(z'-z_a')^2$	Relation between ω, p_1 and p_2
$\varepsilon^0\Delta^0$	$(A-A_a)_1{}^2\exp\{-2i(\omega-p_1)t\}$	$p_1=\omega$
	$(A-A_a)_2{}^2\exp\{-2i(\omega-p_2)t\}$	$p_2=\omega$
	$2(A-A_a)_1(A-A_a)_2\exp\{-i(2\omega-p_1-p_2)t\}$	$p_1+p_2=2\omega$
$\varepsilon^1\Delta^0$	$2(A-A_a)_1(a-a_a)_2\exp\{-i(2\omega-p_1+p_2)t\}$	$p_1-p_2=2\omega$
$\varepsilon^1\Delta^1$	$2(A-A_a)_1(b-b_a)_1\exp\{-2i(2\omega-p_1)t\}$	$p_1=2\omega$
	$2(A-A_a)_2(b-b_a)_2\exp\{-2i(2\omega-p_2)t\}$	$p_2=2\omega$
	$2(A-A_a)_1(b-b_a)_2\exp\{-i(4\omega-p_1-p_2)t\}$	$p_1+p_2=4\omega$
	$2(A-A_a)_2(b-b_a)_1\exp\{-i(4\omega-p_1-p_2)t\}$	$p_1+p_2=4\omega$
$\varepsilon^2\Delta^1$	$2(A-A_a)_1(c-c_a)_2\exp\{-i(4\omega-p_1+p_2)t\}$	$p_1-p_2=4\omega$
	$2(a-a_a)_2(b-b_a)_1\exp\{-i(4\omega-p_1+p_2)t\}$	$p_1-p_2=4\omega$
$\varepsilon^2\Delta^2$	$2(A-A_a)_1(d-d_a)_1\exp\{-2i(3\omega-p_1)t\}$	$p_1=3\omega$
	$(b-b_a)_1{}^2\exp\{-2i(3\omega-p_1)t\}$	$p_1=3\omega$
	$2(A-A_a)_2(d-d_a)_2\exp\{-2i(3\omega-p_2)t\}$	$p_2=3\omega$
	$(b-b_a)_2{}^2\exp\{-2i(3\omega-p_2)t\}$	$p_2=3\omega$
	$2(A-A_a)_1(d-d_a)_2\exp\{-i(6\omega-p_1-p_2)t\}$	$p_1+p_2=6\omega$
	$2(A-A_a)_2(d-d_a)_1\exp\{-i(6\omega-p_1-p_2)t\}$	$p_1+p_2=6\omega$
	$2(b-b_a)_1(b-b_a)_2\exp\{-i(6\omega-p_1-p_2)t\}$	$p_1+p_2=6\omega$

combinations of p_1, p_2 and ω under which unstable vibrations might occur. The amplitudes of these vibrations have a magnitude up to the order of $\varepsilon^2\Delta^2$. If imaginary parts of the constant terms in Table 3. 2 become negative, then the torque T_r in equation (3.7) becomes positive, and unstable vibrations occur. When free vibrations with small amplitudes are considered up to much higher order of small quantities ε and Δ, innumerable unstable regions occur. If a little damping force is applied to the system, the unstable regions disappear, since the magnitude of the negative damping coefficient m is very small in these unstable regions.

As an example of vibratory waves for unstable vibration of a higher order, Fig. 3. 9 (a) shows a vibratory solution derived by an analog computer, the parameters of which are $\sigma=0.1$, $\kappa=1$, $i_p=0$, $\varepsilon=0.8$, $\Delta=0.4$ and $\omega=1.111$. In Fig. 3. 9, a high frequency appeared on x- and x_a-components is $P_1=3.560$, and a low frequency on y- and y_a-components is $P_2=0.880$. In this case, the relation $P_1+P_2\simeq 4\omega$ holds, and this example of vibratory waves is an unstable vibration of the order $\varepsilon^1\Delta^1$ shown by Table 3. 2. A negative damping coefficient m obtained by vibratory waves is $m=0.023$.

Figure 3. 9 (b) shows the vibratory locus of the same unstable vibration of higher order as in Fig. 3. 9 (a) on the $z'-z_a'$ plane. The locus in Fig. 3. 9 (b) indicates the very complicated form, because two vibrations with two frequencies $P_1-\omega$ and $P_2-\omega$ overlap. Thus, the quadrant on a complex plane where the major axis of this locus exists is not clear.

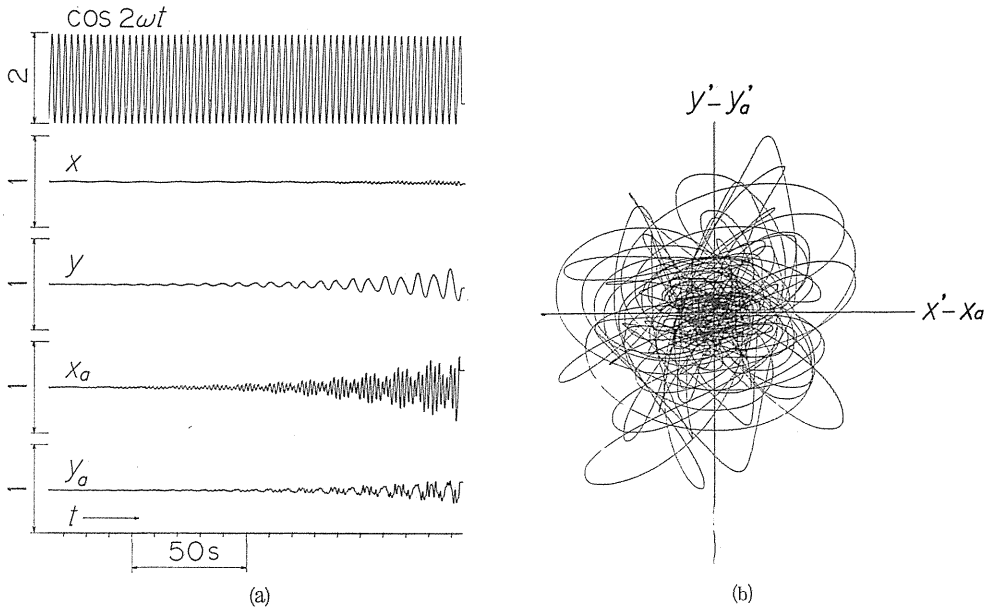

Fig. 3. 9 Vibratory waves of unstable vibration of higher order $\sigma=0.1$, $\kappa=1$, $i_p=0$, $\varepsilon=0.8$, $\Delta=0.4$, $\omega=1.111$, $P_1=3.560$, $P_2=0.880$.

3. 6. *Conclusions*

Conclusions obtained in this chapter may be summarized as follows:

(1) When an asymmetrical shaft is supported by asymmetrically flexible bearings, the necessary condition in which unstable vibrations occur is given by the relation $T_r>0$ of equation (3. 7) for the case in which a rotor moves in parallel to upper and lower pedestals. In the case of a conical motion, the necessary condition is expressed by $T_r>0$ of equation (3. 28).

(2) The condition for statically unstable vibrations is that a constant term $A-A_a$ in $z'-z'_a$ must exist in the second or the fourth quadrant of a complex plane.

(3) The condition for dynamically unstable vibrations is that an arithmetical mean of arguments of two vectors $(A-A_a)_1$ and $(A-A_a)_2$ turning to opposite directions must exist in the second or the fourth quadrant of a complex plane.

(4) These conditions necessary for the occurrence of unstable vibrations can be otherwise expressed that a moment about the bearing center line acted upon by a restoring force (or a component in the direction of bearing center line of a restoring moment) must be externally applied to the shaft end.

(5) It is ascertained that all solutions of unstable vibrations obtained by an analog computer satisfy the condition necessary for the occurrence of unstable vibrations.

(6) When the terms with a higher order of small quantities ε and Δ are considered, a number of very narrow unstable regions can be made to occur, and the examples of vibratory solutions derived by an analog computer are shown.

4. Influence of Unequal Pedestals Stiffness on the Unstable Regions and Mechanism for Occurrence of Unstable Vibrations of an Asymmetrical Rotor[73, 74]

4. 1. *Introduction*

The rotor which has two different principal moments of inertia I_1 and I_2 about the axes perpendicular to the rotating axis, is called an asymmetrical rotor[57]. A few papers[56, 61~63] are reported on the unstable vibrations of a shaft having an asymmetrical rotor, both ends of which are supported by flexible pedestals with a directional inequality in stiffness. These studies concern the unstable vibration of an overhung shaft with an asymmetrical rotor[56], an asymmetrical rotor mounted the shaft with the statically directional inequality in stiffness[61], an asymmetrical rotor with a uniformly distributed mass supported by massless pedestals[62], and the case that both pedestals are rigid in the longitudinal direction of the pedestal but flexible only in its lateral direction[63] (i. e., directional inequality of pedestal rigidity $\varepsilon=1$).

This chapter deals with conical motions of an asymmetrical rotor, the shaft ends of which are supported by flexible pedestals, each with a directional inequality in stiffness $\varepsilon=0\sim1$ and a concentrated mass. The position, width and number of these unstable regions are approximately obtained by a similar analysis to Chapter 1[70] and Chapter 2[71]. The approximate result in this case coincides well with the vibratory solutions obtained by an analog computer. The conditions under which unstable vibrations occur, just as input energy into the rotating shaft system tends to increase the whirling amplitudes of the shaft, are clearly given. The solutions obtained by an analog computer are found to satisfy these conditions.

4. 2. *Equations of Motion and Frequency Equation*

4. 2. 1. *Equations of motion*

Rotor inclination and lateral displacement are not interconnected in a rotating shaft system shown in Fig. 4. 1, because an asymmetrical rotor is mounted on the midpoint of shaft S. This chapter only deals with the conical motions of an asymmetrical rotor. Let O-xy be a stationary rectangular coordinate system, z-axis of which coincides with a bearing center line O_aO_b in equilibrium. Eulerian angles θ, ϕ and ψ as shown in Fig. 4. 1 (a) denote the angular position of a rectangular coordinate system S-XYZ which consists of three principal axes of inertia passing through the rotor center S. The principal axis of inertia SZ coincides with a bearing center line Oz in an equilibrium state, because the rotor has no static unbalance and dynamic one. The x_a- and x_b-axes are parallel to x-axis, and also y_a- and y_b-axes are parallel to y-axis. Let us consider that the upper and lower pedestals move symmetrically to the origin O, that is, $x_a=-x_b$ and $y_a=-y_b$. The upper and lower flexible pedestals B, A shown in Fig. 4. 1 (b) are dynamically alike, i. e., pedestals A and B possess the equivalent concentrated masses m_a and m_b ($m_a=m_b$), and the directional difference in stiffness $k_a\pm\Delta k_a$ and $k_b\pm\Delta k_b$ ($k_a=k_b$, $\Delta k_a=\Delta k_b$). Mass of the asymmetrical rotor is m_0, and principal moments of inertia about axes SX, SY and SZ are I_1, I_2 and I_p ($I_2<I_1$), respectively. Let θ_x and θ_y be the projectional angles of rotor inclination $\theta=\angle ZSz$ to xz- and

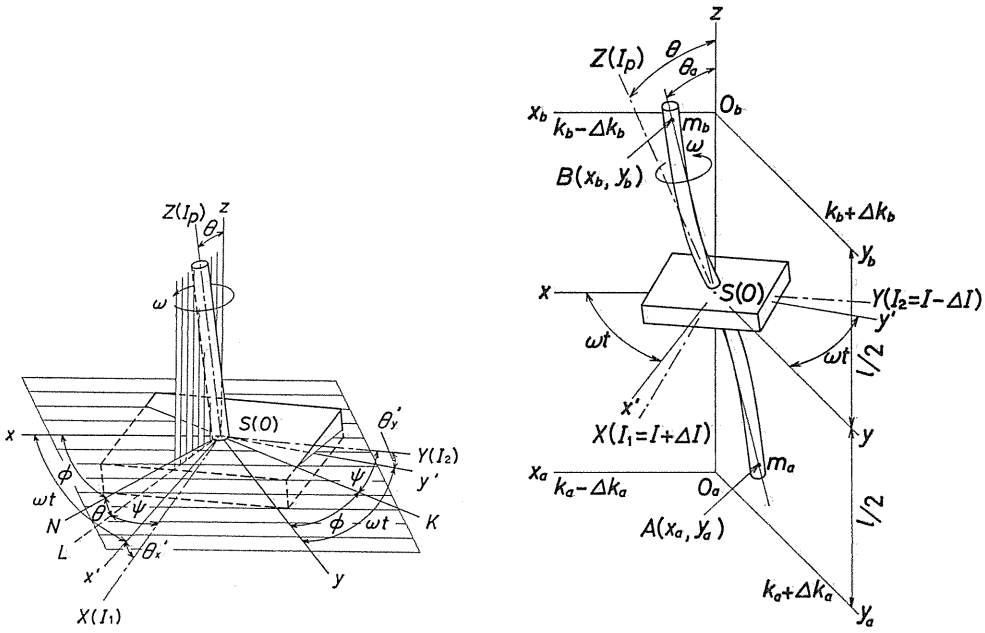

(a) (b)

Fig. 4. 1 An asymmetrical rotor and Eulerian angles θ, ϕ, ψ.

yz-planes, respectively, and let θ_{ax} and θ_{ay} be the projectional angles of the inclination $\theta_a=\angle BSz$ of the bearing center line AB to xz- and yz-planes. A unit deflectional angle of shaft $\angle ZSB$ yields a restoring moment δ. The total kinetic energy T and the potential energy V of this system are expressed as follows[57]:

$$\left.\begin{aligned} 2T &= I_p\{\dot{\theta}^2+\dot{\theta}(\dot{\theta}_x\theta_y-\theta_x\dot{\theta}_y)\}+I(\dot{\theta}_x^2+\dot{\theta}_y^2) \\ &\quad -\Delta I\{(\dot{\theta}_x^2-\dot{\theta}_y^2)\cos 2\theta+2\dot{\theta}_x\dot{\theta}_y\sin 2\theta\}+2m_a(\dot{x}_a^2+\dot{y}_a^2) \\ 2V &= \delta\{(\theta_x-\theta_{ax})^2+(\theta_y-\theta_{ay})^2\}+2(k_a-\Delta k_a)x_a^2+2(k_a+\Delta k_a)y_a^2 \end{aligned}\right\} \quad (4.1)$$

where

$$\theta=\phi+\psi, \quad I=(I_1+I_2)/2, \quad \Delta I=(I_1-I_2)/2 \quad (4.2)$$

Θ is rotational angle of shaft, and ΔI is inertia asymmetry of rotor. When equation (4.1) is substituted into Lagrange's equation, and the second order terms of small quantities are neglected, the equation of motion in regard to Θ is obtained as

$$\dot{\theta}=\omega=\text{Constant}, \quad \theta=\omega t \quad (4.3)$$

The equations of motion regarding θ_x, θ_y, x_a and y_a are obtained as follows:

$$\left.\begin{aligned}
&I\ddot{\theta}_x+I_p\omega\dot{\theta}_y+\delta(\theta_x-\theta_{ax})=\Delta I\frac{\mathrm{d}}{\mathrm{d}t}(\dot{\theta}_x\cos 2\omega t+\dot{\theta}_y\sin 2\omega t)\\
&I\ddot{\theta}_y-I_p\omega\dot{\theta}_x+\delta(\theta_y-\theta_{ay})=\Delta I\frac{\mathrm{d}}{\mathrm{d}t}(\dot{\theta}_x\sin 2\omega t-\dot{\theta}_y\cos 2\omega t)\\
&m_a\ddot{x}_a+(k_a-\Delta k_a)x_a+\delta(\theta_x-\theta_{ax})/l=0\\
&m_a\ddot{y}_a+(k_a+\Delta k_a)y_a+\delta(\theta_y-\theta_{ay})/l=0
\end{aligned}\right\}\quad(4.4)$$

Use equations (2.2) and (2.6), add the first equation of equation (4.4) to the second equation multiplied by i, and also add the third equation to the fourth equation multiplied by i; then the following equations are obtained:

$$\left.\begin{aligned}
&I\ddot{\theta}_z-iI_p\omega\dot{\theta}_z+\delta(\theta_z-\theta_{az})=\Delta I\frac{\mathrm{d}}{\mathrm{d}t}(\dot{\bar{\theta}}_z\mathrm{e}^{2i\omega t})\\
&m_al^2\ddot{\theta}_{az}+k_al^2\theta_{az}-\Delta k_al^2\bar{\theta}_{az}-2\delta(\theta_z-\theta_{az})=0
\end{aligned}\right\}\quad(4.5)$$

For simplicity, ε in equation (1.6), dimensionless quantities (2.7), and the following dimensionless one are introduced:

$$\Delta I/I=\Delta_0 \tag{4.6}$$

Hereafter, the primes of the dimensionless quantities are omitted, and the dots over the dimensionless ones mean the differential coefficient with respect to t'. The equations of motion for dimensionless quantities are then given as:

$$\left.\begin{aligned}
&\ddot{\theta}_z-ii_p\omega\dot{\theta}_z+\theta_z-\theta_{az}=\Delta_0\frac{\mathrm{d}}{\mathrm{d}t}(\dot{\bar{\theta}}_z\mathrm{e}^{2i\omega t})\\
&\sigma\ddot{\theta}_{az}+(1+\kappa)\theta_{az}-\theta_z=\kappa\varepsilon\bar{\theta}_{az}
\end{aligned}\right\}\quad(4.7)$$

4. 2. 2. Frequency equation

The solutions of free vibration (2.9) is substituted into the equations of motion (4.7), and the determinant of the 10th order consisting of the coefficients of complex amplitudes A, A_a, $\bar{a}$, $\bar{a}_a$, $\bar{B}$, $\bar{B}_a$, b, b_a, C and C_a, is put equal to zero, that is,

$$F=\begin{vmatrix}
H_1(p) & -1 & 0 & 0 & -\Delta_0 p\hat{p} & 0 & 0 & 0 & 0 & 0\\
-1 & G(p) & 0 & -\kappa\varepsilon & 0 & 0 & 0 & 0 & 0 & 0\\
0 & 0 & H_1(-p) & -1 & 0 & 0 & 0 & 0 & \Delta_0 p(2\omega+p) & 0\\
0 & -\kappa\varepsilon & -1 & G(-p) & 0 & 0 & 0 & 0 & 0 & 0\\
-\Delta_0 p\hat{p} & 0 & 0 & 0 & H_1(\hat{p}) & -1 & 0 & 0 & 0 & 0\\
0 & 0 & 0 & 0 & -1 & G(\hat{p}) & 0 & -\kappa\varepsilon & 0 & 0\\
0 & 0 & 0 & 0 & 0 & 0 & H_1(-\hat{p}) & -1 & 0 & 0\\
0 & 0 & 0 & 0 & 0 & -\kappa\varepsilon & -1 & G(-\hat{p}) & 0 & 0\\
0 & 0 & \Delta_0 p(2\omega+p) & 0 & 0 & 0 & 0 & 0 & H_1(2\omega+p) & -1\\
0 & 0 & 0 & 0 & 0 & 0 & 0 & 0 & -1 & G(2\omega+p)
\end{vmatrix}=0$$

Expanding this determinant, a frequency equation is derived as the following simple form:

$$F=f_1(2\omega+p)\Phi_1(p)\Phi_1(\hat{p})-\Delta_0^2\{(p\hat{p})^2f_1(2\omega+p)k_1(p)k_1(\hat{p})$$
$$+(-p)^2(2\omega+p)^2G(2\omega+p)\Phi_1(\hat{p})k_1(-p)\}$$
$$+\Delta_0^4\{p^2\hat{p}(2\omega+p)\}^2G(2\omega+p)k_1(\hat{p})\{G(p)G(-p)-\kappa^2\varepsilon^2\}=0 \qquad (4.8)$$

where $H_1(p)$, $G(p)$, $f_1(p)$ and $\Phi_1(p)$ are defined by equations (1.11), (2.11) and (2.13), and $k_1(p)$ is defined as follows:

$$k_1(p)=f_1(-p)G(p)-\kappa^2\varepsilon^2H_1(-p) \qquad (4.9)$$

4. 3. *Occurrence of Unstable Vibrations, and the Position, Width and Number of Unstable Regions*

4. 3. 1. *Case of a small directional inequality of pedestal stiffness*

The following relation[57] holds between the principal moments of inertia I_1, I_2 and I_p for an asymmetrical rotor:

$$I_1-I_2\leqq I_p\leqq I_1+I_2 \quad (2\Delta_0\leqq i_p\leqq 2)$$

When ε^2 is smaller than Δ_0, and terms including ε^2 are neglected, the frequency equation (4.8) is approximated as follows:

$$F\simeq f_1(-\hat{p})F_1(p)F_1(-p)=0 \qquad (4.10)$$

The term $f_1(-\hat{p})$ in equation (4.10) does not contain Δ_0 and has no relation to the occurrence of unstable vibrations. Because the equation

$$F_1(p)=f_1(p)f_1(\hat{p})-\Delta_0^2(p\hat{p})^2G(p)G(\hat{p})=0 \qquad (4.11)$$

and the equation $F_1(-p)=0$ in equation (4.10) have symmetrical roots with respect to the axis of the abscissa $p=0$ in the ω, p plane, we may consider equation (4.11) alone. Four real roots derived from $f_1(p)=0$ are defined as p_i ($i=1, 2, 3, 4$), and two roots derived from $G(p)=0$ are defined as p_{Gi} ($i=1, 2$). For parameters $\sigma=1$, $\kappa=1$, $\varepsilon=0$ and $i_p=0.8$, the roots p_i and $\hat{p}_i$, and p_{Gi} and $\hat{p}_{Gi}$ are shown by solid lines and dotted lines on the $p-\omega$ diagram of Fig. 4.2, respectively. The real roots p derived from equation (4.11) may exist in the unhatched area where the sign of $f_1(p)f_1(\hat{p})G(p)G(\hat{p})$ is positive. Unstable regions are restricted in the neighbourhood of the four intersections C_1, C_2, D_1 and D_2 where the curves $f_1(p)=0$ and $f_1(\hat{p})=0$ cross each other and the real roots p separate right and left. When inertia asymmetry of rotor Δ_0 is assumed to be small, the coordinate near the intersecting points C_1, C_2, D_1 and D_2 in Fig. 4.2 may be put as

$$\omega=\omega_{ij}+\xi, \quad p=p_i+\eta_i \qquad (4.12)$$

The frequency equation (4.11) is expanded by equation (4.12) in Taylor's series at these intersections. If small quantities Δ_0, ξ and η_i are counted to the second order, the frequency equation becomes as follows:

$$F_1 \simeq \left\{\left(\frac{\partial f_1}{\partial p}\right)_i \eta_i + \left(\frac{\partial f_1}{\partial \omega}\right)_i \xi\right\}\left\{\left(\frac{\partial \hat{f}_1}{\partial p}\right)_i \eta_i + \left(\frac{\partial \hat{f}_1}{\partial \omega}\right)_i \xi\right\} - \Delta_0^2 (p\hat{p})_i^2 (G\hat{G})_i = 0 \quad (4.13)$$

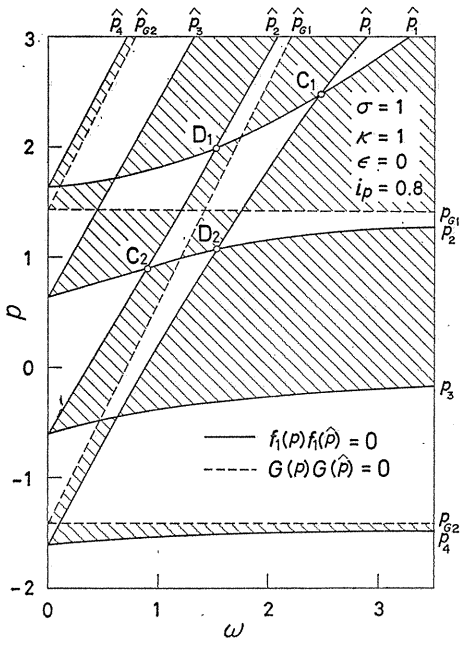

Fig. 4. 2 $p-\omega$ diagram ($\varepsilon=0$).

Equation (4. 13) is reduced to a quadratic equation for η_i, and the solutions for this equation are obtained as follows:

$$\eta_i = \frac{1}{2}\left[-\left\{\frac{(\partial f_1/\partial \omega)_i}{(\partial f_1/\partial p)_i} + \frac{(\partial \hat{f}_1/\partial \omega)_i}{(\partial \hat{f}_1/\partial p)_i}\right\}\xi \right.$$
$$\left. \pm\sqrt{\left\{\frac{(\partial f_1/\partial \omega)_i}{(\partial f_1/\partial p)_i} - \frac{(\partial \hat{f}_1/\partial \omega)_i}{(\partial \hat{f}_1/\partial p)_i}\right\}^2 \xi^2 + \frac{4\Delta_0^2 (p\hat{p})_i^2 (G\hat{G})_i}{(\partial f_1/\partial p)_i (\partial \hat{f}_1/\partial p)_i}}\right] \quad (4.14)$$

When a square root in equation (4. 14) becomes imaginary, the root η_i becomes a complex number, and an unstable vibration occurs. A limiting value ξ_0 of the unstable region $-|\xi_0|<\xi<|\xi_0|$ is obtained as follows:

$$\xi_0 = \frac{\pm 2\Delta_0 \sqrt{-(p\hat{p})_i^2 (G\hat{G})_i / (\partial f_1/\partial p)_i (\partial \hat{f}_1/\partial p)_i}}{|\{(\partial f_1/\partial \omega)_i/(\partial f_1/\partial p)_i\} - \{(\partial \hat{f}_1/\partial \omega)_i/(\partial \hat{f}_1/\partial p)_i\}|} \quad (4.15)$$

The negative damping coefficient m and its maximum value $m_{\max}$ become

$$m = m_{\max}\sqrt{1-(\xi/\xi_0)^2}, \quad m_{\max} = \Delta_0 \sqrt{-(p\hat{p})_i^2 (G\hat{G})_i \Big/ \left(\frac{\partial f_1}{\partial p}\right)_i \left(\frac{\partial \hat{f}_1}{\partial p}\right)_i} \quad (4.16)$$

When the asymmetry of shaft stiffness Δ and symbol g_1 is replaced for Δ_0 and

p^2G, equations (4.15) and (4.16) coincide with equation (2.33) which gives ξ_0 and m_{max} of an asymmetrical shaft for the case in which $\varepsilon \ll 1$.

4. 3. 2. Case of a not small directional inequality of pedestal stiffness

The fifth equation $\Phi_1(p)=0$ in equation (2.13) is a frequency equation for the case that $\Delta_0=0$ and $\varepsilon \neq 0$. When ε is not small, unstable vibrations occur in the neighbourhood where roots p_i $(i=1\sim8)$ derived from $\Phi_1(p)=0$ and roots $\hat{p}_i$ derived from $\Phi_1(\hat{p})=0$ cross each other on the ω, p plane in Fig. 4.3. The higher-order terms smaller than Δ_0^4 and $\Delta_0^2\Phi_1(\hat{p})$ in the frequency equation (4.8) are neglected, and then the following equation is derived:

$$F \simeq f_1(2\omega+p)F_3(p)=0 \qquad (4.17)$$

where the term $f_1(2\omega+p)$ without Δ_0 has no relation to unstable vibrations, and

$$F_3(p)=\Phi_1(p)\Phi_1(\hat{p}) - \Delta_0^2(p\hat{p})^2k_1(p)k_1(\hat{p})=0 \qquad (4.18)$$

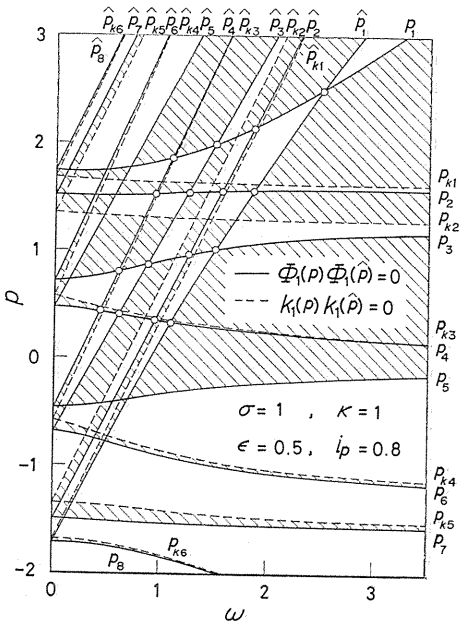

Fig. 4. 3 $p-\omega$ diagram ($\varepsilon=0.5$).

Figure 4.3 shows the $p-\omega$ diagram for $\sigma=1$, $\kappa=1$, $\varepsilon=0.5$ and $i_p=0.8$. In Fig. 4.3, p_{ki} $(i=1\sim6)$ are defined as the roots derived from $k_1(p)=0$. Occurrence of unstable vibrations is limited in the neighbourhood of 16 intersections shown by the ○ indication in Fig. 4.3 where the roots p_i derived from $\Phi_1(p)=0$ and roots $\hat{p}_i$ from $\Phi_1(\hat{p})=0$ cross each other, because a real root p derived from equation (4.18) may exist in the unhatched area where $\Phi_1(p)\Phi_1(\hat{p})k_1(p)k_1(\hat{p})$ is positive. The values ξ_0 and m_{max} are derived as follows:

$$\eta_i=\frac{1}{2}\left[-\left\{\frac{(\partial\Phi_1/\partial\omega)_i}{(\partial\Phi_1/\partial p)_i}+\frac{(\partial\hat{\Phi}_1/\partial\omega)_i}{(\partial\hat{\Phi}_1/\partial p)_i}\right\}\xi \pm\sqrt{\left\{\frac{(\partial\Phi_1/\partial\omega)_i}{(\partial\Phi_1/\partial p)_i}-\frac{(\partial\hat{\Phi}_1/\partial\omega)_i}{(\partial\hat{\Phi}_1/\partial p)_i}\right\}^2\xi^2+\frac{4\Delta_0^2(p\hat{p})_i^2(k_1\hat{k}_1)_i}{(\partial\Phi_1/\partial p)_i(\partial\hat{\Phi}_1/\partial p)_i}}\right] \qquad (4.19)$$

$$\left.\begin{aligned}\xi_0&=\frac{\pm2\Delta_0\sqrt{-(p\hat{p})_i^2(k_1\hat{k}_1)_i/(\partial\Phi_1/\partial p)_i(\partial\hat{\Phi}_1/\partial p)_i}}{|\{(\partial\Phi_1/\partial\omega)_i/(\partial\Phi_1/\partial p)_i\}-\{(\partial\hat{\Phi}_1/\partial\omega)_i/(\partial\hat{\Phi}_1/\partial p)_i\}|}\\ m_{max}&=\Delta_0\sqrt{-(p\hat{p})_i^2(k_1\hat{k}_1)_i/(\partial\Phi_1/\partial p)_i(\partial\hat{\Phi}_1/\partial p)_i}\end{aligned}\right\} \qquad (4.20)$$

The width of the unstable region $2|\xi_0|$, and the negative damping coefficient m given by equation (4.20) are shown by solid lines in Figs. 4. 4 (a) and (b) for $\sigma=1$, $\kappa=1$, $\Delta_0=0.2$, $i_p=0.8$, and $\varepsilon=0.1$ and 0.5. Vertical dot-dash lines in Fig. 4. 4 show the rotating speed ω_{ij} of intersections between p_i and $\hat{p}_j$ in Fig. 4. 3. Because the width of unstable region $2|\xi_0|$ is fairly wide for $\omega_{11}=2.489$ ($\varepsilon=0.1$), and for $\omega_{11}=2.491$ ($\varepsilon=0.5$) in Fig. 4. 4, approximation (4.20) assuming that ξ is enough small

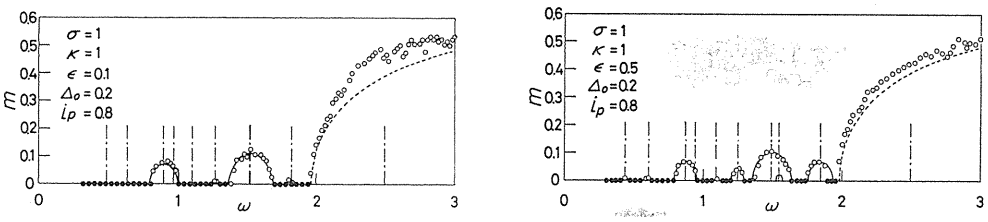

(a) $\varepsilon=0.1$ (b) $\varepsilon=0.5$.

Fig. 4. 4 m$-\omega$ diagram (○, ●: unstable and stable solutions by analog computer).

cannot apply. Thus, the imaginary part m of complex roots p obtained by solving the frequency equation (4.18) is shown by dotted lines in Fig. 4. 4. The circles in Fig. 4. 4 show the value m obtained by an analog computer ALS-200X. Solid and blank circles indicate stable solutions ($m=0$) and unstable ones ($m>0$), respectively. The solid and dotted lines agree well with the circles derived by an analog computer. When the directional inequality of pedestal ε increases, the unstable regions near the four intersecting points C_1, C_2, D_1 and D_2 in Fig. 4. 2 split up into many unstable regions as shown in Fig. 4. 4.

Figure 4. 5 shows how the unstable regions change with the coefficient of the gyroscopic term $i_p=0.4\sim2$ for $\sigma=1$, $\kappa=1$, $\varepsilon=0.5$ and $\Delta_0=0.2$. Solid lines are given by equation (4.20), and dotted lines by the frequency equation (4.18). Vertical dot-dash lines in Fig. 4. 5 show the abscissa ω_{ij} of the intersection of p_i and $\hat{p}_j$ in Fig. 4. 3, where unstable vibrations may occur. The circles in Fig. 4. 5 are derived from the analog computer solutions, and the rotating speed between the two ○ indications shows the unstable region for a certain value of i_p.

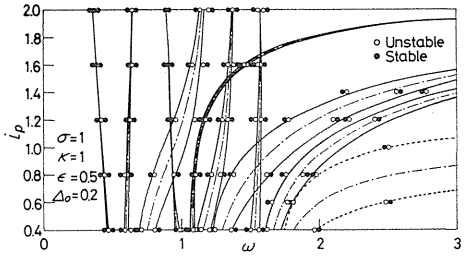

Fig. 4. 5 $i_p-\omega$ diagram ($i_p=0.4\sim2$).

For the conical motion of a rotor mounted on an asymmetrical shaft which is supported by flexible pedestals with a directional inequality in stiffness (cf. Chapter 2), unstable regions near the intersecting points C_2, D_1 and D_2 disappear on a curve in $i_p-\omega$ diagram where the relation $i_p\omega=\sqrt{\kappa/\sigma}$ holds, but this tendency is not shown by Fig. 4. 5. When the value $(p\hat{p})^2(G\hat{G})$ is equal to zero, the relations $\xi_0=0$ and $m_{\max}=0$ are obtained from equation (4.15) and (4.16). Both values $f_1(p)$ and $f_1(\hat{p})$ are not equal to zero simultaneously at the point where $(p\hat{p})^2(G\hat{G})$

$=0$ is satisfied. Namely, the relations $f_1(p)=\kappa$ and $f_1(p)=H_1G-1=-1$ hold on the straight lines $p=0$ and $p=p_{Gi}$ satisfying $G=0$, respectively, and thus $f_1(p)$ is never equal to zero. When the value $\hat{p}^2\hat{G}$ equal to zero, the relation $f_1(\hat{p})\neq 0$ is obtained by replacing p and G with $\hat{p}$ and $\hat{G}$, respectively. Consequently, a point where three values $(p\hat{p})^2G\hat{G}$, $f(p)$ and $f(\hat{p})$ are simultaneously equal to zero, does not exist on the $p-\omega$ diagram.

4. 4. *Mechanism for the Occurrence of Unstable Vibrations*[73]

4. 4. 1. *Increase in rate of total energy*

The increase in rate of kinetic energy T and potential energy V is given by differentiating equation (4. 1) with respect to time t and using equation (4. 3):

$$\left.\begin{aligned}2\dot{T}&=I_p\omega(\ddot{\theta}_x\theta_y-\theta_x\ddot{\theta}_y)+2I(\dot{\theta}_x\ddot{\theta}_x+\dot{\theta}_y\ddot{\theta}_y)\\&\quad-\Delta I\frac{\mathrm{d}}{\mathrm{d}t}\{(\dot{\theta}_x^2-\dot{\theta}_y^2)\cos 2\omega t+2\dot{\theta}_x\dot{\theta}_y\sin 2\omega t\}+4m_a(\dot{x}_a\ddot{x}_a+\dot{y}_a\ddot{y}_a)\\2\dot{V}&=2\delta\{(\theta_x-\theta_{ax})(\dot{\theta}_x-\dot{\theta}_{ax})+(\theta_y-\theta_{ay})(\dot{\theta}_y-\dot{\theta}_{ay})\}\\&\quad+4k_a(x_a\dot{x}_a+y_a\dot{y}_a)-4\Delta k_a(x_a\dot{x}_a-y_a\dot{y}_a)\end{aligned}\right\}\quad(4.21)$$

Equation (4. 21) is rewritten by use of the relations (3. 24) between inclinational angles θ_z, θ_{az} in view of the stationary coordinate system O-xy and angles θ'_z, θ'_{az} in view of the rotating coordinate system O-$x'y'$:

$$\left.\begin{aligned}2\dot{T}&=I_p\omega\mathrm{Im}[\theta_z\ddot{\bar{\theta}}_z]+2I\mathrm{Re}[\dot{\bar{\theta}}_z\ddot{\theta}_z]-\Delta I\frac{\mathrm{d}}{\mathrm{d}t}\{\mathrm{Re}[\dot{\theta}_z'^2]\\&\quad-2\omega\mathrm{Im}[\theta'_z\dot{\theta}'_z]-\omega^2\mathrm{Re}[\theta_z'^2]\}+m_al^2\mathrm{Re}[\dot{\bar{\theta}}_{az}\ddot{\theta}_{az}]\\2\dot{V}&=2\delta\mathrm{Re}[(\theta_z-\theta_{az})(\dot{\bar{\theta}}_z-\dot{\bar{\theta}}_{az})]+k_al^2\mathrm{Re}[\theta_{az}\dot{\bar{\theta}}_{az}]-\Delta k_al^2\mathrm{Re}[\theta_{az}\dot{\theta}_{az}]\end{aligned}\right\}\quad(4.22)$$

When the first equation in equation (4. 5) is multiplied by $2\dot{\bar{\theta}}_z$, the second equation by $\dot{\bar{z}}_a$, and the real parts are substituted into equation (4. 22), the increase in rate of total energy $\dot{T}+\dot{V}$ is given as follows:

$$\dot{T}+\dot{V}=-\Delta I\omega\mathrm{Im}[(-\omega\theta'_z+i\dot{\theta}'_z)^2]-\frac{1}{2}I_p\omega\mathrm{Im}[\bar{\theta}_z\ddot{\theta}_z]\qquad(4.23)$$

Because torque T_r applied to the shaft end is a generalized force with respect to rotation angle Θ, the application of equation (4. 1) to Lagrange's equation of motion gives the following:

$$T_r=\frac{\mathrm{d}}{\mathrm{d}t}\left(\frac{\partial T}{\partial\dot{\theta}}\right)-\frac{\partial T}{\partial\theta}+\frac{\partial V}{\partial\theta}=-\Delta I\mathrm{Im}[(-\omega\theta'_z+i\dot{\theta}'_z)^2]-\frac{1}{2}I_p\mathrm{Im}[\bar{\theta}_z\ddot{\theta}_z]\quad(4.24)$$

From equations (4. 23) and (4. 24), the relation

$$\omega T_r=\dot{T}+\dot{V}\qquad(4.25)$$

holds. It can be confirmed that the time rate of work ωT_r applied to the shaft system is identified with the increase in rate of total energy.

4. 4. 2. Torque applied to shaft end

Let us obtain the relation of equation (4. 24) by using Eulerian angles θ, ϕ and ψ. The angular velocities ω_X, ω_Y and ω_Z about the principal axes SX, SY and SZ in Fig. 4. 1 (a) are expressed as follows[61]:

$$\left.\begin{aligned} &\omega_X=\dot{\theta}\sin\psi-\dot{\phi}\sin\theta\cos\psi, \quad \omega_Y=\dot{\theta}\cos\psi+\dot{\phi}\sin\theta\sin\psi, \\ &\omega_Z=\dot{\phi}\cos\theta+\dot{\psi} \end{aligned}\right\} \quad (4.26)$$

The X-, Y- and Z-components of the time rate of the angular momentum are given by the following Euler's equations:

$$\left.\begin{aligned} &M_X=I_1\dot{\omega}_X-(I_2-I_p)\omega_Y\omega_Z, \quad M_Y=I_2\dot{\omega}_Y-(I_p-I_1)\omega_Z\omega_X, \\ &M_Z=I_p\dot{\omega}_Z-(I_1-I_2)\omega_X\omega_Y \end{aligned}\right\} \quad (4.27)$$

When higher terms than the second power of θ are neglected hereafter, the following relations hold:

$$\left.\begin{aligned} &\theta_z=\theta e^{i\phi}, \quad \theta_x=\theta\cos\phi, \quad \theta_y=\theta\sin\phi, \\ &\theta'_z=\theta_z e^{-i\Theta}=\theta e^{-i\psi}, \quad \theta'_x=\theta\cos\psi, \quad \theta'_y=-\theta\sin\psi \end{aligned}\right\} \quad (4.28)$$

Equation (4. 26) is rewritten by use of equations (2. 2), (4. 3) and (4. 28) as follows:

$$\omega_X=-\dot{\theta}'_y-\omega\theta'_x, \quad \omega_Y=\dot{\theta}'_x-\omega\theta'_y, \quad \omega_Z=\omega-\frac{1}{2}(\dot{\phi}\theta^2) \quad (4.29)$$

By substituting equation (4. 29) into equation (4. 27), the following relations are reduced:

$$\left.\begin{aligned} &M_X=-(I+\Delta I)\ddot{\theta}'_y-(2I-I_p)\omega\dot{\theta}'_x-(I_p-I+\Delta I)\omega^2\theta'_y \\ &M_Y=(I-\Delta I)\ddot{\theta}'_x-(2I-I_p)\omega\dot{\theta}'_y+(I_p-I-\Delta I)\omega^2\theta'_x \\ &M_Z=-\frac{1}{2}I_p\frac{d}{dt}(\dot{\phi}\theta^2)+2\Delta I(\dot{\theta}'_y+\omega\theta'_x)(\dot{\theta}'_x-\omega\theta'_y) \end{aligned}\right\} \quad (4.30)$$

When the X- and Y-components of restoring moment, that is,

$$M_X=\delta(\theta'_y-\theta'_{ay}), \quad M_Y=-\delta(\theta'_x-\theta'_{ax}) \quad (4.31)$$

are replaced for the left hand side of equation (4. 30), the equations of motion can be obtained[68] for an asymmetrical rotor with respect to the rotating coordinates θ'_x and θ'_y. The Z-component of torque T_r, i. e., $T_r\cos|\theta'_z-\theta'_{az}|$, is identified with the moment M_Z about SZ axis. When the terms including the third power of small quantity θ are neglected, and the relations

$$\left.\begin{aligned} &\frac{d}{dt}(\dot{\phi}\theta^2)=\frac{d}{dt}(\theta_x\dot{\theta}_y-\dot{\theta}_x\theta_y)=\mathrm{Im}[\bar{\theta}_z\ddot{\theta}_z] \\ &2(\dot{\theta}'_y+\omega\theta'_x)(\dot{\theta}'_x-\omega\theta'_y)=-\mathrm{Im}[(-\omega\theta'_z+i\dot{\theta}'_z)^2] \end{aligned}\right\} \quad (4.32)$$

are used, the torque applied to the shaft end is given as the following equation from the third equation of equation (4. 30) :

$$T_r = M_Z = -\Delta I \mathrm{Im}[(-\omega\theta_z' + i\dot{\theta}_z')^2] - \frac{1}{2} I_p \mathrm{Im}[\bar{\theta}_z \ddot{\theta}_z] \tag{4. 33}$$

Equation (4. 33) agrees precisely with equation (4. 24) which is reduced by Lagrange's equation.

4. 4. 3. Condition necessary for the occurrence of unstable vibration

When the right hand side of equation (4. 23) is positive, the total energy of shaft system increases with time, and unstable vibrations occur. A time average of the second term $-(1/2)I_p\omega\mathrm{Im}[\bar{\theta}_z\ddot{\theta}_z]$ of equation (4. 23) becomes zero in a steady-state vibration[72]. Since the inclinational angle of rotor θ_z gradually increases in the case of unstable vibration, a time average of this term does not become zero. Thus, this second term of equation (4. 23) has an effect on torque T_r in the unstable region, but has no connection with the condition for the occurrence of unstable vibration. The condition for the occurrence of unstable vibration is represented by the condition under which a time average of the first term of equation (4. 23) is positive, that is,

$$-\Delta I \omega \mathrm{Im}[K] > 0 \tag{4. 34}$$

where

$$K = \text{Constant terms of } (-\omega\theta_z' + i\dot{\theta}_z')^2 \tag{4. 35}$$

4. 4. 3. 1. Condition necessary for the occurrence of statically unstable vibration

In statically unstable regions in which a whirling natural frequency p coincides with an angular velocity of shaft ω, the solutions for free vibration are put in the following form[72]:

$$\theta_z = A\mathrm{e}^{i\omega t} + a\mathrm{e}^{-i\omega t} + C\mathrm{e}^{3i\omega t} + c\mathrm{e}^{-3i\omega t} + F\mathrm{e}^{5i\omega t} + f\mathrm{e}^{-5i\omega t} + H\mathrm{e}^{7i\omega t} \cdots \tag{4. 36}$$

By using equations (3. 24) and (4. 36), the term $(-\omega\theta_z' + i\dot{\theta}_z')^2$ in equation (4. 34) is derived as follows:

$$(-\omega\theta_z' + i\dot{\theta}_z')^2 = (i\dot{\theta}_z\mathrm{e}^{-i\omega t})^2 = \omega^2(A - a\mathrm{e}^{-2i\omega t} + 3C\mathrm{e}^{2i\omega t} - 3c\mathrm{e}^{-4i\omega t}$$
$$+ 5F\mathrm{e}^{4i\omega t} - 5f\mathrm{e}^{-6i\omega t} + 7H\mathrm{e}^{6i\omega t} - \cdots)^2 \tag{4. 37}$$

When all time-varying terms $\mathrm{e}^{2Ni\omega t}$ (N=integers except zero) in the expanded terms of equation (4. 37) are averaged for a cycle $2\pi/\omega$, these terms become zero, and they hardly influence the condition whether or not statical unstable vibrations occur. Therefore, the term K in the condition for instability (4. 34) is expressed as follows:

$$K = \omega^2(A^2 - 6aC - 30cF - 70fH - \cdots) \tag{4. 38}$$

Since all but the first term in equation (4. 38) are real numbers as seen from the equations of motion (4. 7), the condition for instability (4. 34) is given by

$$\mathrm{Im}[A^2]<0 \tag{4.39}$$

The symbol arg is used in equation (4.39), so

$$(2N-1)\pi<2\arg A<2N\pi \tag{4.40}$$

The condition necessary for the occurrence of statically unstable vibration (4.40) means that a constant term ωA of $-\omega\theta_z'+i\dot{\theta}_z'$ in equation (4.37) must exist in the second or the fourth quadrant of a complex plane.

4. 4. 3. 2. *Condition necessary for the occurrence of dynamically unstable vibration*

The solutions for free vibration have the following form[72]:

$$\theta_z=\sum_{j=1}^{2}\{A_j e^{ip_jt}+a_j e^{-ip_jt}+C_j e^{i(2\omega+p_j)t}+c_j e^{-i(2\omega+p_j)t}+F_j e^{i(4\omega+p_j)t}$$
$$+f_j e^{-i(4\omega+p_j)t}+H_j e^{i(6\omega+p_j)t}+\cdots\} \tag{4.41}$$

The term $(-\omega\theta_z'+i\dot{\theta}_z')^2$ is rewritten by use of equations (3.24) and (4.41):

$$(-\omega\theta_z'+i\dot{\theta}_z')^2=[\sum_{j=1}^{2}\{p_jA_je^{-i(\omega-p_j)t}-p_ja_je^{-i(\omega+p_j)t}+(2\omega+p_j)C_je^{i(\omega+p_j)t}$$
$$-(2\omega+p_j)c_je^{-i(3\omega+p_j)t}+(4\omega+p_j)F_je^{i(3\omega+p_j)t}$$
$$-(4\omega+p_j)f_je^{-i(5\omega+p_j)t}+(6\omega+p_j)H_je^{j(5\omega+p_j)t}-\cdots\}]^2 \tag{4.42}$$

Only a constant term K in the expanded terms of equation (4.42) affects the occurrence of dynamically unstable vibrations. The constant term K is expressed:

$$K=2p_1p_2A_1A_2-2p_1(2\omega+p_1)a_1C_1-2p_2(2\omega+p_2)a_2C_2$$
$$-2(2\omega+p_1)(4\omega+p_1)c_1F_1-2(2\omega+p_2)(4\omega+p_2)c_2F_2$$
$$-2(4\omega+p_1)(6\omega+p_1)f_1H_1-2(4\omega+p_2)(6\omega+p_2)f_2H_2-\cdots \tag{4.43}$$

Because any but the first term in equation (4.43) is real and it has no effect upon the condition for instability, the condition under which dynamically unstable vibrations occur is given by

$$\mathrm{Im}[A_1A_2]<0 \tag{4.44}$$

Equation (4.44) is rewritten by using the arguments of complex numbers A_1 and A_2 as follows:

$$(2N-1)\pi<\arg A_1+\arg A_2<2N\pi \tag{4.45}$$

If an arithmetical mean of the arguments of complex amplitudes A_1 and A_2 exists in the second or the fourth quadrant of a complex plane, the dynamically unstable vibrations occur.

In the case in which either of pedestals has no directional inequality ($\varepsilon=0$) or ε is much less than Δ_0, the solutions for free vibration θ_z can be represented only by the first term in the right hand side of equation (4.41). A term $-\omega\theta_z'+i\dot{\theta}_z'$ describes an elliptic locus on a complex plane. The length of the major axis of

the ellipse is $2(|A_1|+|A_2|)$, and the length of the minor one is $2(|A_1|\sim|A_2|)$[72]. The angle between the major principal axis of the ellipse and the real axis is $(1/2)\times(\arg A_1+\arg A_2)$. When the major axis of an ellipse exists in the second or the fourth quadrant, satisfying equation (4.45), the dynamically unstable vibrations may occur. In the case that ε is not negligible, the vibrations with small amplitudes derived from ε and Δ_0 are added to the ellipse, and a locus of $-\omega\theta'_z+i\dot{\theta}'_z$ expressed on a complex plane is very complicated [see Fig. 4.8 (b)].

4. 4. 4. *Solutions of vibration obtained by analog computer and condition necessary for the occurrence of unstable vibriaton*

In order to substantiate whether the conditions for the occurrence of unstable vibration (4.40) and (4.45) are satisfied, the vibratory solutions with regard to rotating coordinates θ'_z and θ'_{az} are obtained by an analog computer ALS-200X. Figure 4.6 shows a simulation circuit in an analog computer which satisfies simultaneously both the real and imaginary parts of the following equation:

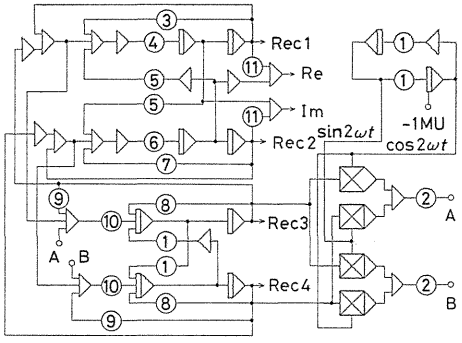

Fig. 4. 6 Simulation circuit for analog computer
Rec 1: θ'_x, Rec 2: θ'_y, Rec 3: θ'_{ax},
Rec 4: θ'_{ay}, Re: $-\omega\theta'_x-\dot{\theta}'_y$,
Im: $-\omega\theta'_y+\dot{\theta}'_x$
Potentiometers ①: 2ω, ②: $\kappa\varepsilon$,
③: $(1+\Delta_0-i_p)\omega^2$, ④: $1/(1-\Delta_0)$,
⑤: $(2-i_p)\omega$, ⑥: $1/(1+\Delta_0)$,
⑦: $(1-\Delta_0-i_p)\omega^2$, ⑧: ω^2, ⑨: κ,
⑩: $1/\sigma$, ⑪: ω.

$$\left.\begin{aligned}&\ddot{\theta}'_z+i(2-i_p)\omega\dot{\theta}'_z+(i_p-1)\omega^2\theta'_z+\theta'_z-\theta'_{az}=\Delta_0(\ddot{\bar{\theta}}'_z+\omega^2\bar{\theta}'_z)\\&\sigma(\ddot{\theta}'_{az}+2i\omega\dot{\theta}'_{az}-\omega^2\theta'_{az})+(1+\kappa)\theta'_{az}-\theta'_z=\kappa\varepsilon\bar{\theta}'_{az}e^{-2i\omega t}\end{aligned}\right\}\quad(4.46)$$

Let us show the results on a complex plane in which the real part ($\mathrm{Re}=-\omega\theta'_x-\dot{\theta}'_y$) and the imaginary one ($\mathrm{Im}=-\omega\theta'_y+\dot{\theta}'_x$) are derived by an analog computer, and they are put into the abscissa and the ordinate of an X-Y recorder.

Examples of statically unstable vibrations are shown in Figs. 4.7 (a) and (b) for $\varepsilon=0$ and $\varepsilon=0.5$, respectively, and other parameters are set as $\sigma=1$, $\kappa=1$, $\Delta_0=0.2$, $i_p=0.8$ and $\omega=0.88$. The loci of $-\omega\theta'_z+i\dot{\theta}'_z$ on a complex plane always exist in the second quadrant, and the necessary condition for static instability (4.40) is satisfied. Because of the pedestal inequality ε, Fig. 4.7 (b) shows that the terms with frequencies $\pm2\omega$, $\pm4\omega$, $\cdots$ are added to the straight line motion resulting from the constant term ωA in equation (4.37).

Figures 4.8 (a) and (b) show examples of dynamically unstable vibrations for the same parameters as Fig. 4.7 except $\omega=1.50$. The locus of dynamically unstable vibration describes an ellipse in Fig. 4.8 (a). This ellipse is composed of two rotating vectors, one whirling at a counterclockwise velocity $p_1-\omega>0$ with amplitude $|p_1A_1|$, and the other whirling at a clockwise velocity $\omega-p_1<0$ with

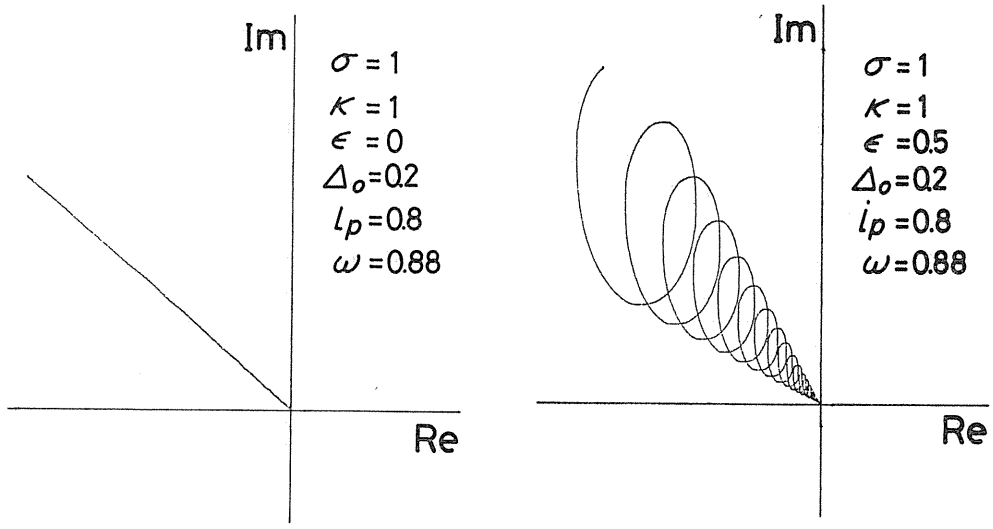

(a) (b)

Fig. 4. 7 Unstable vibration expressed on a complex plane $-\omega\theta_z'+i\dot{\theta}_z'$.

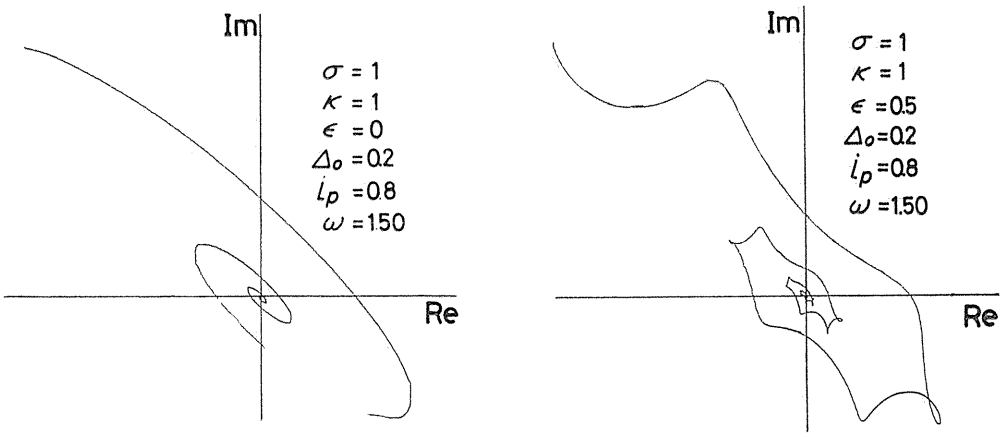

(a) (b)

Fig. 4. 8 Unstable vibration expressed on a complex plane $-\omega\theta_z'+i\dot{\theta}_z'$.

amplitude $|p_2A_2|$. The major axis of the ellipse always exists in the second and the fourth quadrants, and the condition for dynamic instability (4. 45) is always satisfied. Figure 4. 8 (b) shows a complicated locus, because very small vibrations with frequencies $\pm(\omega+p_1)$, $\pm(\omega+p_2)$, $\pm(3\omega+p_1)$, $\pm(3\omega+p_2)$ $\cdots$ overlap upon an elliptical locus of Fig. 4. 8 (a). Nevertheless, the major axis of an ellipse composed of two motions whirling in an opposite direction with frequencies $\pm(p_1-\omega)$ exists in the second and the fourth quadrants, and the condition for the increase of the total energy of this systen is satisfied.

4. 5. *Conclusions*

Conclusions obtained in this chapter may be summarized as follows:

(1) The analysis of unstable vibrations for conical motions of an asymmetrical rotor supported by unequally flexible pedestals is carried out by a similar approximation applied to an asymmetrical shaft supported by unequally flexible ones in Chapter 2.

(2) When the approximate analysis is applied by assuming the two cases in which ε^2 is either negligibly small or not so, the approximate results coincide with the solutions obtained by an analog computer.

(3) For the conical motion of a rotor mounted an asymmetrical shaft in Chapter 2, unstable regions near the intersecting points C_2, D_1 and D_2 disappear at the angular velocity $\omega=\sqrt{\kappa/\sigma}/i_p$, but such a phenomenon does not occur for an asymmetrical rotor.

(4) When a shaft with an asymmetrical rotor is supported by unequally flexible pedestals, the condition necessary for occurrence of unstable vibrations is given by the relation (4.34) under which the total energy of the shaft system increases.

(i) The condition for static instability means that a constant term ωA in a complex plane of $-\omega\theta_z'+i\dot{\theta}_z'$ must exist in the second or the fourth quadrant.

(ii) The condition for dynamic instability means that the locus of $-\omega\theta_z'+i\dot{\theta}_z'$ in a complex plane describes an ellipse, and the major axis of this ellipse must exist in the second or the fourth quadrant.

(5) It is ascertained that all solutions of unstable vibrations obtained by an analog computer satisfy the necessary condition under which unstable vibrations occur.

5. On the Shaft End Torque and the Unstable Vibrations of an Asymmetrical Shaft Carrying an Asymmetrical Rotor[75]

5. 1. *Introduction*

In a rotating asymmetrical shaft carrying an asymmetrical rotor[25, 26, 46, 48, 64~66] as well as in a rotating asymmetrical shaft[70~73], and in an asymmetrical rotor[73, 74], there occur two types of unstable vibrations[25, 26, 57, 59, 70~74]. It is obtained from analytical and experimental studies[25, 26] that the width of the unstable regions changes with the orientation angle between the inequality of shaft stiffness and that of rotor inertia.

In this chapter, in order to clarify the dependence of the orientation angle ζ upon the occurrence of unstable vibration, the condition is obtained, under which input energy supplied at the shaft end increases the whirling amplitudes of the shaft, so that these two types of unstable vibrations occur. T. Yamamoto, H. Ōta and K. Kōno[25, 26] indicate analytically and experimentally that the width of the statically unstable region[57] becomes narrower as the orientation angle ζ increases from zero to $\pi/2$, and on the other hand the width of the dynamically unstable one[59] becomes greater as ζ increases. The condition necessary for occurrence of instability depends on the angle ζ, and the analytical results agree qualitatively with that of the experimental ones[25, 26]. Furthermore, when inertia asymmetry

Δ_0 and stiffness asymmetry Δ_{ij} are combined suitably, the condition under which the unstable region vanishes is realized. It is ascertained that the solutions of the unstable vibration obtained with an analog computer satisfy the condition necessary for instability.

5. 2. *Equations of Motion*

The principal moments of inertia about three principal axes of inertia SX_2, SY_2 and SZ_1 through the center S of an asymmetrical rotor in Fig. 5. 1 are denoted by I_1, I_2 and $I_p(I_2>I_1)$, respectively, and $I=(I_1+I_2)/2$ and $\Delta I=(I_1-I_2)/2$. The mass of the rotor is m_0, but the mass of the shaft is assummed to be negligibly small. Let the bearing center line be Oz. The rectangular coordinate system O-xyz is parallel to the rectangular coordinate system S-XYZ; thus, xy-plane coincides with XY-plane. The rectangular coordinate systems S-$X_2Y_2Z_1$ and S-$X_3Y_3Z_1$ are fixed to the rotor, the angular positions of which are denoted by Eulerian angles θ, ϕ and ψ. The rectangular coordinate system S-NKZ is obtained by rotating the rectangular system S-XYZ about the vertical axis SZ by ϕ, and then the system S-LKZ_1 is obtained by inclining the coordinate system S-NKZ about the axis SK by θ. Next, the coordinate systems S-$X_2Y_2Z_1$ and S-$X_3Y_3Z_1$ are obtained by rotating the system S-LKZ_1 about the axis of inertia SZ_1 by ψ and $\psi+\zeta$, respectively. The orientation angle between the inequality of shaft stiffness and that of rotor inertia is defined as $\zeta=\angle X_2SX_3=\angle Y_2SY_3$. The stiffnesses of the asymmetrical shaft are $\alpha\pm\Delta\alpha$, $\gamma\pm\Delta\gamma$ and $\delta\pm\Delta\delta$ in which the lower negative signs correspond to the displacement in the SX_3-direction, and upper positive ones to that in the SY_3-direction. Let two components of displacement vector $\overrightarrow{OS}$ be x and y, and let projectional angles of inclination angle $\theta=\angle ZSZ_1$ to xz- and yz-planes be θ_x and θ_y, respectively.

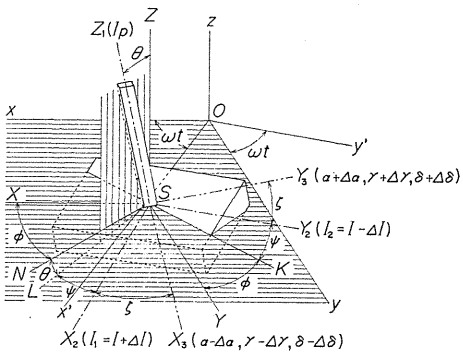

Fig. 5. 1 Eulerian angles θ, ϕ and ψ, and orientation angle ζ.

When the terms higher than the 3 rd order of small quantities θ_x and θ_y are neglected, the kinetic energy of the asymmetrical rotor T both of translation and rotation is represented as follows:

$$2T=m_0(\dot{x}^2+\dot{y}^2)+I_p\{\dot{\theta}^2+\dot{\theta}(\dot{\theta}_x\theta_y-\theta_x\dot{\theta}_y)\}+I(\dot{\theta}_x^2+\dot{\theta}_y^2)$$
$$-\Delta I\{(\dot{\theta}_x^2-\dot{\theta}_y^2)\cos 2\Theta+2\dot{\theta}_x\dot{\theta}_y\sin 2\Theta\} \tag{5.1}$$

where Θ is the rotational angle of the shaft end. Let the projections of the displacement vector $\overrightarrow{OS}$ to X_3SZ and Y_3SZ planes be x_3' and y_3', respectively, and let the projectional angles of inclination angle θ to X_3SZ and Y_3SZ planes be θ_{x3}' and θ_{y3}', respectively. The potential energy of the asymmetrical shaft V is represented as follows[57]:

$$2V=(\alpha-\Delta\alpha)x_3'^2+2(\gamma-\Delta\gamma)x_3'\theta_{x3}'+(\delta-\Delta\delta)\theta_{x3}'^2+(\alpha+\Delta\alpha)y_3'^2$$

$$+2(\gamma+\Delta\gamma)y_3'\theta_{y3}'+(\delta+\Delta\delta)\theta_{y3}'^2 \tag{5.2}$$

When the following relations

$$\begin{matrix} x_3' \\ \theta_{x3}' \end{matrix}=\begin{matrix} x \\ \theta_x \end{matrix}\cos(\theta+\zeta)+\begin{matrix} y \\ \theta_y \end{matrix}\sin(\theta+\zeta),\quad \begin{matrix} y_3' \\ \theta_{y3}' \end{matrix}=-\begin{matrix} x \\ \theta_x \end{matrix}\sin(\theta+\zeta)+\begin{matrix} y \\ \theta_y \end{matrix}\cos(\theta+\zeta) \tag{5.3}$$

are used, equation (5.2) is rewritten as follows[57]:

$$\begin{aligned} 2V=&\alpha(x^2+y^2)+2\gamma(x\theta_x+y\theta_y)+\delta(\theta_x^2+\theta_y^2)-\Delta\alpha\{(x^2-y^2)\cos 2(\theta+\zeta)\\ &+2xy\sin 2(\theta+\zeta)\}-2\Delta\gamma\{(x\theta_x-y\theta_y)\cos 2(\theta+\zeta)+(x\theta_y+y\theta_x)\sin 2(\theta+\zeta)\}\\ &-\Delta\delta\{(\theta_x^2-\theta_y^2)\cos 2(\theta+\zeta)+2\theta_x\theta_y\sin 2(\theta+\zeta)\} \end{aligned} \tag{5.4}$$

Substituting equations (5.1) and (5.4) into Lagrange's equation of motion, and neglecting the terms higher than the 2nd order of θ_x and θ_y, the equation of motion regarding angle Θ is derived as $\ddot{\Theta}=0$, which leads to

$$\dot{\theta}=\omega=\text{Constant},\quad \theta=\omega t \tag{5.5}$$

The equations of motion[25, 26] regarding x, y, θ_x and θ_y are obtained by using equations (5.1). (5.4) and (5.5):

$$\left.\begin{aligned} m_0\ddot{x}+\alpha x+\gamma\theta_x=&\Delta\alpha\{x\cos 2(\omega t+\zeta)+y\sin 2(\omega t+\zeta)\}\\ &+\Delta\gamma\{\theta_x\cos 2(\omega t+\zeta)+\theta_y\sin 2(\omega t+\zeta)\}\\ m_0\ddot{y}+\alpha y+\gamma\theta_y=&\Delta\alpha\{x\sin 2(\omega t+\zeta)-y\cos 2(\omega t+\zeta)\}\\ &+\Delta\gamma\{\theta_x\sin 2(\omega t+\zeta)-\theta_y\cos 2(\omega t+\zeta)\}\\ I\ddot{\theta}_x+I_p\omega\dot{\theta}_y+\gamma x+\delta\theta_x=&\Delta I\frac{\mathrm{d}}{\mathrm{d}t}(\dot{\theta}_x\cos 2\omega t+\dot{\theta}_y\sin 2\omega t)\\ &+\Delta\gamma\{x\cos 2(\omega t+\zeta)+y\sin 2(\omega t+\zeta)\}\\ &+\Delta\delta\{\theta_x\cos 2(\omega t+\zeta)+\theta_y\sin 2(\omega t+\zeta)\}\\ I\ddot{\theta}_y-I_p\omega\dot{\theta}_x+\gamma y+\delta\theta_y=&\Delta I\frac{\mathrm{d}}{\mathrm{d}t}(\dot{\theta}_x\sin 2\omega t-\dot{\theta}_y\cos 2\omega t)\\ &+\Delta\gamma\{x\sin 2(\omega t+\zeta)-y\cos 2(\omega t+\zeta)\}\\ &+\Delta\delta\{\theta_x\sin 2(\omega t+\zeta)-\theta_y\cos 2(\omega t+\zeta)\} \end{aligned}\right\} \tag{5.6}$$

Complex variables (1.7) and (2.6) are introduced into equation (5.6), and the equations of motion regarding z and θ_z are expressed as:

$$\left.\begin{aligned} &m_0\ddot{z}+\alpha z+\gamma\theta_z=(\Delta\alpha\cdot\bar{z}+\Delta\gamma\cdot\bar{\theta}_z)\mathrm{e}^{2i(\omega t+\zeta)}\\ &I\ddot{\theta}_z-iI_p\omega\dot{\theta}_z+\gamma z+\delta\theta_z=\Delta I\frac{\mathrm{d}}{\mathrm{d}t}(\dot{\bar{\theta}}_z\mathrm{e}^{2i\omega t})+(\Delta\gamma\cdot\bar{z}+\Delta\delta\cdot\bar{\theta}_z)\mathrm{e}^{2i(\omega t+\zeta)} \end{aligned}\right\} \tag{5.7}$$

5. 3. *Mechanism for the Occurrence of Unstable Vibrations*

5. 3. 1. *Increase in rate of total energy* $\dot{T}+\dot{V}$

By differentiating equations (5. 1) and (5. 4) with respect to time t and using equation (5. 5), the increase in rate of kinetic energy and potential energy are obtained :

$$\left.\begin{aligned}
\dot{T}&=m_0(x\ddot{x}+y\ddot{y})+(I_p/2)\,\omega(\ddot{\theta}_x\theta_y-\theta_x\ddot{\theta}_y)+I(\dot{\theta}_x\ddot{\theta}_x+\dot{\theta}_y\ddot{\theta}_y)\\
&\quad-(\varDelta I/2)\frac{\mathrm{d}}{\mathrm{d}t}\{(\dot{\theta}_x^2-\dot{\theta}_y^2)\cos 2\omega t+2\dot{\theta}_x\dot{\theta}_y\sin 2\omega t\}\\
\dot{V}&=\alpha(x\dot{x}+y\dot{y})+\gamma(x\dot{\theta}_x+\dot{x}\theta_x+y\dot{\theta}_y+\dot{y}\theta_y)+\delta(\theta_x\dot{\theta}_x+\theta_y\dot{\theta}_y)\\
&\quad-\varDelta\alpha\{(2\omega xy+x\dot{x}-y\dot{y})\cos 2(\omega t+\zeta)-(\omega x^2-\omega y^2-x\dot{y}-\dot{x}y)\sin 2(\omega t+\zeta)\}\\
&\quad-\varDelta\gamma\{(2\omega x\theta_y+2\omega y\theta_x+x\dot{\theta}_x+\dot{x}\theta_x-y\dot{\theta}_y-\dot{y}\theta_y)\cos 2(\omega t+\zeta)\\
&\quad-(2\omega x\theta_x-2\omega y\theta_y-x\dot{\theta}_y-\dot{x}\theta_y-y\dot{\theta}_x-\dot{y}\theta_x)\sin 2(\omega t+\zeta)\\
&\quad-\varDelta\delta\{(2\omega\theta_x\theta_y+\theta_x\dot{\theta}_x-\theta_y\dot{\theta}_y)\cos 2(\omega t+\zeta)\\
&\quad-(\omega\theta_x^2-\omega\theta_y^2-\theta_x\dot{\theta}_y-\dot{\theta}_x\theta_y)\sin 2(\omega t+\zeta)\}
\end{aligned}\right\}\tag{5·8}$$

Use of complex variables (1. 7) and (2. 6) in equation (5. 8) gives the following equation ;

$$\left.\begin{aligned}
\dot{T}&=m_0\mathrm{Re}[\dot{\bar{z}}\ddot{z}]+(I_p/2)\,\omega\mathrm{Im}[\theta_z\ddot{\bar{\theta}}_z]+I\mathrm{Re}[\dot{\bar{\theta}}_z\ddot{\theta}_z]-(\varDelta I/2)\frac{\mathrm{d}}{\mathrm{d}t}\mathrm{Re}[\dot{\theta}_z^2\mathrm{e}^{-2i\omega t}]\\
\dot{V}&=\alpha\mathrm{Re}[z\dot{\bar{z}}]+\gamma\mathrm{Re}[\dot{\bar{z}}\theta_z+z\dot{\bar{\theta}}_z]+\delta\mathrm{Re}[\theta_z\dot{\bar{\theta}}_z]-\varDelta\alpha\mathrm{Re}[z\dot{z}\mathrm{e}^{-2i(\omega t+\zeta)}]\\
&\quad-\varDelta\alpha\omega\mathrm{Im}[z^2\mathrm{e}^{-2i(\omega t+\zeta)}]-\varDelta\gamma\mathrm{Re}[(z\dot{\theta}_z+\dot{z}\theta_z)\mathrm{e}^{-2i(\omega t+\zeta)}]\\
&\quad-\varDelta\gamma\omega\mathrm{Im}[2z\theta_z\mathrm{e}^{-2i(\omega t+\zeta)}]-\varDelta\delta\mathrm{Re}[\theta_z\dot{\theta}_z\mathrm{e}^{-2i(\omega t+\zeta)}]\\
&\quad-\varDelta\delta\omega\mathrm{Im}[\theta_z^2\mathrm{e}^{-2i(\omega t+\zeta)}]
\end{aligned}\right\}\tag{5. 9}$$

When the first equation in equation (5. 7) is multiplied by $\dot{\bar{z}}$, the second one by $\dot{\bar{\theta}}_z$, and these are added together, the following equation is given from the real part of the derived equation :

$$\begin{aligned}
&m_0\mathrm{Re}[\dot{\bar{z}}\ddot{z}]+\alpha\mathrm{Re}[z\dot{\bar{z}}]+\gamma\mathrm{Re}[\dot{\bar{z}}\theta_z+z\dot{\bar{\theta}}_z]+I\mathrm{Re}[\dot{\bar{\theta}}_z\ddot{\theta}_z]+\delta\mathrm{Re}[\theta_z\dot{\bar{\theta}}_z]\\
&\quad=\mathrm{Re}[\varDelta I\dot{\bar{\theta}}_z\frac{\mathrm{d}}{\mathrm{d}t}(\dot{\bar{\theta}}_z\mathrm{e}^{2i\omega t})+\{\varDelta\alpha\bar{z}\dot{\bar{z}}+\varDelta\gamma(\dot{\bar{z}}\bar{\theta}_z+\bar{z}\dot{\bar{\theta}}_z)+\varDelta\delta\bar{\theta}_z\dot{\bar{\theta}}_z\}\mathrm{e}^{2i(\omega t+\zeta)}]
\end{aligned}\tag{5. 10}$$

By substituting equations (3. 1), (3. 24) and (5. 10) into equation (5. 9), the increase in rate of total energy $\dot{T}+\dot{V}$ is given as

$$\begin{aligned}
\dot{T}+\dot{V}=&-\omega\mathrm{Im}[\varDelta I(-\omega\theta_z'+i\dot{\theta}_z')^2+(\varDelta\alpha\cdot z'^2+2\varDelta\gamma\cdot z'\theta_z'+\varDelta\delta\cdot\theta_z'^2)\mathrm{e}^{-2i\zeta}\\
&+(I_p/2)\bar{\theta}_z\ddot{\theta}_z]
\end{aligned}\tag{5. 11}$$

Torque T_r supplied at the shaft end is a generalized force with respect to shaft end rotation Θ. When equations (5.1) and (5.4) are substituted into Lagrange's equation of motion, and equations (3.1), (3.24) and (5.5) are used, torque T_r is obtained as follows:

$$T_r=\frac{\mathrm{d}}{\mathrm{d}t}\left(\frac{\partial T}{\partial\dot{\theta}}\right)-\frac{\partial T}{\partial\theta}+\frac{\partial V}{\partial\theta}=-\mathrm{Im}[\varDelta I(-\omega\theta_z'+i\dot{\theta}_z')^2$$
$$+(\varDelta\alpha\cdot z'^2+2\varDelta\gamma\cdot z'\theta_z'+\varDelta\delta\cdot\theta_z'^2)\mathrm{e}^{-2i\zeta}+(I_p/2)\bar{\theta}_z\ddot{\theta}_z] \tag{5.12}$$

From equations (5.11) and (5.12), the relation

$$\omega T_r=\dot{T}+\dot{V} \tag{5.13}$$

is obtained. Equation (5.13) means that the time rate of work applied to the shaft end ωT_r agrees with the increase in rate of total energy[72~74].

5. 3. 2. Frequency equation

For simplicity, i_p in equation (2.7), $\varDelta_0$ in equation (4.6) and the following dimensionless quantities are introduced:

$$\left.\begin{array}{l} x/\sqrt{I/m_0}=x',\quad y/\sqrt{I/m_0}=y',\quad t\sqrt{\alpha/m_0}=t',\quad p/\sqrt{\alpha/m_0}=p',\\ \omega/\sqrt{\alpha/m_0}=\omega',\quad \gamma\sqrt{m_0/I}/\alpha=\gamma',\quad m_0\delta/(\alpha I)=\delta',\quad \varDelta\alpha/\alpha=\varDelta_{11},\\ \varDelta\gamma/\gamma=\varDelta_{12},\quad \varDelta\delta/\delta=\varDelta_{22},\quad m_0T_r/(\alpha I)=T_r' \end{array}\right\} \tag{5.14}$$

The primes in the dimensionless quantities (5.14) are omitted hereafter. The dots over the dimensionless ones mean the differential coefficient with respect to t'. The equations of motion (5.7) regarding z and θ_z are rewritten by using dimensionless quantities (2.7), (4.6) and (5.14):

$$\left.\begin{array}{l} \ddot{z}+z+\gamma\theta_z=(\varDelta_{11}\bar{z}+\gamma\varDelta_{12}\bar{\theta}_z)\mathrm{e}^{2i(\omega t+\zeta)}\\ \ddot{\theta}_z-i\cdot i_p\omega\dot{\theta}_z+\gamma z+\delta\theta_z=\varDelta_0\dfrac{\mathrm{d}}{\mathrm{d}t}(\dot{\bar{\theta}}_z\mathrm{e}^{2i\omega t})+(\gamma\varDelta_{12}\bar{z}+\delta\varDelta_{22}\bar{\theta}_z)\mathrm{e}^{2i(\omega t+\zeta)} \end{array}\right\} \tag{5.15}$$

The existence of the rotating inequalities $\varDelta_0$ and $\varDelta_{ij}$ yields a pair of natural frequencies p and $2\omega-\bar{p}$ ($\bar{p}$ is a conjugate complex number of p), and the solutions for the free vibration of equation (5.15) are represented as follows:

$$z=A\mathrm{e}^{ipt}+A'\mathrm{e}^{i(2\omega-\bar{p})t},\quad \theta_z=B\mathrm{e}^{ipt}+B'\mathrm{e}^{i(2\omega-\bar{p})t} \tag{5.16}$$

where amplitudes A, A', B and B' are complex numbers. When equation (5.16) is substituted into equation (5.15), the 4th order determinant which consists of coefficients of A, $\bar{A}'\mathrm{e}^{2i\zeta}$, B and $\bar{B}'\mathrm{e}^{2i\zeta}$ gives the frequency equation (5.17),

$$F=\begin{vmatrix} H(p) & -\varDelta_{11} & \gamma & -\gamma\varDelta_{12}\\ -\varDelta_{11} & H(\hat{p}) & -\gamma\varDelta_{12} & \gamma\\ \gamma & -\gamma\varDelta_{12} & G(p) & -\delta\varDelta_{22}-\varDelta_0p\hat{p}\mathrm{e}^{-2i\zeta}\\ -\gamma\varDelta_{12} & \gamma & -\delta\varDelta_{22}-\varDelta_0p\hat{p}\mathrm{e}^{2i\zeta} & G(\hat{p}) \end{vmatrix}=0 \tag{5.17}$$

where

$$H(p)=1-p^2, \quad G(p)=\delta+i_p\omega p-p^2 \tag{5.18}$$

Expanding equation (5.17) and using the relation $e^{2i\zeta}+e^{-2i\zeta}=2\cos 2\zeta$, a frequency equation is derived as follows:

$$\begin{aligned}F=&f(p)f(\hat{p})+[-\varDelta_0^2p^2\hat{p}^2H(p)H(\hat{p})-\varDelta_{11}^2G(p)G(\hat{p})\\&-\gamma^2\varDelta_{12}^2\{H(p)G(\hat{p})+H(\hat{p})G(p)\}-\delta^2\varDelta_{22}^2H(p)H(\hat{p})\\&+2\gamma^2\varDelta_{11}\varDelta_{12}\{G(p)+G(\hat{p})\}+2\delta\gamma^2\varDelta_{12}\varDelta_{22}\{H(p)+H(\hat{p})\}\\&-2(\delta\varDelta_{11}\varDelta_{22}+\gamma^2\varDelta_{12}^2)\gamma^2+2\varDelta_0p\hat{p}\{-\gamma^2\varDelta_{11}+\gamma^2\varDelta_{12}H(p)+\gamma^2\varDelta_{12}H(\hat{p})\\&-\delta\varDelta_{22}H(p)H(\hat{p})\}\cos 2\zeta]+\{(\delta\varDelta_{11}\varDelta_{22}-\gamma^2\varDelta_{12}^2)^2+\varDelta_0^2\varDelta_{11}^2p^2\hat{p}^2\\&+2\varDelta_0\varDelta_{11}p\hat{p}(\delta\varDelta_{11}\varDelta_{22}-\gamma^2\varDelta_{12}^2)\cos 2\gamma\}=0\end{aligned} \tag{5.19}$$

where

$$f(p)=H(p)G(p)-\gamma^2 \tag{5.20}$$

5. 3. 3. Condition necessary for the occurrence of unstale vibration

The increase in rate of the total energy (5.11) is rewritten by use of dimensionless quantities (2.7), (4.6) and (5.14):

$$\begin{aligned}\omega T_r=\dot{T}+\dot{V}=&-\omega\mathrm{Im}[\varDelta_0(-\omega\theta_z'+i\dot{\theta}_z')^2+(\varDelta_{11}z'^2+2\gamma\varDelta_{12}z'\theta_z'+\delta\varDelta_{22}\theta_z'^2)e^{-2i\zeta}\\&+(i_p/2)\bar{\theta}_z\ddot{\theta}_z]\end{aligned} \tag{5.21}$$

The condition under which the input energy is supplied to the shaft system and the unstable vibration occurs, coincides with the condition where a time average of the increase in rate of total energy represented by equation (5.21) is positive.

5. 3. 3. 1. Condition necessary for the occurrence of statically unstable vibration

When the root p derived from equation (5.19) is not a real number but an imaginary one, an unstable vibration occurs. In the statically unstable region[57] in which the real part of a complex root p coincides with an angular velocity of shaft ω, whirling natural frequencies in equation (5.16) may be replaced by $p=\omega\pm im$ and $2\omega-\bar{p}=\omega\pm im$, and the solutions of free vibration are given as follows:

$$z=A_1e^{i(\omega+im)t}+A_2e^{i(\omega-im)t}, \quad \theta_z=B_1e^{i(\omega+im)t}+B_2e^{i(\omega-im)t} \tag{5.22}$$

If the imaginary part m of a complex root p is positive, then the first term of the right hand side of equation (5.22) decreases exponentially with time as e^{-mt} regardless of the initial condition. This first term in equation (5.22) may be neglected unlike the second one which increases exponentially as e^{mt}. Thus, only the second term in equation (5.22) is considered, and the subscript 2 is omitted:

$$z=Ae^{(m+i\omega)t}, \quad \theta_z=Be^{(m+i\omega)t} \tag{5.23}$$

In a statically unstable region, the increase in rate of total energy (5.21) is rewritten by use of equation (3.1), (3.24) and (5.23) as follows:

$$\omega T_r = \dot{T} + \dot{V} = -\omega e^{2mt} \mathrm{Im}[J] \tag{5.24}$$

where

$$J = \Delta_0(\omega - im)^2 B^2 + (\Delta_{11} A^2 + 2\gamma \Delta_{12} AB + \delta \Delta_{22} B^2) e^{-2i\zeta} - (i_p/2)(\omega - im)^2 B\bar{B} \tag{5.25}$$

The condition under which unstable vibrations occur is given by the relation in which equation (5.24) is positive; that is,

$$\mathrm{Im}[J] = -T_r e^{-2mt} < 0 \tag{5.26}$$

Let the arguments of the complex numbers A and B be $\arg A$ and $\arg B$, respectively, and the imaginary part of equation (5.25) is expressed as follows:

$$\begin{aligned}\mathrm{Im}[J]/|B|^2 = {} & \Delta_0(\omega^2 - m^2) \sin 2 \arg B - 2\Delta_0 m\omega \cos 2 \arg B \\ & + \Delta_{11} |A/B|^2 \sin 2(\arg A - \zeta) + 2\gamma \Delta_{12} |A/B| \sin(\arg A + \arg B - 2\zeta) \\ & + \delta \Delta_{22} \sin 2(\arg B - \zeta) + i_p m\omega \end{aligned} \tag{5.27}$$

If the equations of motion (5.15) have the free vibration (5.23), the following determinant consisting of the coefficients of $\mathrm{Re}[A]$, $\mathrm{Im}[A]$, $\mathrm{Re}[B]$ and $\mathrm{Im}[B]$ must satisfy the following relation:

$$\begin{vmatrix} 1 - \Delta_{11}\cos 2\zeta - \omega^2 + m^2 & -\Delta_{11}\sin 2\zeta - 2m\omega & \gamma(1 - \Delta_{12}\cos 2\zeta) & -\gamma\Delta_{12}\sin 2\zeta \\ -\Delta_{11}\sin 2\zeta + 2m\omega & 1 + \Delta_{11}\cos 2\zeta - \omega^2 + m^2 & -\gamma\Delta_{12}\sin 2\zeta & \gamma(1 + \Delta_{12}\cos 2\zeta) \\ \gamma(1 - \Delta_{12}\cos 2\zeta) & -\gamma\Delta_{12}\sin 2\zeta & \begin{matrix}\delta(1 - \Delta_{22}\cos 2\zeta) \\ + (i_p - 1 - \Delta_0)\omega^2 \\ + (1 - \Delta_0) m^2\end{matrix} & \begin{matrix} -\delta\Delta_{22}\sin 2\zeta \\ - (2 - i_p) m\omega \end{matrix} \\ -\gamma\Delta_{12}\sin 2\zeta & \gamma(1 + \Delta_{12}\cos 2\zeta) & \begin{matrix} -\delta\Delta_{22}\sin 2\zeta \\ + (2 - i_p) m\omega \end{matrix} & \begin{matrix}\delta(1 + \Delta_{22}\cos 2\zeta) \\ + (i_p - 1 + \Delta_0)\omega^2 \\ + (1 + \Delta_0) m^2\end{matrix} \end{vmatrix} = 0 \tag{5.28}$$

The cofactor of each row ($i=1, 2, 3, 4$) of the determinant (5.28) has the following relation:

$$A_{i1} : A_{i2} : A_{i3} : A_{i4} = \mathrm{Re}[A] : \mathrm{Im}[A] : \mathrm{Re}[B] : \mathrm{Im}[B] \tag{5.29}$$

Thus, the absolute value of ampltude ratio $|A/B|$ and arguments $\arg A$ and $\arg B$ in equation (5.27) can be calculated as follows:

$$\left|\frac{A}{B}\right| = \sqrt{\frac{A_{i1}^2 + A_{i2}^2}{A_{i3}^2 + A_{i4}^2}}, \quad \arg A = \tan^{-1}\frac{A_{i2}}{A_{i1}}, \quad \arg B = \tan^{-1}\frac{A_{i4}}{A_{i3}} \tag{5.30}$$

The condition necessary for occurrence of unstable vibration coincides with the condition under which the right hand side of equation (5.27) is negative.

An appropriate combination of inertia asymmetry Δ_0 and stiffness asymmetry Δ_{ij} makes the imaginary part of a complex number J of equation (5.25) zero, and the unstable region may almost vanish.

5. 3. 3. 2. Condition necessary for the occurrence of dynamically unstable vibration

When whirling natural frequencies of a shaft system are put as

$$p=P_1\pm im,\quad 2\omega-\bar{p}=P_2\pm im\ \ (0<P_2<\omega<P_1) \tag{5.31}$$

a dynamically unstable vibration[59] is considered which certainly satisfies the relation

$$P_1+P_2=2\omega \tag{5.32}$$

and in which both amplitudes of frequencies P_1 and P_2 increase exponentially as e^{mt}. In this unstable region, the solutions of free vibration (5.16) are rewritten as follows:

$$\left.\begin{aligned} z&=A_1e^{i(P_1+im)t}+A_2e^{i(P_1-im)t}+A_1'e^{i(P_2+im)t}+A_2'e^{i(P_2-im)t}\\ \theta_z&=B_1e^{i(P_1+im)t}+B_2e^{i(P_1-im)t}+B_1'e^{i(P_2+im)t}+B_2'e^{i(P_2-im)t}\end{aligned}\right\} \tag{5.33}$$

As with equation (5.22), the first and third terms in the right hand side of equation (5.33) may be negligible. Thus, the second and fourth terms of equation (5.33) are adopted as the solutions of free vibration, and subscript 2 is omitted. Thus,

$$z=Ae^{(m+iP_1)t}+A'e^{(m+iP_2)t},\quad \theta_z=Be^{(m+iP_1)t}+B'e^{(m+iP_2)t} \tag{5.34}$$

When equation (5.34) is transformed by using equations (3.1) and (3.24), and substituted into equation (5.21), the increase in rate of total energy is given as follows:

$$\begin{aligned}\omega T_r=\dot{T}+\dot{V}=&-\omega e^{2mt}\mathrm{Im}[\Delta_0(P_1-im)^2B^2e^{2i(P_1-\omega)t}\\ &+\underline{2\Delta_0(P_1-im)(P_2-im)BB'}+\Delta_0(P_2-im)^2B'^2e^{-2i(P_1-\omega)t}\\ &+\{\Delta_{11}A^2e^{2i(P_1-\omega)t}+\underline{2\Delta_{11}AA'}+\Delta_{11}A'^2e^{-2i(P_1-\omega)t}+2\gamma\Delta_{12}ABe^{2i(P_1-\omega)t}\\ &+\underline{2\gamma\Delta_{12}(AB'+A'B)}+2\gamma\Delta_{12}A'B'e^{-2i(P_1-\omega)t}+\delta\Delta_{22}B^2e^{2i(P_1-\omega)t}+\underline{2\delta\Delta_{22}BB'}\\ &+\delta\Delta_{22}B'^2e^{-2i(P_1-\omega)t}\}e^{-2i\zeta}-(i_p/2)\{\underline{(P_1-im)^2B\bar{B}}+(P_2-im)^2\bar{B}B'e^{-i(P_1-P_2)t}\\ &+(P_1-im)^2B\bar{B}'e^{i(P_1-P_2)t}+\underline{(P_2-im)^2B'\bar{B}'}\}]\end{aligned} \tag{5.35}$$

The sum of the constant terms shown by underlines in equation (5.33) is defined by J, and a time average of torque T_r is expressed by T_{rm}. The condition under which an unstable vibration occurs is reduced as follows:

$$\mathrm{Im}[J]=-T_{rm}e^{-2mt}<0 \tag{5.36}$$

By using the argument of a complex number and equation (5.32), $\mathrm{Im}[J]$ in equation

(5.36) is obtained in the following form:

$$\begin{aligned}\mathrm{Im}[J]/2|BB'| &= \Delta_0(P_1P_2-m^2)\sin(\arg B+\arg B') \\ &-2\Delta_0 m\omega\cos(\arg B+\arg B')+\Delta_{11}|AA'/BB'|\sin(\arg A+\arg A'-2\zeta) \\ &+\gamma\Delta_{12}\{|A/B|\sin(\arg A+\arg B'-2\zeta)+|A'/B'|\sin(\arg A'+\arg B-2\zeta)\} \\ &+\delta\Delta_{22}\sin(\arg B+\arg B'-2\zeta)+(i_p/2)m(P_1|B/B'|+P_2|B'/B|) \qquad (5.37)\end{aligned}$$

Amplitude ratio and argument of complex amplitudes A, B, A' and B' are necessary in order to calculate the right hand side of equation (5.37). For the whirling solutions of free vibration (5.34), the cofactors of determinant (5.17) into which $p=P_1-im$ and $2\omega-p=2\omega-P_1+im=P_2+im$ are inserted have the following relation:

$$A_{i1}:A_{i2}:A_{i3}:A_{i4}=A:\overline{A}'e^{2i\zeta}:B:\overline{B}'e^{2i\zeta} \qquad (5.38)$$

which gives absolute values of amplitude ratio and arguments regarding the complex amplitudes A, B, A' and B' as follows:

$$\left|\frac{A}{B}\right|=\left|\frac{A_{i1}}{A_{i3}}\right|,\quad \left|\frac{A'}{B'}\right|=\left|\frac{A_{i2}}{A_{i4}}\right|,\quad \left|\frac{B}{B'}\right|=\left|\frac{A_{i3}}{A_{i4}}\right| \qquad (5.39)$$

$$\left.\begin{aligned}&\arg A=\arg A_{i1},\quad \arg A'=2\zeta-\arg A_{i2}\\ &\arg B=\arg A_{i3},\quad \arg B'=2\zeta-\arg A_{i4}\end{aligned}\right\} \qquad (5.40)$$

Because the right hand side of equation (5.37) includes the orientation angle ζ, the condition under which a dynamically unstable vibration occurs changes remarkably with the angle ζ.

The right hand side of equation (5.37) can be made zero with an appropriate combination of inertia asymmetry Δ_0 and stiffness asymmetry Δ_{ij}, and thus, the unstable region may almost vanish.

5. 3. 3. 3. *Approximate equation for the condition under which unstable vibration occurs*

As the imaginary part m is much smaller than the real parts P_1 and P_2 for complex natural frequencies $p=P_1\pm im$ and $2\omega-\bar{p}=P_2\pm im$ shown by equation (5.31), the imaginary part m is ignored in this section. Free vibrations in a steady state are assumed by putting $p=P_1$ and $2\omega-\bar{p}=P_2$ in equation (5.16), and the sum of constant terms J in $[\cdots]$ of equation (5.35) is rewritten as follows:

$$\begin{aligned}J &= 2\Delta_0P_1P_2BB'+2\{\Delta_{11}AA'+\gamma\Delta_{12}(AB'+A'B)+\delta\Delta_{22}BB'\}e^{-2i\zeta} \\ &-(i_p/2)(P_1^2|B|^2+P_2^2|B'|^2) \qquad (5.41)\end{aligned}$$

The third term in equation (5.41) is omitted hereafter, because this term is always a real number and does not influence the instability condition (5.36).

The amplitude ratios A/B and $\overline{A}'/\overline{B}'$ of equation (5.16) are obtained by substituting the cofactor A_{ij} of determinant (5.17) into equation (5.38). Hence,

$$\left.\begin{aligned}\frac{A}{B}&=\frac{A_{31}}{A_{33}}\\&=\frac{-\gamma[f(\hat{p})-\{\Delta_{12}H(\hat{p})-\Delta_{11}\}\{\delta\Delta_{22}+\Delta_0 p\hat{p}e^{2i\zeta}\}-\Delta_{12}\{\Delta_{11}G(\hat{p})-\gamma^2\Delta_{12}\}]}{H(p)f(\hat{p})+2\gamma^2\Delta_{11}\Delta_{12}-\gamma^2\Delta_{12}^2H(\hat{p})-\Delta_{11}^2G(\hat{p})}\\\frac{\overline{A}'}{\overline{B}'}&=\frac{A_{42}}{A_{44}}\\&=\frac{-\gamma[f(p)-\{\Delta_{12}H(p)-\Delta_{11}\}\{\delta\Delta_{22}+\Delta_0 p\hat{p}e^{-2i\zeta}\}-\Delta_{12}\{\Delta_{11}G(p)-\gamma^2\Delta_{12}\}]}{H(\hat{p})f(p)+2\gamma^2\Delta_{11}\Delta_{12}-\gamma^2\Delta_{12}^2H(p)-\Delta_{11}^2G(p)}\end{aligned}\right\}\tag{5.42}$$

When the terms higher than the 2nd order of small quantities Δ_0 and Δ_{ij} are neglected, equation (5.42) is represented as follows:

$$\frac{A}{B}=\frac{-\gamma}{H(p)},\quad \frac{\overline{A}'}{\overline{B}'}=\frac{-\gamma}{H(\hat{p})}=\frac{A'}{B'}\tag{5.43}$$

The substitution of equation (5.43) into the first and second terms in equation (5.41) yields the following relation:

$$H(p)H(\hat{p})J/2BB'=Qe^{-2i\zeta}+R\tag{5.44}$$

where

$$\left.\begin{aligned}Q&=\gamma^2\Delta_{11}-\gamma^2\Delta_{12}\{H(p)+H(\hat{p})\}+\delta\Delta_{22}H(p)H(\hat{p})\\R&=\Delta_0 p\hat{p}H(p)H(\hat{p})\end{aligned}\right\}\tag{5.45}$$

Let the absolute value of equation (5.44) be J',

$$J'=|H(p)H(\hat{p})J/2BB'|=|Qe^{-2i\zeta}+R|=\sqrt{Q^2+R^2+2QR\cos 2\zeta}\tag{5.46}$$

which is in proportion to $\mathrm{Im}[J]$ of equation (5.36), the width of dynamically unstable region, and the negative damping coefficient irrespective of the argument of B and B'. When the product QR is positive, the absolute value J' takes the maximum value $|Q|+|R|$ for $\zeta=0$ and the minimum one $|Q|\sim|R|$ for $\zeta=\pi/2$. When QR is negative, value J' has the minimum $|Q|\sim|R|$ for $\zeta=0$, and the maximum $|Q|+|R|$ for $\zeta=\pi/2$. In order to eliminate the dynamically unstable region, the parameters of shaft system must satisfy the relation $J'=0$, that is, $|Q|=|R|$ and $\cos 2\zeta=-QR/|QR|$. The above-mentioned analyses can be applied to the statically unstable vibration by putting $p=\omega$ in equations (5.43)$\sim$(5.46).

5. 3. 4. Effect of orientation angle ζ upon unstable regions

According to the experimental results[25, 26] reported by T. Yamamoto, H. Ōta and K. Kōno, and Figs. 5. 5, 5. 6, 5. 8 and 5. 9, the statically unstable region becomes narrower as the orientation angle ζ increases from zero to $\pi/2$, and on the other hand, the dynamically unstable one becomes wider as ζ increases. This tendency can be explained later.

5. 3. 4. 1. Statically unstable vibration

In statically unstable region, substitution of $m=0$ into equation (5. 23) yields the solutions for free vibration $z=Ae^{i\omega t}$ and $\theta_z=Be^{i\omega t}$. When the complex amplitude B exists in the second or fourth quadrant (hatched parts in Fig. 5. 2) of a complex plane with the real axis (x') and the imaginary one (y'), the unstable vibration occurs in an asymmetrical rotor (cf. Section *4. 4. 3. 1*). When the amplitudes A and B exist in the second or fourth quadrant of the coordinate O-$x_3'y_3'$ which is obtained by turning the coordinate O-$x'y'$ counterclockwise by an angle ζ in Fig. 5. 2, the unstable vibration occurs in an asymmetrical shaft. Therefore, the two unstable quadrants superimpose when $\zeta=0$, and so the statically unstable vibration occurs vigorously. On the other hand, when $\zeta=\pi/2$, these two quadrants do not superimpose, and the statically unstable vibration hardly occurs.

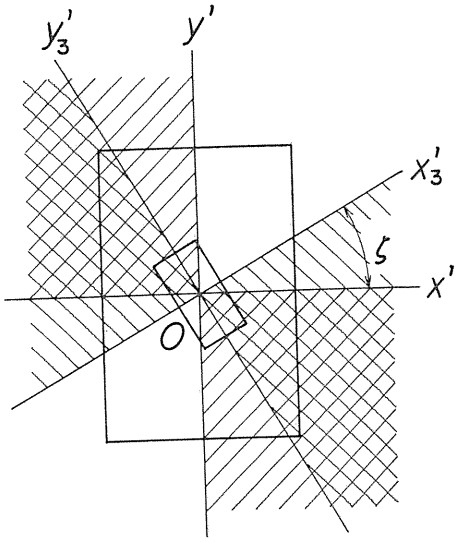

Fig. 5. 2 Superposition of two rotating coordinate systems $O-x'y'$ and $O-x_3'y_3'$.

The condition under which the time average of torque is positive are given from equation (5. 25) as follows:

$$\mathrm{Im}[J]=\mathrm{Im}[\Delta_0\omega^2B^2+(\Delta_{11}A^2+2\gamma\Delta_{12}AB+\delta\Delta_{22}B^2)e^{-2i\zeta}]<0 \qquad (5.47)$$

The vector J is composed of two vectors as shown in Fig. 5. 3 (a). Magnitude of the first term is $\Delta_0\omega^2|B|^2$, and that of the second term is $\Delta_{11}|A|^2\pm2\gamma\Delta_{12}|AB|+\delta\Delta_{22}|B|^2$. The magnitude of the vector J is given by sum of the two absolute

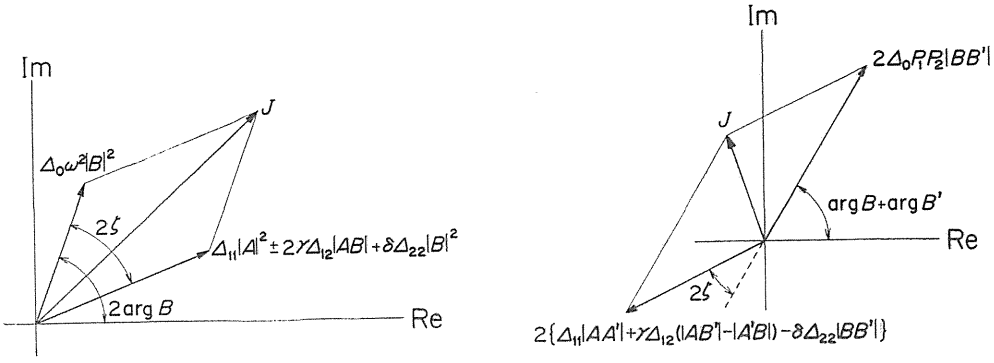

(a) Statically unstable vibration (b) Dynamically unstable vibration.

Fig. 5. 3

values when $\zeta=0$, and by difference when $\zeta=\pi/2$. From equation (5. 24), the shaft end torque has a maximum for $\zeta=0$, and so the unstable region becomes widest.

On the other hand, the shaft end torque has a minimum for $\zeta=\pi/2$, and the unstable region becomes narrowest.

5. 3. 4. 2. Dynamically unstable vibration

When solutions for free vibration $z=Ae^{iP_1t}+A'e^{iP_2t}$ and $\theta_z=Be^{iP_1t}+B'e^{iP_2t}$ are obtained by substituting $m=0$ into equation (5. 34), the condition under which the time average of the shaft end torque is positive is given by the following condition:

$$\mathrm{Im}[J]=\mathrm{Im}[2\Delta_0P_1P_2BB'+2\{\Delta_{11}AA'+\gamma\Delta_{12}(AB'+A'B)+\delta\Delta_{22}BB'\}e^{-2i\zeta}]<0 \tag{5. 48}$$

Because the relations $A/B<0$ for $p=P_1$ and $A'/B'>0$ for $p=P_2$ hold from equation (5. 43), the vector J is composed from two vectors. Magnitude of the first term is $2\Delta_0P_1P_2|BB'|$, and that of the second term is $2\{\Delta_{11}|AA'|+\gamma\Delta_{12}(|AB'|-|A'B|)-\delta\Delta_{22}|BB'|\}$. The magnitude of vector J is given by difference of absolute values of these two vectors when $\zeta=0$, and by sum of those when $\zeta=\pi/2$. The dependence ζ for the dynamically unstable vibration is completely contrary to that for the statically unstable one.

5. 4. Solutions for Free Vibration Obtained by Analog Computer

Substitution of equations (3. 1) and (3. 24) into equation (5. 15) yields the following equations of motion regarding z' and θ'_z:

$$\left.\begin{aligned}
\ddot{x}'=&-(1-\Delta_{11}\cos 2\zeta-\omega^2)x'+2\omega\dot{y}'+\Delta_{11}\sin 2\zeta\cdot y'\\
&-\gamma(1-\Delta_{12}\cos 2\zeta)\theta'_x+\gamma\Delta_{12}\sin 2\zeta\cdot\theta'_y\\
\ddot{y}'=&-(1+\Delta_{11}\cos 2\zeta-\omega^2)y'-2\omega\dot{x}'+\Delta_{11}\sin 2\zeta\cdot x'\\
&-\gamma(1+\Delta_{12}\cos 2\zeta)\theta'_y+\gamma\Delta_{12}\sin 2\zeta\cdot\theta'_x\\
\ddot{\theta}'_x=&[-\{\delta(1-\Delta_{22}\cos 2\zeta)+(i_p-1-\Delta_0)\omega^2\}\theta'_x+(2-i_p)\omega\dot{\theta}'_y\\
&+\delta\Delta_{22}\sin 2\zeta\cdot\theta'_y-\gamma(1-\Delta_{12}\cos 2\zeta)x'+\gamma\Delta_{12}\sin 2\zeta\cdot y']/(1-\Delta_0)\\
\ddot{\theta}'_y=&[-\{\delta(1+\Delta_{22}\cos 2\zeta)+(i_p-1+\Delta_0)\omega^2\}\theta'_y-(2-i_p)\omega\dot{\theta}'_x\\
&+\delta\Delta_{22}\sin 2\zeta\cdot\theta'_x-\gamma(1+\Delta_{12}\cos 2\zeta)y'+\gamma\Delta_{12}\sin 2\zeta\cdot x']/(1+\Delta_0)
\end{aligned}\right\} \tag{5. 49}$$

Torque T_r of equation (5. 21) is given by using equations (3. 1) and (3. 24) as follows:

$$\begin{aligned}
T_r=&\{\Delta_{11}(x'^2-y'^2)+2\gamma\Delta_{12}(x'\theta'_x-y'\theta'_y)+\delta\Delta_{22}(\theta'^2_x-\theta'^2_y)\}\sin 2\zeta\\
&-2\{\Delta_{11}x'y'+\gamma\Delta_{12}(x'\theta'_y+y'\theta'_x)+\delta\Delta_{22}\theta'_x\theta'_y\}\cos 2\zeta\\
&-2\Delta_0(\omega\theta'_x+\dot{\theta}'_y)(\omega\theta'_y-\dot{\theta}'_x)-(i_p/2)\{\theta'_x\ddot{\theta}'_y-\ddot{\theta}'_x\theta'_y+2\omega(\theta'_x\dot{\theta}'_x+\theta'_y\dot{\theta}'_y)\}
\end{aligned} \tag{5. 50}$$

Figures 5. 4 (a) and (b) show the simulation circuits which satisfy equations (5. 49) and (5. 50). A time average of the fourth term $-(i_p/2)\{\theta'_x\ddot{\theta}'_y-\ddot{\theta}'_x\theta'_y+2\omega(\theta'_x\dot{\theta}'_x+$

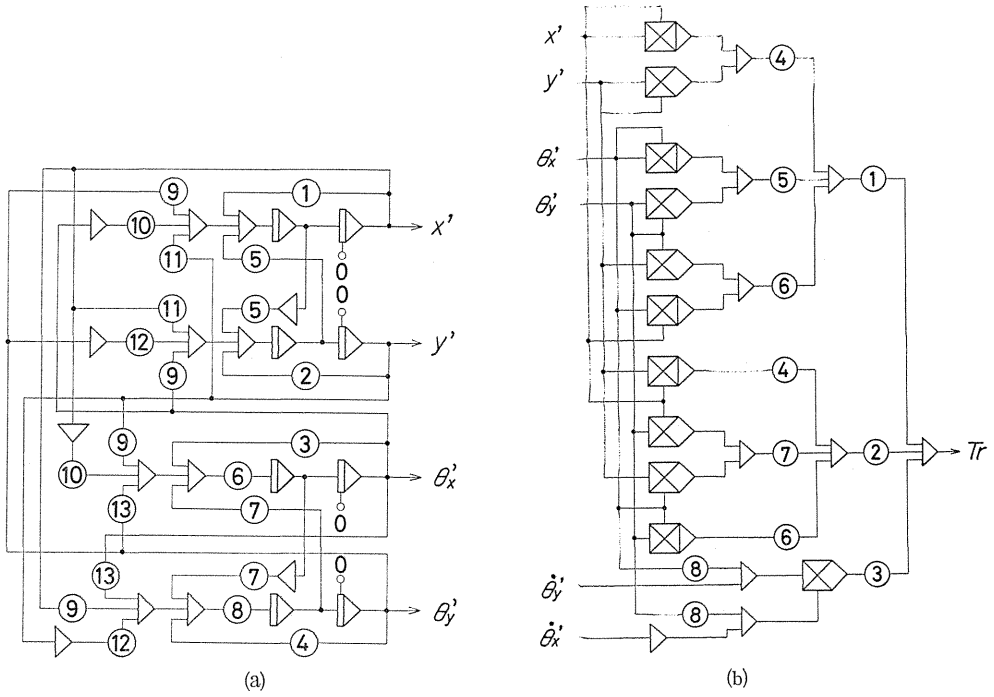

Fig. 5. 4 Simulation circuit for analog computer
(a) Potentiometers ①: $1-\Delta_{11}\cos 2\zeta-\omega^2$, ②: $1+\Delta_{11}\cos 2\zeta-\omega^2$, ③: $\delta(1-\Delta_{22}\cos 2\zeta)+(i_p-1-\Delta_0)\omega^2$, ④: $\delta(1+\Delta_{22}\cos 2\zeta)+(i_p-1+\Delta_0)\omega^2$, ⑤: 2ω, ⑥: $1/(1-\Delta_0)$, ⑦: $(2-i_p)\omega$, ⑧: $1/(1+\Delta_0)$, ⑨: $\gamma\Delta_{12}\sin 2\zeta$, ⑩: $\gamma(1-\Delta_{12}\cos 2\zeta)$, ⑪: $\Delta_{11}\sin 2\zeta$, ⑫: $\gamma(1+\Delta_{12}\cos 2\zeta)$, ⑬: $\delta\Delta_{22}\sin 2\zeta$
(b) Potentiometers ①: $\sin 2\zeta$, ②: $2\cos 2\zeta$, ③: $2\Delta_0$, ④: Δ_{11}, ⑤: $2\gamma\Delta_{12}$, ⑥: $\delta\Delta_{22}$, ⑦: $\gamma\Delta_{12}$, ⑧: ω.

$\theta_y'\dot{\theta}_y')\}$ in equation (5. 50) becomes zero[72] in a steady state vibration or as small as the negative damping coefficient m in a nonsteady state vibration [cf. equations (5. 27) and (5. 37)]. Thus, this term is omitted in Fig. 5. 4 (b).

5. 4. 1. *Solutions for statically unstable vibration*

The vibratory waves x', y', θ_x' and θ_y' obtained by an analog computer ALS-200X are shown in Fig. 5. 5 when the orientation angle ζ is changed to 0, $\pi/4$ and $\pi/2$ with other parameters[25, 26] fixed as $i_p=1.993$, $\delta=1.797$, $\gamma=-1.050$, $\Delta_0=0.304$, $\Delta_{11}=0.058$, $\Delta_{12}=0.051$, $\Delta_{22}=0.069$ and $\omega=0.725$. Because the number of poten-

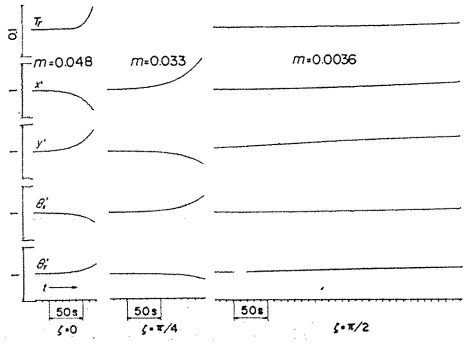

Fig. 5. 5 Vibratory waves of statically unstable vibration ($\omega=0.725$).

tiometers and multipliers of an analog computer is short for $\zeta=\pi/4$, torque T_r is not shown in Fig. 5. 5. A torque applied to the shaft end and the negative damping

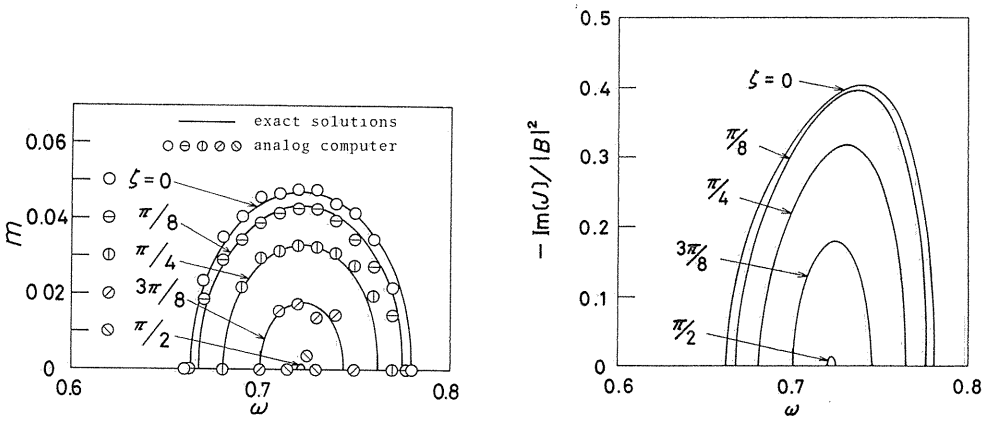

(a) $m-\omega$ diagram (b) Im$[J]-\omega$ diagram

Fig. 5. 6 Statically unstable vibration
$i_p=1.993$, $\delta=1.797$, $\gamma=-1.050$,
$\Delta_0=0.304$, $\Delta_{11}=0.058$, $\Delta_{12}=0.051$, $\Delta_{22}=0.069$.

coefficient decrease as the orientation angle ζ increases. The tendency of Fig. 5. 5 agrees with that of the experimental results[25] for the same parameters.

The negative damping coefficient m and Im$[J]/|B|^2$ calculated by using equations (5. 27)～(5. 30), are plotted against the shaft speed ω in Figs. 5. 6 (a) and (b) for the same parameters as Fig. 5. 5 but $\zeta=0$, $\pi/8$, $\pi/4$, $3\pi/8$ and $\pi/2$. The circles in Fig. 5. 6 (a) indicate the negative damping coefficient m measured from the vibratory solution of an analog computer, and the solid lines represent the imaginary part m of the exact complex root p calculated from equation (5. 19). When the angle ζ increases from 0 to $\pi/2$, the negative damping coefficient m decreases, and the width of the unstable region is also reduced. Because Im$[J]$ has a negative value in the statically unstable region, it satisfies the condition (5. 25) under which a statically unstable vibration occurs.

When inertia asymmetry Δ_0 is changed from 0 to 0. 5 and the orientation angle ζ is fixed as $\pi/2$ with the

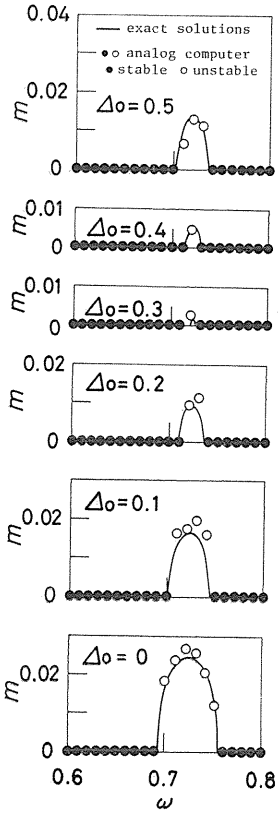

Fig. 5. 7 Effect of inertia asymmetry Δ_0 on negative damping coefficient m for statically unstable vibration
$\zeta=\pi/2$, $i_p=1.993$, $\delta=1.797$, $\gamma=-1.050$,
$\Delta_{11}=0.058$, $\Delta_{12}=0.051$, $\Delta_{22}=0.069$.

other parameters being same as Fig. 5. 5, the negative damping coefficient m is shown as in Fig. 5. 7. The circles and the solid lines in Fig. 5. 7 have the same meaning as those in Fig. 5. 6 (a). From Fig. 5. 7, it is clear that the unstable region is narrowest in the neighbourhood of $\Delta_0=0.34$.

5. 4. 2. *Solutions for dynamically unstable vibration*

The vibratory waves x', y' θ'_x and θ'_y for dynamically unstable vibration obtained with an analog computer are shown in Fig. 5. 8 when the orientation angle ζ is changed to 0, $\pi/4$ and $\pi/2$ with the other parameters[26] fixed as $i_p=0.7536$, $\delta=14.179$, $\gamma=-3.253$, $\Delta_0=0.0903$, $\Delta_{11}=0.1032$, $\Delta_{12}=0.0880$, $\Delta_{22}=0.0780$ and $\omega=2.760$. Torque T_r for $\zeta=\pi/4$ is not shown because the number of potentiometers and multipliers is short. A torque applied to the shaft end is equal to zero when $\zeta=0$, and the vibration is always stable. On the other hand, the torque T_r increases rapidly with time when $\zeta=\pi/2$, and an unstable vibration occurs. The tendency of Fig. 5. 8 agrees with that of the experimental results[26] for the same parameters.

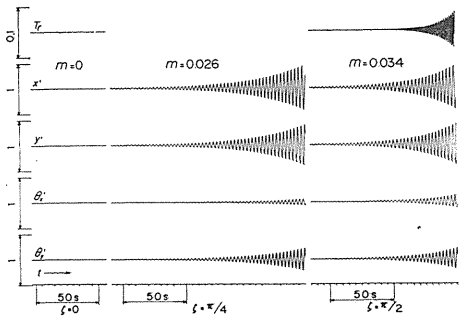

Fig. 5. 8 Vibratory waves of dynamical instability ($\omega=2.760$).

Figures 5. 9 (a) and (b) for the same parameters as Fig. 5. 8 except ζ show the measured results and exact solutions of the negative damping coefficient m,

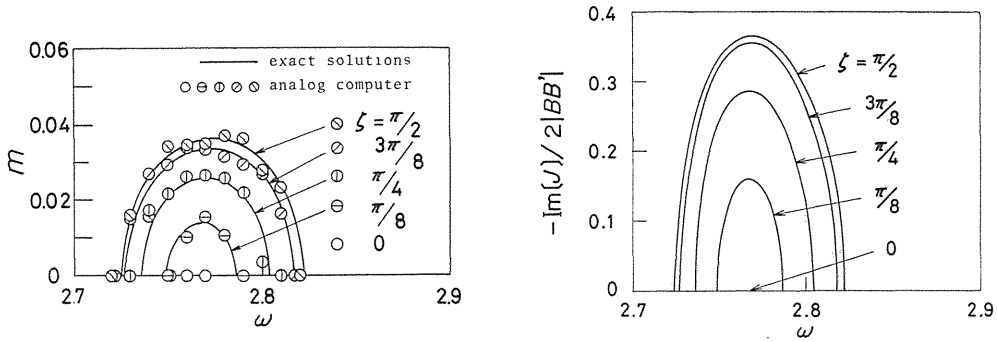

(a) m $-\omega$ diagram (b) Im[J]$-\omega$ diagram

Fig. 5. 9 Dynamically unstable vibration.
$i_p=0.7536$, $\delta=14.179$, $\gamma=-3.257$, $\Delta_0=0.0903$, $\Delta_{11}=0.1032$, $\Delta_{12}=0.088$, $\Delta_{22}=0.078$

and Im[J]/2$|BB'|$ calculated from equation (5. 37). The circles in Fig. 5. 9 (a) indicate the negative damping coefficient m measured from vibratory solutions of an analog computer, and the solid lines correspond to the imaginary part m of exact complex root p calculated from a frequency equation (5. 19). An unstable vibration does not occur when $\zeta=0$. As ζ increases till $\pi/2$, the negative damping

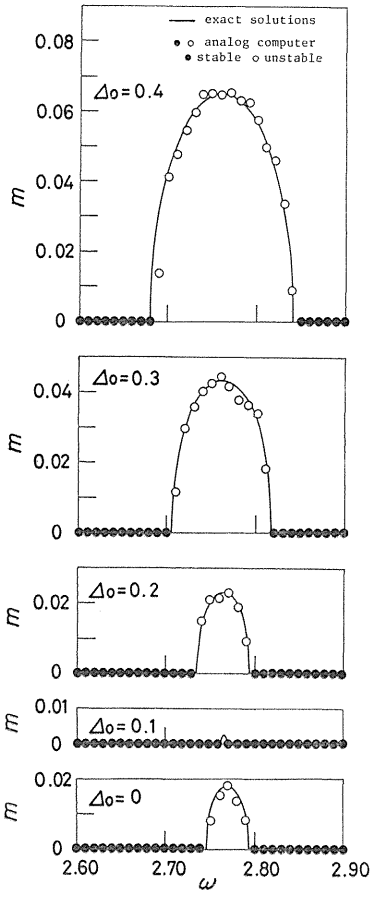

coefficient m increases, and also the width of the unstable region becomes greater. Because Im[J] has a negative value in the unstable region, it satisfies the condition under which a dynamically unstable vibration occurs.

Figure 5. 10 shows the negative damping coefficient m, which changes with the magnitude of Δ_0 for the same parameters as Fig. 5. 8 except $\zeta=0$. A dynamically unstable vibration does not occur in the neighbourhood of $\Delta_0=0.09$ as shown in Figs. 5. 8 and 5. 9.

Fig. 5. 10 Effect of inertia asymmetry Δ_0 on negative damping coefficient m for dynamically unstable vibration
$\zeta=0$, $i_p=0.7536$, $\gamma=-3.253$, $\delta=14.179$, $\Delta_{11}=0.1032$, $\Delta_{12}=0.088$, $\Delta_{22}=0.078$.

5. 5. *Conclusions*

Conclusions obtained in this chapter may be summarized as follows:

(1) In a rotating asymmetrical shaft carrying an asymmetrical rotor, the increase in rate of the total energy of the shaft system is identified with the time rate of work, and it is given by equation (5. 21).

(2) The condition under which a statically unstable vibration occurs means that Im[J] of equation (5. 27) is negative, and this condition depends on the orientation angle ζ between stiffness asymmetry and inertia asymmetry. As ζ increases from 0 to $\pi/2$, the statically unstable region becomes narrow in the present study, and the negative damping coefficient m decreases.

(3) The condition under which a dynamically unstable vibration occurs means that Im[J] of equation (5. 37) is negative, and this condition also depends on the orientation angle ζ. When $\zeta=0$, an unstable vibration does not occur in the present study. Width of the dynamically unstable region becomes greater and the negative damping coefficient m increases as ζ increases to $\pi/2$.

(4) Im[J] of equations (5. 27) and (5. 37) becomes negative in the region in which the vibratory solutions obtained with an analog computer are unstable. Thus, it is apparent that the necessary conditions for instability (5. 27) and (5. 37) are

correct.

(5) An appropriate combination of inertia asymmetry Δ_0 and stiffness asymmetry Δ_{ij} may give the condition under which an unstable vibration does not occur. This condition holds in each case of the statically unstable vibration and the dynamically unstable one, which is ascertained by the vibration solutions obtained with an analog computer.

6. On the Shaft End Torque and Forced Vibrations of an Asymmetrical Shaft Carrying an Asymmetrical Rotor[76]

6. 1. *Introduction*

It has been reported[24~28] that the response curve is considerably influenced by the angles between the principal axis of inertia of an asymmetrical shaft or an asymmetrical rotor, and the direction of rotor unbalances. T. Yamamoto and H. Ōta[24] report analytical results that the response curve for an asymmetrical rotor and an asymmetrical shaft changes with the angular position of static unbalance. T. Yamamoto, H. Ōta and K. Kōno[25, 26] obtained the relation between the angular position of rotor unbalances and the response curve of a rotating asymmetrical shaft with an asymmetrical rotor. K. Okijima and Y. Kondo[27] discuss the effect of the angular position of rotor unbalance on the response curve of a rotating asymmetrical shaft, both ends of which are supported by flexible pedestals with directional inequality in stiffness. T. A. Henry and B. E. Okah-Avae[28] indicate that the response curve depends on the angle between a crack and rotor unbalance when a crack takes place in a rotating shaft system.

This chapter clarifies the effect of two angular positions ξ, η of the static unbalance e_0 and the dynamic unbalance τ on the increase in rate of total energy and the torque[72~75] applied to the shaft end in an asymmetrical shaft carrying an asymmetrical rotor. When a rotor is mounted on the middle of an asymmetrical shaft, the parallel motion of a rotor is not connected with its conical motion, and so a torque applied to the shaft end is directly obtained from the equilibrium of forces and moments acting upon the rotor. Moreover, it is shown in an asymmetrical shaft and/or in an asymmetrical rotor that the shaft end torque changes with the orientation angles ξ, η of rotor unbalances in a manner similar to the response curve.

6. 2. *Equations of Motion*

A rotating shaft system as shown in Fig. 5. 1 is considered. Let c_1 and c_2 be viscous damping coefficients for rotor displacement and inclination, respectively. Dissipation function F is given as

$$2F = c_1(\dot{x}^2 + \dot{y}^2) + c_2(\dot{\theta}_x^2 + \dot{\theta}_y^2) \tag{6. 1}$$

Substituting the kinetic energy (5. 1), the potential energy (5. 4) and dissipation function (6. 1) into Lagrange's equation of motion (6. 2);

$$\frac{\mathrm{d}}{\mathrm{d}t}\left(\frac{\partial T}{\partial \dot{q}_s}\right) - \frac{\partial T}{\partial q_s} + \frac{\partial V}{\partial q_s} + \frac{\partial F}{\partial \dot{q}_s} = 0 \tag{6. 2}$$

taking generalized coordinate q_s as Θ, x, y, θ_x and θ_y, and using equations (1.7), (2.6) and (5.5), the equations of motion for z and θ_z are obtained as follows:

$$\left.\begin{aligned}&\underline{m_0\ddot{z}}+c_1\dot{z}+\alpha z+\gamma\theta_z-(\Delta\alpha\cdot\bar{z}+\Delta\gamma\cdot\bar{\theta}_z)e^{2i(\omega t+\zeta)}=0\\&\underline{I\ddot{\theta}_z}-\underline{iI_p\omega\dot{\theta}_z}+c_2\dot{\theta}_z+\gamma z+\delta\theta_z-\underline{\Delta I\frac{d}{dt}(\dot{\bar{\theta}}_z e^{2i\omega t})}\\&\qquad-(\Delta\gamma\cdot\bar{z}+\Delta\delta\cdot\bar{\theta}_z)e^{2i(\omega t+\zeta)}=0\end{aligned}\right\}\quad(6.3)$$

In general, there are both the static unbalance $e_0=\overline{SG}$ and the dynamic one $\tau=\angle Z_1SZ_0$ as shown in Fig. 6. 1. Displacements x_g and y_g of the gravity center G of a rotor are represented by complex variable $z_g=x_g+iy_g$, and the projected angles θ_{1x} and θ_{1y} of the principal axis SZ_1 by $\theta_{1z}=\theta_{1x}+i\theta_{1y}$. When the four terms underlined in equation (6.3), that is, $m_0\ddot{z}$, $I\ddot{\theta}_z$, $-iI_p\omega\dot{\theta}_z$ and $-\Delta I\frac{d}{dt}(\dot{\bar{\theta}}_z e^{2i\omega t})$, are replaced by $m_0\ddot{z}_g$, $I\ddot{\theta}_{1z}$, $-iI_p\omega\dot{\theta}_{1z}$ and $-\Delta I\frac{d}{dt}(\dot{\bar{\theta}}_{1z}e^{2i\omega t})$, respectively, the equations of motion with rotor unbalances are rewritten as follows:

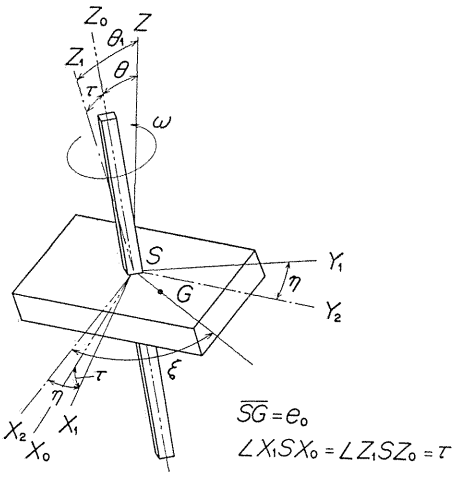

Fig. 6. 1 Angular positions ξ and η of static unbalance e_0 and dynamic unbalance τ.

$$\left.\begin{aligned}&m_0\ddot{z}_g+c_1\dot{z}+\alpha z+\gamma\theta_z-(\Delta\alpha\cdot\bar{z}+\Delta\gamma\cdot\bar{\theta}_z)e^{2i(\omega t+\zeta)}=0\\&\underline{I\ddot{\theta}_{1z}-iI_p\omega\dot{\theta}_{1z}}+c_2\dot{\theta}_z+\gamma z+\delta\theta_z-\Delta I\frac{d}{dt}(\dot{\bar{\theta}}_{1z}e^{2i\omega t})\\&\qquad-(\Delta\gamma\cdot\bar{z}+\Delta\delta\cdot\bar{\theta}_z)e^{2i(\omega t+\zeta)}=0\end{aligned}\right\}\quad(6.4)$$

As shown in Fig. 6. 1, the gravity center G exists in the SG-direction given by a rotation of the SX_2-axis about the SZ_1-axis by angle $\xi=\angle X_2SG$, and the dynamic unbalance τ exists in the $X_1Z_1(X_0Z_0)$ plane which is perpendicular to the SY_1-axis of the rotated SY_2-axis about the SZ_1-axis by angle $\eta=\angle Y_2SY_1=\angle X_2SX_1$. The following relations[69] are obtained by neglecting terms higher than the 3 rd order term of small quantities:

$$z_g = z + e_0 e^{i(\omega t+\xi)}, \quad \theta_{1z} = \theta_z + \tau e^{i(\omega t+\eta)} \tag{6.5}$$

Substituting equation (6.5) into equation (6.4), the equations of motion are rewritten as follows[25, 26, 69]:

$$\left.\begin{aligned} & m_0\ddot{z} + c_1\dot{z} + \alpha z + \gamma\theta_z - (\Delta\alpha\cdot\bar{z} + \Delta\gamma\cdot\bar{\theta}_z)e^{2i(\omega t+\zeta)} = m_0 e_0 \omega^2 e^{i(\omega t+\xi)} \\ & I\ddot{\theta}_z - iI_p\omega\dot{\theta}_z + c_2\dot{\theta}_z + \gamma z + \delta\theta_z - \Delta I\frac{d}{dt}(\dot{\bar{\theta}}_z e^{2i\omega t}) - (\Delta\gamma\cdot\bar{z} + \Delta\delta\cdot\bar{\theta}_z)e^{2i(\omega t+\zeta)} \\ & \qquad = -\tau\omega^2\{(I_p - I)e^{i(\omega t+\eta)} - \Delta I e^{i(\omega t-\eta)}\} \end{aligned}\right\} \tag{6.6}$$

6. 3. *Relation between Shaft End Torque and Increase in Rate of Total Energy*

In the case that rotor unbalances e_0 and τ both exist, the increase in rate of kinetic energy $\dot{T}$ is obtained by replacing $\ddot{z}$, $\dot{\bar{z}}$, θ_z, $\dot{\theta}_z$, $\ddot{\theta}_z$, $\dot{\bar{\theta}}_z$ and $\ddot{\bar{\theta}}_z$ in the first equation in equation (5.9) with $\ddot{z}_g$, $\dot{\bar{z}}_g$, θ_{1z}, $\dot{\theta}_{1z}$, $\ddot{\theta}_{1z}$, $\dot{\bar{\theta}}_{1z}$ and $\ddot{\bar{\theta}}_{1z}$, respectively. Thus,

$$\begin{aligned} \dot{T} = {} & m_0 \mathrm{Re}[\dot{\bar{z}}_g \ddot{z}_g] + (I_p/2)\omega \mathrm{Im}[\theta_{1z}\ddot{\bar{\theta}}_{1z}] + I\mathrm{Re}[\dot{\bar{\theta}}_{1z}\ddot{\theta}_{1z}] \\ & - (\Delta I/2)\frac{d}{dt}\mathrm{Re}[\dot{\theta}_{1z}^2 e^{-2i\omega t}] \end{aligned} \tag{6.7}$$

The increase in rate of potential energy $\dot{V}$ is the same as the second equation in equation (5.9). The first equation in equation (6.4) is multiplied by $\dot{\bar{z}}$, the second one by $\dot{\bar{\theta}}_z$, and these two equations are added together, the real part of which gives the following equation:

$$\begin{aligned} & m_0\mathrm{Re}[\dot{\bar{z}}\ddot{z}_g] + c_1|\dot{z}|^2 + \alpha\mathrm{Re}[z\dot{\bar{z}}] + \gamma\mathrm{Re}[\dot{\bar{z}}\theta_z + z\dot{\bar{\theta}}_z] + I\mathrm{Re}[\dot{\bar{\theta}}_z\ddot{\theta}_{1z}] + c_2|\dot{\theta}_z|^2 \\ & + \delta\mathrm{Re}[\theta_z\dot{\bar{\theta}}_z] - \mathrm{Re}[\Delta I\dot{\bar{\theta}}_z\frac{d}{dt}(\dot{\bar{\theta}}_{1z}e^{2i\omega t}) + \{\Delta\alpha\bar{z}\dot{\bar{z}} + \Delta\gamma(\dot{\bar{z}}\bar{\theta}_z + \bar{z}\dot{\bar{\theta}}_z) \\ & + \Delta\delta\bar{\theta}_z\dot{\bar{\theta}}_z\}e^{2i(\omega t+\zeta)}] = 0 \end{aligned} \tag{6.8}$$

Using equations (3.1), (3.24), (6.7), (6.8) and the second equation in equation (5.9), the increase in rate of total energy $\dot{T}+\dot{V}$ is given as:

$$\begin{aligned} \dot{T} + \dot{V} = {} & -\omega\mathrm{Im}[\Delta I(-\omega\theta_z' + i\dot{\theta}_z')^2 + (\Delta\alpha\cdot z'^2 + 2\Delta\gamma\cdot z'\theta_z' + \Delta\delta\cdot\theta_z'^2)e^{-2i\zeta} \\ & + (I_p/2)\bar{\theta}_z\ddot{\theta}_z - m_0 e_0\ddot{\bar{z}}e^{-i(\omega t+\xi)} + \tau\ddot{\bar{\theta}}_z\{(I_p - I)e^{-i(\omega t+\eta)} - \Delta I e^{-i(\omega t-\eta)}\}] \\ & - c_1|\dot{z}|^2 - c_2|\dot{\theta}_z|^2 \end{aligned} \tag{6.9}$$

Applied torque T_r to the shaft end should be a generalized force with respect to rotation of shaft end Θ, so the torque is obtained by putting $q_s = \Theta$ in Lagrange's equation of motion (6.2):

$$T_r = \frac{d}{dt}\left(\frac{\partial T}{\partial\dot{\Theta}}\right) - \frac{\partial T}{\partial\Theta} + \frac{\partial V}{\partial\Theta} + \frac{\partial F}{\partial\dot{\Theta}}$$

$$=-\mathrm{Im}[\Delta I(-\omega\theta_z'+i\dot{\theta}_z')^2+(\underline{\Delta\alpha\cdot z'^2}+2\Delta\gamma\cdot z'\theta_z'+\underline{\underline{\Delta\delta\cdot\theta_z'^2}})\mathrm{e}^{-2i\zeta}+(\underline{\underline{I_p/2)\bar{\theta}_z\ddot{\theta}_z}}$$
$$-\underline{m_0e_0\ddot{z}\mathrm{e}^{-i(\omega t+\xi)}}+\underline{\underline{\tau\ddot{\theta}_z\{(I_p-I)\mathrm{e}^{-i(\omega t+\eta)}}}-\Delta I\mathrm{e}^{-i(\omega t-\eta)}\}] \tag{6.10}$$

From equations (6.1), (6.9) and (6.10), the following relation holds:

$$\omega T_r=\dot{T}+\dot{V}+2F \tag{6.11}$$

Equation (6.11) means that the time rate of work applied to the shaft end ωT_r agrees with the sum of the increase in rate of total energy and the dissipated rate by damping forces. The amplitude of whirling motion changes with the orientation angle ζ between the inequality of shaft stiffness and that of rotor inertia, the angular position ξ of static unbalance e_0 and η of dynamic unbalance τ, because the right hand side of equation (6.10) contains the three angles ζ, ξ and η.

6. 4. *Effect of Angular Position of Rotor Unbalances on Shaft End Torque for Asymmetrical Shaft*

6. 4. 1. *Case of parallel motion of rotor*

Let us consider only a parallel motion of a rotor mounted on the middle of an asymmetrical shaft ($\theta_z=0$), and put $\zeta=0$. Three force vectors F, D and P in Fig. 6. 2 indicate restoring, damping and inertial forces, respectively; the restoring and damping forces act upon the rotor center S, and an inertial force acts upon the gravity center of the rotor G. A restoring force vector F does not point[72,73] to the direction of lateral displacement OS. Components of a restoring force F in x'- and y'-directions are expressed as follows:

$$F_x'=-(\alpha-\Delta\alpha)x',\quad F_y'=-(\alpha+\Delta\alpha)y' \tag{6.12}$$

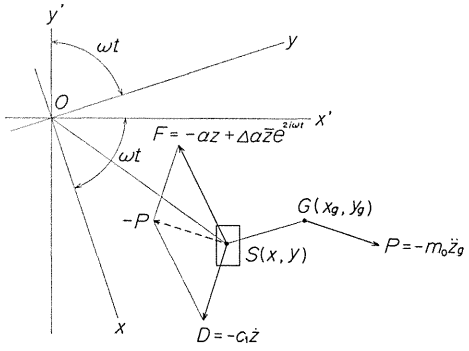

Fig. 6. 2 Three force vectors F, P and D acting upon rotor with parallel motion ($\theta_z=0$, $\zeta=0$).

Let F_2 be the perpendicular component of F to the OS-axis. In order to turn the shaft end at a constant velocity ω, a counter-torque T_{r1} must be applied to the shaft end against a moment produced by a reaction force $-F_2$ about the bearing center line Oz:

$$T_{r1}=F_2|z'|=-F_x'y'+F_y'x'=-2\Delta\alpha\cdot x'y'=-\Delta\alpha\mathrm{Im}[z'^2] \tag{6.13}$$

As shown in Fig. 6. 2, an inertial force $P=-m_0\ddot{z}_g$ acting upon G is in balance to a vector sum $-P$ shown by a dotted line consisting of two vectors F and $D=-c_1\dot{z}$. By using equation (6.15), an inertial force P is expressed as

$$P=P_x+iP_y=-m_0\{\ddot{z}-e_0\omega^2\mathrm{e}^{i(\omega t+\xi)}\} \tag{6.14}$$

An inertial force P makes a moment about S, because vector P does not point to

the direction SG. The following counter-torque T_{r2} against a moment produced by P

$$T_{r2}=P_x(y_g-y)-P_y(x_g-x)=m_0e_0\mathrm{Im}[\ddot{z}e^{-i(\omega t+\xi)}] \tag{6.15}$$

must be applied to the shaft end in order to turn a shaft at a constant velocity ω.

Therefore, the applied torque T_r is obtained from equations (6.13) and (6.15) as follows:

$$T_r=T_{r1}+T_{r2}=-\mathrm{Im}[\Delta\alpha\cdot z'^2-m_0e_0\ddot{z}e^{-i(\omega t+\xi)}] \tag{6.16}$$

Equation (6.16) agrees precisely with the underlined terms obtained by setting $\zeta=0$ in equation (6.10) excepting θ_z terms.

Next, let us investigate how the shaft end torque and the amplitude change with the angular position ξ of the static unbalance e_0.

The solutions for forced vibration of equation (6.6) are represented by

$$z=Ae^{i\omega t},\quad z'=ze^{-i\omega t}=A \tag{6.17}$$

where A is a complex constant. Substituting the solution (6.17) into equation (6.16), the torque is given as follows:

$$T_r=-\mathrm{Im}[\Delta\alpha A^2+m_0e_0\omega^2Ae^{-i\xi}] \tag{6.18}$$

Using the argument of complex number, equation (6.18) is rewritten in the following form:

$$T_r=-\Delta\alpha|A|^2\sin 2\arg A-m_0e_0\omega^2|A|\sin(\arg A-\xi) \tag{6.19}$$

When the solutions of forced vibration (6.17) are substituted into the first equation of equation (6.6), the real and imaginary parts of this derived equation are as follows:

$$\begin{aligned}(\alpha-\Delta\alpha-m_0\omega^2)|A|\cos\arg A-c_1\omega|A|\sin\arg A&=m_0e_0\omega^2\cos\xi\\ c_1\omega|A|\cos\arg A+(\alpha+\Delta\alpha-m_0\omega^2)|A|\sin\arg A&=m_0e_0\omega^2\sin\xi\end{aligned} \tag{6.20}$$

$|A|\cos\arg A$ and $|A|\sin\arg A$ in equation (6.20) can be solved as follows[24]:

$$\left.\begin{aligned}|A|\cos\arg A&=\frac{m_0e_0\omega^2\{(\alpha+\Delta\alpha-m_0\omega^2)\cos\xi+c_1\omega\sin\xi\}}{(\alpha-m_0\omega^2)^2-\Delta\alpha^2+c_1^2\omega^2}\\ |A|\sin\arg A&=\frac{m_0e_0\omega^2\{-c_1\omega\cos\xi+(\alpha-\Delta\alpha-m_0\omega^2)\sin\xi\}}{(\alpha-m_0\omega^2)^2-\Delta\alpha^2+c_1^2\omega^2}\end{aligned}\right\} \tag{6.21}$$

Substitution of equation (6.21) into equation (6.19) gives a driving torque T_r. Thus,

$$T_r=\frac{m_0^2e_0^2c_1\omega^5\{2c_1\omega\Delta\alpha\sin 2\xi+2\Delta\alpha(\alpha-m_0\omega^2)\cos 2\xi+(\alpha-m_0\omega^2)+\Delta\alpha^2+c_1^2\omega^2\}}{\{(\alpha-m_0\omega^2)^2-\Delta\alpha^2+c_1^2\omega^2\}^2} \tag{6.22}$$

The dimensionless torque $T_r/(\alpha e_0^2)$ and amplitude $|A|/e_0$ derived from equations (6. 21) and (6. 22) are indicated by solid lines in Figs. 6. 3(a) and (b) where ξ is $-\pi/4$, 0, $\pi/4$ and $\pi/2$ for $\Delta\alpha/\alpha=0.322$ and $c_1/\sqrt{m_0\alpha}=0.5$. For the sake of comparison, the calculated values for a symmetrical shaft are also indicated by dotted lines in Fie. 6. 3. The shaft end torque shows a qualitative tendency similar to the response curve. The shaft end torque and response curve have the maxima for the angular position $\xi=\pi/4$, and have the minima for $\xi=-\pi/4$.

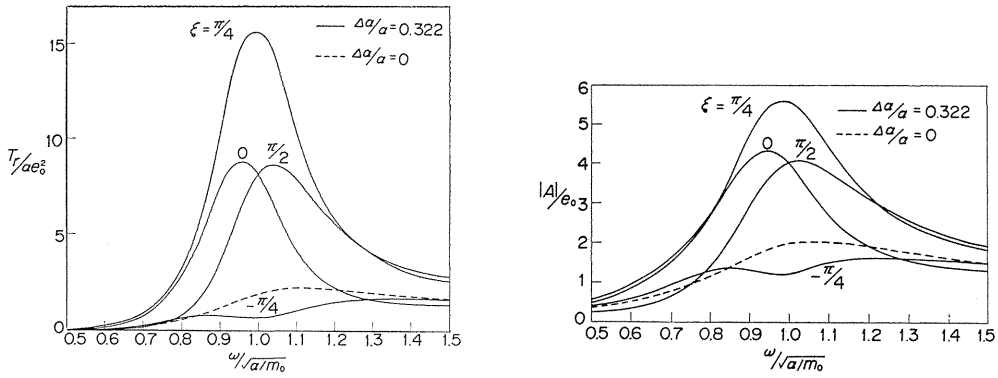

(a) Shaft end torque (b) Response curve

Fig. 6. 3 Shaft end torque and response curve for parallel motion of a rotor mounted on an asymmetrical shaft.

6. 4. 2. *Case of conical motion of rotor*

Let us consider only a conical motion of a rotor mounted on the middle of an asymmetrical shaft ($z=0$) putting $\zeta=0$, and derive applied torque T_r by using the equilibrium of moments shown in Figs. 6. 4(a) and (b). Take two parallel planes to the xy-plane having a short distance h as shown in Fig. 6. 4 (a). The tangent TT' at the origin O intersects those two planes at T and T', and the principal axis of rotor inertia UU' intersects those at U and U'. Restoring moment M_t, the damping moment M_d and the moment by inertia M_p are indicated by three vectors in Fig. 6. 4 (a). Two vectors M_t and M_d drawn from O exist on the plane perpendicular to the tangent OT, and the vector M_p drawn from O exist on the plane perpendicular to the principal axis of inertia OU. When the 2nd order terms of small quantities in θ and θ_1 are neglected, three vectors projected on the xy-plane [Fig. 6. 4 (b)] can be represented by the same symbols M_t, M_d and M_p as those in Fig. 6. 4 (a). Components of restoring moment M_t in x'- and y'-directions are expressed as

$$M'_{tx}=(\delta+\Delta\delta)\theta'_y, \quad M'_{ty}=-(\delta-\Delta\delta)\theta'_x \tag{6. 23}$$

The component M_{t2} of M_t on TOz plane encourages a conical motion of the rotor. The restoring moment M_t can be equivalently replaced by two forces F and $-F$ which act on two points T and T'. In order to maintain the shaft end revolution at a constant velocity ω against the reaction of M_{t2}, the following torque T_{r1} must be applied[72]:

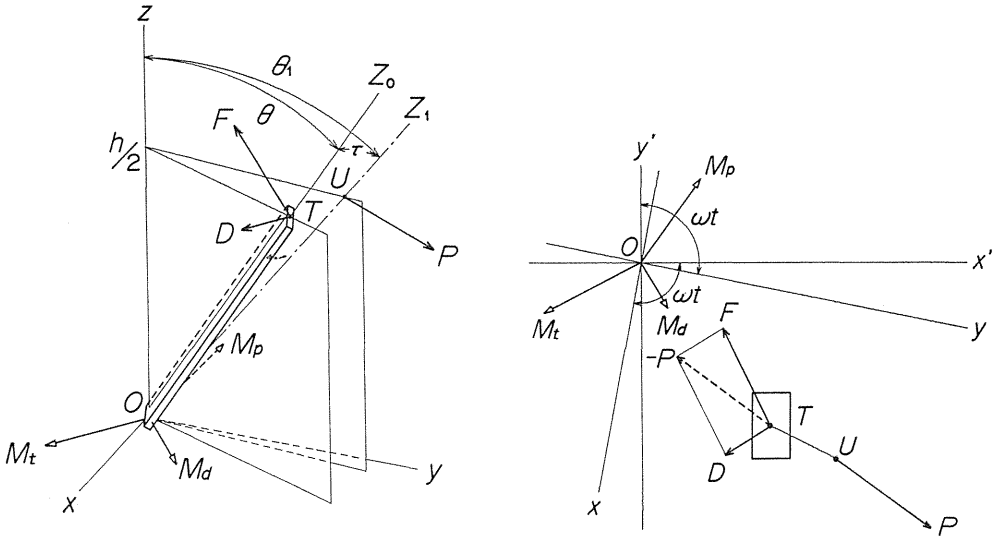

(a) (b)

Fig. 6. 4 Three moment vectors M_t, M_p and M_d acting upon rotor with conical motion ($z=0$, $\zeta=0$).

$$T_{r1}=M_{t2}=-M'_{tx}\theta'_x-M'_{ty}\theta'_y=-2\Delta\delta\theta'_x\theta'_y=-\Delta\delta\mathrm{Im}[\theta'^2_z] \tag{6.24}$$

Components of moment by inertia M_p in x- and y-directions are obtained from the underlined terms in equation (6. 4) as follows:

$$\left.\begin{aligned} M_{px}&=I\ddot{\theta}_{1y}-I_p\omega\dot{\theta}_{1x}=I\ddot{\theta}_y-I_p\omega\dot{\theta}_x+(I_p-I)\tau\omega^2\sin(\omega t+\eta)\\ M_{py}&=-(I\ddot{\theta}_{1x}+I_p\omega\dot{\theta}_{1y})=-I\ddot{\theta}_x-I_p\omega\dot{\theta}_y-(I_p-I)\tau\omega^2\cos(\omega t+\eta)\end{aligned}\right\} \tag{6.25}$$

The moment by inertia M_p can be equivalently replaced by the couple of inertia forces P and $-P$ which act on the two points U and U'. Equivalent inertia forces P and $-P$ produce a moment about TOT' axis. The counter-torque T_{r2} to this moment is obtained as follows:

$$\begin{aligned} T_{r2}&=M_{px}(\theta_{1x}-\theta_x)+M_{py}(\theta_{1y}-\theta_y)\\ &=I\tau\mathrm{Im}[\ddot{\theta}_z e^{-i(\omega t+\eta)}]-I_p\tau\omega\mathrm{Re}[\dot{\theta}_z e^{-i(\omega t+\eta)}]\end{aligned} \tag{6.26}$$

Thus, equations (6. 24) and (6. 26) give the torque T_r required to turn an asymmetrical shaft at a constant velocity ω:

$$T_r=T_{r1}+T_{r2}=-\mathrm{Im}[\Delta\delta\cdot\theta'^2_z-I\tau\ddot{\theta}_z e^{-i(\omega t+\eta)}]-I_p\tau\omega\mathrm{Re}[\dot{\theta}_z e^{-(\omega t+\eta)}] \tag{6.27}$$

When a rotor behaves with a conical motion, the solutions of forced vibration of equation (6. 6) are expressed by

$$\theta_z=Be^{i\omega t},\quad \theta'_z=\theta_z e^{-i\omega t}=B \tag{6.28}$$

The shaft end torque T_r is obtained by substituting $\zeta=0$ and the solution (6. 28)

into the double-underlined terms in equation (6.10);

$$T_r = -\mathrm{Im}[\Delta\delta B^2 - \tau\omega^2 B(I_p - I)e^{-i\eta}] \tag{6.29}$$

When the solution (6.28) is substituted into equation (6.27) which is derived directly from balance of moments, equation (6.27) agrees with equation (6.29). Using an argument of a complex number, equation (6.29) is rewritten as

$$T_r = -\Delta\delta|B|^2 \sin 2\arg B + \tau\omega^2(I_p - I)|B| \sin(\arg B - \eta) \tag{6.30}$$

When the solution (6.28) is applied to a conical motion in which zero is put for z, $\bar{z}$, ΔI and ζ in the second equation in equation (6.6), the real and imaginary parts are

$$\left.\begin{aligned} &\{\delta - \Delta\delta + (I_p - I)\omega^2\}|B|\cos\arg B - c_2\omega|B|\sin\arg B = -\tau\omega^2(I_p - I)\cos\eta \\ &c_2\omega|B|\cos\arg B + \{\delta + \Delta\delta + (I_p - I)\omega^2\}|B|\sin\arg B = -\tau\omega^2(I_p - I)\sin\eta \end{aligned}\right\} \tag{6.31}$$

Equation (6.31) is solved for $|B|\cos\arg B$ and $|B|\sin\arg B$. Thus:

$$\left.\begin{aligned} |B|\cos\arg B &= \frac{-\tau\omega^2(I_p - I)[\{\delta + \Delta\delta + (I_p - I)\omega^2\}\cos\eta + c_2\omega\sin\eta]}{\{\delta + (I_p - I)\omega^2\}^2 - \Delta\delta^2 + c_2^2\omega^2} \\ |B|\sin\arg B &= \frac{-\tau\omega^2(I_p - I)[-c_2\omega\cos\eta + \{\delta - \Delta\delta + (I_p - I)\omega^2\}\sin\eta]}{\{\delta + (I_p - I)\omega^2\}^2 - \Delta\delta^2 + c_2^2\omega^2} \end{aligned}\right\} \tag{6.32}$$

Substituting equation (6.32) into equation (6.30), the shaft end torque T_r is given as

$$\begin{aligned} T_r = {} & (I_p - I)^2\tau^2 c_2\omega^5[2\Delta\delta\{\delta + (I_p - I)\omega^2\}\cos 2\eta + 2c_2\omega\Delta\delta\sin 2\eta \\ & + \{\delta + (I_p - I)\omega^2\}^2 + \Delta\delta^2 + c_2^2\omega^2]/[\{\delta + (I_p - I)\omega^2\}^2 - \Delta\delta^2 + c_2^2\omega^2]^2 \end{aligned} \tag{6.33}$$

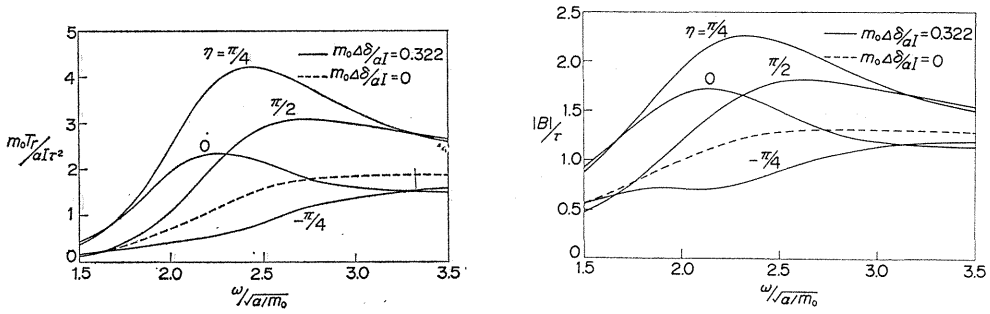

(a) Shaft end torque (b) Response curve

Fig. 6.5 Shaft end torque and response curve for conical motion of a rotor mounted on an asymmetrical shaft.

the value of which changes with the angle η.

On the conical motion of a rotor mounted on an asymmetrical shaft, dimensionless torque $m_0T_r/(\alpha I\tau^2)$ and amplitude $|B|/\tau$ are indicated by solid lines in Figs 6. 5 (a) and (b) where $\eta=-\pi/4$, 0, $\pi/4$ and $\pi/2$ for $i_p=0.8$, $m_0\delta/(\alpha I)=1.060$, $m_0\Delta\delta/(\alpha I)=0.322$ and $c_2\sqrt{m_0/\alpha}/I=0.3$. For the sake of comparison, the calculated values for a symmetrical shaft ($\Delta\delta=0$) are indicated by dotted lines in Fig. 6. 5. The shaft end torque and the response curve in Fig. 6. 5 show a similar tendency to Fig. 6. 3 for the parallel motion.

6. 5. *Effect of Angular Position of Rotor Unbalances on Shaft End Torque for an Asymmetrical Rotor*

Let us consider a coupled motion of an asymmetrical rotor mounted on a symmetrical shaft. When the solutions of forced vibration (6. 17) and (6. 28) are substituted into the equations of motion (6. 6) and shaft asymmetries $\Delta\alpha$, $\Delta\gamma$ and $\Delta\delta$ are considered to be zero, the real and imaginary parts are represented as follows:

$$\left.\begin{aligned}
&(\alpha-m_0\omega^2)|A|\cos\arg A-c_1\omega|A|\sin\arg A+\gamma|B|\cos\arg B=m_0e_0\omega^2\cos\xi\\
&c_1\omega|A|\cos\arg A+(\alpha-m_0\omega^2)|A|\sin\arg A+\gamma|B|\sin\arg B=m_0e_0\omega^2\sin\xi\\
&\gamma|A|\cos\arg A+\{\delta+(I_p-I-\Delta I)\omega^2\}|B|\cos\arg B-c_2\omega|B|\sin\arg B\\
&\qquad\qquad=-(I_p-I-\Delta I)\tau\omega^2\cos\eta\\
&\gamma|A|\sin\arg A+c_2\omega|B|\cos\arg B+\{\delta+(I_p-I+\Delta I)\omega^2\}|B|\sin\arg B\\
&\qquad\qquad=-(I_p-I+\Delta I)\tau\omega^2\sin\eta
\end{aligned}\right\}\tag{6. 34}$$

Substituting solutions of forced vibration (6. 17) and (6. 28) into equation (6. 10) and putting zero for $\Delta\alpha$, $\Delta\gamma$ and $\Delta\delta$, a torque T_r applied to the shaft end is derived as

$$\begin{aligned}
T_r=&-\mathrm{Im}[\Delta I(-\omega B)^2+(I_p/2)(-\omega^2B\overline{B})+m_0e_0\omega^2A\mathrm{e}^{-i\xi}\\
&-\tau\omega^2B\{(I_p-I)\mathrm{e}^{-i\eta}-\Delta I\mathrm{e}^{i\eta}\}]\\
=&-\Delta I\omega^2|B|^2\sin 2\arg B-m_0e_0\omega^2|A|\sin(\arg A-\xi)\\
&+\tau\omega^2|B|\{(I_p-I)\sin(\arg B-\eta)-\Delta I\sin(\arg B+\eta)\}
\end{aligned}\tag{6. 35}$$

When $|A|\cos\arg A$, $|A|\sin\arg A$, $|B|\cos\arg B$ and $|B|\sin\arg B$ obtained by solving equation (6. 34) are substituted into equation (6. 35), the shaft end torque can be calculated. Only amplitude A regarding the parallel motion of the rotor is shown hereafter, because the rotor's parallel motion is larger than the conical one at the first major critical speed.

6. 5. 1. *Influence of angular position ξ upon torque*

Let us examine the influence of the angular position ξ where e_0 exists in case only the static unbalance e_0 exists and no dynamic one. Putting zero for τ in

equation (6.34), the real and imaginary parts of amplitudes A and B are expressed as follows[24]:

$$\left.\begin{aligned}
|A|\cos\arg A &= (m_0e_0\omega^2/K_0)[\{(\alpha-m_0\omega^2)(X_1X_2+c_2^2\omega^2)-\gamma^2X_1\}\cos\xi \\
&\quad +\{c_1(X_1X_2+c_2^2\omega^2)+\gamma^2c_2\}\omega\sin\xi] \\
|A|\sin\arg A &= (m_0e_0\omega^2/K_0)[-\{c_1(X_1X_2+c_2^2\omega^2)+\gamma^2c_2\}\omega\cos\xi \\
&\quad +\{(\alpha-m_0\omega^2)(X_1X_2+c_2^2\omega^2)-\gamma^2X_2\}\sin\xi] \\
|B|\cos\arg B &= (m_0e_0\gamma\omega^2/K_0)[-\{(\alpha-m_0\omega^2)X_2-c_1c_2\omega^2-\gamma^2\}\cos\xi \\
&\quad -\{c_2(\alpha-m_0\omega^2)+c_1X_2\}\omega\sin\xi] \\
|B|\sin\arg B &= (m_0e_0\gamma\omega^2/K_0)[\{c_2(\alpha-m_0\omega^2)-c_1X_1\}\omega\cos\xi \\
&\quad -\{(\alpha-m_0\omega^2)X_1-c_1c_2\omega^2-\gamma^2\}\sin\xi]
\end{aligned}\right\} \quad (6.36)$$

where

$$\left.\begin{aligned}
K_0 &= \{(\alpha-m_0\omega^2)X_1-\gamma^2\}\{(\alpha-m_0\omega^2)X_2-\gamma^2\}+c_1^2\omega^2X_1X_2 \\
&\quad +c_2^2\omega^2(\alpha-m_0\omega^2)^2+2c_1c_2\gamma^2\omega^2+c_1^2c_2^2\omega^4 \\
X_1 &= \delta+(I_p-I-\Delta I)\omega^2, \quad X_2=\delta+(I_p-I+\Delta I)\omega^2
\end{aligned}\right\} \quad (6.37)$$

The shaft end torque can be calculated numerically by substituting equation (6.36) into equation (6.35) and putting zero for τ.

For $i_p=1.987$, $\Delta_0=0.322$, $\gamma\sqrt{m_0/I}/\alpha=-0.855$, $m_0\delta/(\alpha I)=1.060$, $c_1/\sqrt{m_0\alpha}=0.1$ and $c_2\sqrt{m_0/\alpha}/I=0.1$, dimensionless torque $T_r/(\alpha e_0^2)$ and amplitude $|A|/e_0$ are

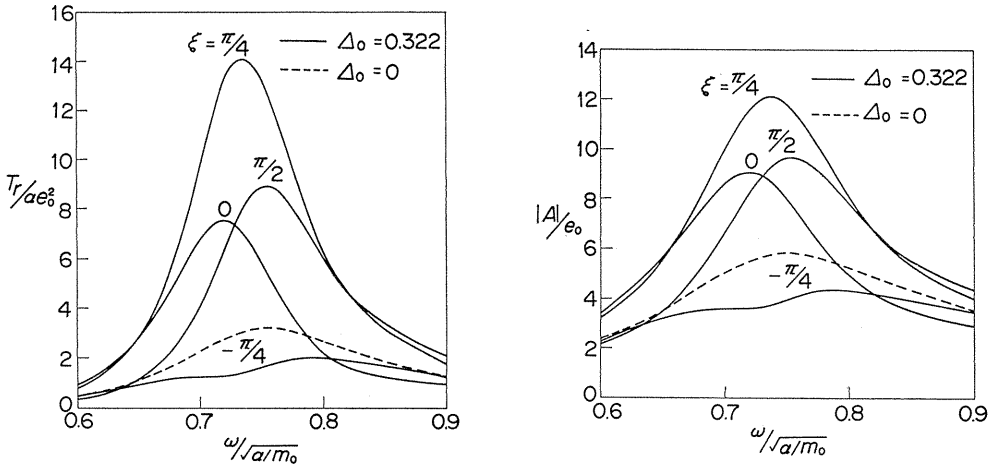

(a) Shaft end torque (b) Response curve

Fig. 6. 6 Shaft end torque and response curve for an asymmetrical rotor ($\tau=0$).

indicated by solid lines with the parameter ξ in Figs. 6. 6 (a) and (b). The calculated results for a symmetrical rotor ($\Delta_0=0$) are indicated by dotted lines. The shaft end torque and the amplitude with respect to an asymmetrical rotor show a tendency similar to that of an asymmetrical shaft. When $\xi=\pi/4$, the torque and the amplitude have maxima. When $\xi=-\pi/4$, on the other hand, the torque and the amplitude have minima, and they are smaller than those of the dotted lines.

6. 5. 2. Influence of angular position η upon torpue

The real and imaginary parts of amplitudes A and B are obtained[24] from equation (6. 34) by putting $e_0=0$ when there is no static unbalance but only the dynamic unbalance τ :

$$\left.\begin{aligned}
|A|\cos\arg A&=(\gamma\tau\omega^2/K_0)[(I_p-I-\Delta I)\{(\alpha-m_0\omega^2)X_2-c_1c_2\omega^2-\gamma^2\}\cos\eta\\
&\quad+(I_p-I+\Delta I)\{c_1X_1+c_2(\alpha-m_0\omega^2)\}\omega\sin\eta]\\
|A|\sin\arg A&=(\gamma\tau\omega^2/K_0)[-(I_p-I-\Delta I)c_1X_2+c_2(\alpha-m_0\omega^2)\}\omega\cos\eta\\
&\quad+(I_p-I+\Delta I)\{(\alpha-m_0\omega^2)X_1-c_1c_2\omega^2-\gamma^2\}\sin\eta]\\
|B|\cos\arg B&=(\tau\omega^2/K_0)[-(I_p-I-\Delta I)\{(\alpha-m_0\omega^2)^2X_2\\
&\quad-\gamma^2(\alpha-m_0\omega^2)+c_1^2\omega^2X_2\}\cos\eta\\
&\quad-(I_p-I+\Delta I)\{c_2(\alpha-m_0\omega^2)^2+c_1^2c_2\omega^2+c_1\gamma^2\}\omega\sin\eta]\\
|B|\sin\arg B&=(\tau\omega^2/K_0)[(I_p-I-\Delta I)\{c_1(\alpha-m_0\omega^2)^2+c_1^2c_2\omega^2+c_1\gamma^2\}\omega\cos\eta\\
&\quad-(I_p-I+\Delta I)\{(\alpha-m_0\omega^2)^2X_1-\gamma^2(\alpha-m_0\omega^2)+c_1^2\omega^2X_1\}\sin\eta]
\end{aligned}\right\}\tag{6. 38}$$

Torque applied to the shaft end is calculated numerically by substituting equation (6. 38) into equation (6. 35) and putting $e_0=0$.

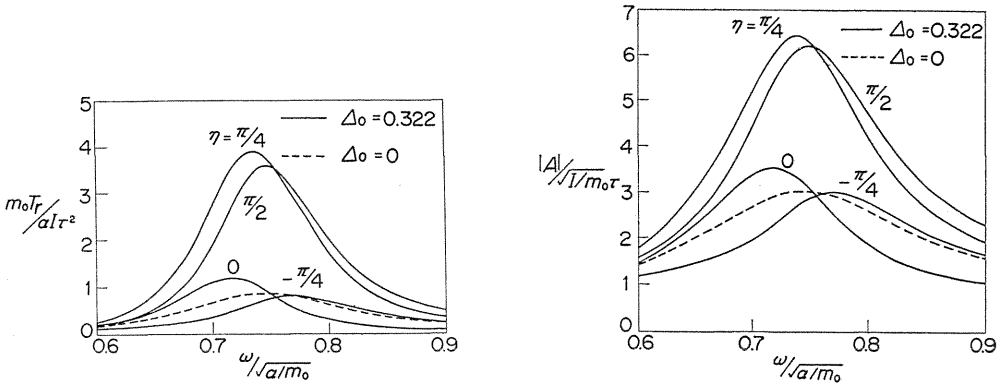

(a) Shaft end torque (b) Response curve

Fig. 6. 7 Shaft end torque and response curve for an asymmetrical rotor ($e_0=0$).

Figures 6. 7 (a) and (b) show the shaft end torque and the response curve which are derived by numerical calculation for the same parameter as for Fig. 6. 6 except $e_0=0$ and $\tau\neq 0$. Figures 6. 7 (a) and (b) show a tendency similar to those of Figs. 6. 6 (a) and (b).

6. 6. Conclusions

Conclusions obtained in this chapter may be summarized as follows:

(1) In an asymmetrical shaft carrying an asymmetrical rotor, the increase in rate of total energy of the shaft system and torque applied to the shaft end are given by equations (6. 9) and (6. 10). These analytical results vary with the angular positions ξ and η in which static unbalance e_0 and dynamic one τ exist.

(2) In the case of parallel motion of a rotor mounted on the middle of an asymmetrical shaft, the shaft end torque can be obtained from the equilibrium of forces. Near the major critical speed, the shaft end torque and the response curve have maxima when $\xi=\pi/4$, and minima when $\xi=-\pi/4$.

(3) In the case of conical motion of a rotor mounted on the middle of an asymmetrical shaft, the shaft end torque can be obtained from the equilibrium of moments. The same as with parallel motion, the shaft end torque shows a tendency similar to the response curves near the major critical speed. The shaft end torque and the response curve have maxima when $\eta=\pi/4$, and minima when $\eta=-\pi/4$.

(4) When parallel motion of an asymmetrical rotor is accompanied by conical motion, the shaft end torque and the response curve are obtained. In the case $\tau=0$, the shaft end torque and the response curve with respect to the parallel motion have maxima near the major critical speed when $\xi=-\pi/4$, and minima when $\xi=\pi/4$.

In the case $e_0=0$, the shaft end torque and the response curve with respect to the parallel motion show a tendency similar to that for the angular position η.

Acknowledgement

The authors are grateful to Mr. N. Yamaguchi for his assistance in preparation of the figures in this article. Analog computation was carried out at Control Mechanics and Components Laboratory in Department of Mechanical Engineering.

References

1) A Stodola, *Dampf- und Gasturbinen*, Springer, (1924).
2) S. Timoshenko, *Vibration Problems in Engineering*, Wiley, (1937).
3) J. P. Den Hartog, *Mechanical Vibration*, McGraw-Hill, (1934).
4) Th. Pöschl, " *Das Anlaufen eines einfachen Schwingers*", Ingenieur-Archiv, Bd. 4, Nr. 1 (1933), S. 98-102.
5) Y. Shimoyama and T. Yamamoto, "*Vibrations Generated on a Rotating Shaft by Passing through its Critical Speed with Some Angular Acceleration*", Trans. of Japan Soc. of Mech. Engrs., Vol. 15, No. 50 (1949), pp. I-113-I-121.
6) F. M. Dimentberg, *Flexural Vibrations of Rotating Shafts*, Butterworths, (1961).
7) S. Yanabe and A. Tamura, "*Vibration on a Shaft Passing through a Critical Speed* (1st Report, *Experiments and Numerical Solutions*)", Bulletin of JSME, Vol. 14, No. 76 (1971

-10), pp. 1050-1058.

8) K. Matsuura, *"A Consideration for Vibration and Velocity Characteristics of an Accelated Unbalanced Rotor"*, Trans. of Japan Soc. of Mech. Engrs., Vol. **37**, No. 302 (1971-10), pp. 1854-1861.

9) S. Aiba, *"On the Vibration of a Rotating Shaft Passing through the Critical Speed"*, Bulletin of JSME, Vol. **19**, No. 128 (1976-2), pp. 95-102.

10) R. Gasch and H. Pfützner, *Rotordynamik*, Springer, (1975).

11) S. Miwa and G. Shimomura, *Kaitenkikai no Tsuriawase*, Corona-sha, (1976).

12) T. Yamamoto, *"On the Critical Speeds of a Shaft"*, Memoirs of the Faculty of Engineering, Nagoya University, Vol. **6**, No. 2 (1954-11), pp. 106-174.

13) A. G. Parkinson, *"The Vibration and Balancing of Shafts Rotating in Asymmetric Bearings"*, J. Sound Vib., Vol. **2**, No. 4 (1965), pp. 477-501.

14) S. Saito and T. Someya, *"Theoretical Investigation into the Vibration of a Rotating Shaft Supported by Anisotropic Springs"*, Trans. of Japan Soc. of Mech. Engrs., Vol. **43**, No. 369 (1977-5), pp. 1687-1693.

15) D. M. Smith, *"The Motion of a Rotor Carried by a Flexible Shaft in Flexible Bearings"*, Proc. Roy. Soc. London, Ser. A, Vol. **142**, No. A846 (1933-10), pp. 92-118.

16) H. D. Taylor, *"Critical-Speed Behavior of Unsymmetrical Shafts"*, J. Appl. Mech., Trans. ASME, Vol. **62**, No. 2 (1940-6), pp. A-71-A-79.

17) W. Kellenberger, *"Forced, Double-Frequency, Flexural Vibrations in a Rotating, Horizontal, Cylindrical Shaft"*, The Brown Boveri Review, Vol. **42**, No. 3 (1955-3), pp. 79-85.

18) R. E. D. Bishop, and A. G. Parkinson, *"Second Order Vibration of Flexible Shafts"*, Phil. Trans. Roy. Soc. London, Ser. A, Vol. **259**, No. A1095(1965-12), pp. 1-31.

19) A. Tondl, *Some Problems of Rotor Dynamics*, Publishing House of the Czechoslovak Academy of Scinces, (1965).

20) A. Föppl, *"Kritische Drehzahlen rasch umlaufender Wellen"*, VDI-Z, Bd. **63**, (1919), S. 866-867.

21) S. Fujii, *"Whirling of an Automotive Propeller Shaft at Lower Speeds* (1st Report)", Trans. of Japan Soc. of Mech. Engrs., Vol. **22**, No. 115 (1956-3), pp. 178-181.

22) S. Fujii, H. Shibata and T. Shigeta, *"Whirling of an Automobile Propeller Shaft at Lower Speeds* (2nd Report)", Trans. of Japan Soc. of Mech. Engrs., Vol. **22**, No. 119 (1956-7), pp. 489-491.

23) T. Yamamoto and K. Kōno, *"On Vibrations of a Rotor with Variable Rotating Speed"*, Bulletin of JSME, Vol. **13**, No. 60 (1970-6) pp. 757-765.

24) T. Yamamoto and H. Ōta, *"On the Forced Vibrations* of the *Shaft Carrying an Unsymmetrical Rotating Body"*, Bulletin of JSME, Vol. **6**, No. 23 (1963-8), pp. 412-420.

25) T. Yamamoto, H. Ōta and K. Kōno, *"The Effect of Flat Shaft on the Unstable Vibrations of a Shaft Carrying an Unsymmetrical Rotor"*, Memoirs of the Faculty of Engineering, Nagoya University, Vol. **21**, No. 1 (1969-5) pp. 122-134, Vol. **21**, No. 2 (1969-11) pp. 287-293.

26) T. Yamamoto, H. Ōta and K. Kōno, *"On the Unstable Vibrations of a Shaft With Unsymmetrical Stiffness Carrying an Unsymmetrical Rotor"*, J. Appl. Mech., Trans. ASME, Vol. **35**, No. 2(1968-6), pp. 313-321.

27) Y. Kondo and K. Okijima, *"On the Critical Speed Regions of an Asymmetric Rotating Shaft Supported by Asymmetrically Elastic Pedestals* (2nd Report, *On the Forced Vibrations)"*, Bulletin of JSME, Vol. **18**, No. 120(1975-6), pp. 597-604.

28) T. A. Henry and B. E. Okah-Avae, *"Vibrations in Cracked Shafts"*, 1st. Int. Conf. on Vibrations in Rotating Machinery (Cambridge), (1976-9), pp. 15-19.

29) R. Kawai, T. Iwatsubo and H. Kanki, *"Transient Vibrations of Asymmetric Rotor at Critical Speeds with Limited Power"*, Trans. of Japan Soc. of Mech. Engrs., Vol. **35**, No. 280 (1969-12), pp. 2325-2333.

30) D. W. Childs, *"A Modal Transient Simulation Model for Flexible Asymmetric Rotors"*, J. Eng. Ind., Trans. ASME, Vol. **98**, No. 1(1976-2), pp. 312-319.

31) A. G. Parkinson, *"On the Balancing of Shafts With Axial Asymmetry"*, Proc. Roy.

Soc. London, Ser. A, Vol. **294**, (1966-9), pp. 66-79.

32) Y. Matsukura, M. Kiso and T. Inoue, *"Convergence of Residual Unbalance of a Rotor with Asymmetrical Cross Section"*, Trans. of Japan Soc. of Mech. Engrs., Vol. **44**, No. 388 (1978-12), pp. 4096-4104.

33) C. S. Hsu, *"On the Parametric Excitation of a Dynamic System Having Multiple Degrees of Freedom"*, J. Appl. Mech., Trans. ASME, Vol. **30**, No. 3 (1963-9), pp. 367-372.

34) T. Yamamoto and A. Saito, *"On the Oscillations of "Summed and Differential Types" under Parametric Excitation"*, Trans. of Japan Soc. of Mech. Engrs., Vol. **33**, No. 246 (1967-2), pp. 215-223.

35) J. Dick, *"The Whirling of Shafts having Sections with Unequal Principal Bending Moduli"* Phil. Mag., Ser. 7, Vol. **39**, (1948), pp. 946-955.

36) W. Kellenberger, *"Biegeschwingungen einer unrunden, rotierenden Welle in Horizontaler Lage"*, Ingenieur-Archiv, Bd. **26**, (1958), S. 302-318.

37) S. T. Ariaratnam, *"The Vibration of Unsymmetrical Rotating Shafts"*, J. Appl. Mech., Trans. ASME, Vol. **32**, No. 1(1965-3), pp. 157-162.

38) R. E. D. Bishop and S. Mahalingam, *"Some Experiments in the Vibration of a Rotating Shaft"*, Proc. Roy. Soc. London, Ser. A, Vol. **292**, No. 1431 (1966-6), pp. 537-561.

39) H. Mitfeld, *"Über ein Paradoxon bei Berechung biegekrischer Drehzahlen: Parametererregung einer anisotropen Lavalwelle"*, ZAMM, Bd. **55**, (1975), S. T70-T72.

40) W. R. Foote, H. Poritsky and J. J. Slade, Jr., *"Critical Speeds of a Rotor With Unequal Shaft Flexibilities, Mounted in Bearings of Unequal Flexibility-I"*, J. Appl. Mech., Trans. ASME, Vol. **10**, No. 2 (1943-6), pp. A-77-A-84.

41) A. Tondl, *"The Stability of Motion of a Rotor with Unsymmetrical Shaft on an Elastically Supported Mass Foundation"*, Ingenieur-Archiv, Bd. **29**, (1960), S. 410-418.

42) G. M. L. Gladwell and C. W. Stammers, *"On the Stability of an Unsymmetrical Rigid Rotor Supported in Unsymmetrical Bearings"*, J. Sound Vib., Vol. **3**, No. 3 (1966), pp. 221-232.

43) H. F. Black and A. J. McTernan, *"Vibration of a Rotating Asymmetric Shaft Supported in Asymmetric Bearings"*, J. Mech. Eng. Sci., Vol. **10**, No. 3 (1968), pp. 252-261.

44) H. F. Black, *"Parametrically Excited Lateral Vibrations of an Asymmetric Slender Shaft in Asymmetrically Flexible Bearings"*, J. Mech. Eng. Sci., Vol. **11**, No. 1 (1969), pp. 57-67.

45) K. Okijima and Y. Kondo, *"On the Critical Speed Regions of an Asymmetric Rotating Shaft Supported by Asymmetrically Elastic Pedestals* (1st Report, *On the Unstable Regions)"*, Bulletin of JSME, Vol. **18**, No. 120 (1975-6), pp. 587-596.

46) D. Ardayfio and D. A. Frohrib, *"Vibration of an Asymmetrically Mounted Rotor With Gyroscopic Effects"*, J. Eng. Ind., Trans. ASME, Vol. **98**, No. 1 (1976-2), pp. 372-331.

47) L. Forrai, *"Vibrations of a Rotating Asymmetric Shaft Carrying Two Disks, Supported in Asymmetric Bearings"*, 1st Int. Conf. on Vibrations in Rotating Machinery (Cambridge), (1976-9), pp. 43-48.

48) D. Ardayfio and D. A. Frohrib, *"Instabilities of an Asymmetric Rotor With Asymmetric Shaft Mounted on Symmetric Elastic Supports"*, J. Eng. Ind., Trans. ASME, Vol. **98**, No. 4 (1976-11), pp. 1161-1165.

49) T. Iwatsubo, *"Stability of Rotor Systems Having Asymmetric Elements"*, Ingenieur-Archiv, Bd. **47**, Nr. 5 (1978), S. 293-302.

50) A. A. Müller and P. C. Müller, *"Parameter- und Kombinationsresonanzen bei Rotorsystemen mit Unsymmetrien"*, Ingenieur-Archiv, Bd. **48**, Nr. 1 (1978), S. 65-72.

51) K. Kelkel, *"Parametererregte Schwingungen elastischer Rotoren"* ZAMM, Bd. **59**, Nr. 5 (1979), S. T129-T132.

52) T. Iwatsubo, R. Kawai and T. Miyaji, *"On the Stability of a Rotating Asymmetric Shaft Supported by Asymmetric Bearings"*, Bulletin of JSME, Vol. **23**, No. 180 (1980-6) pp. 934-937.

53) T. Kotera, *"A New Method of Determining Regions of Instability of Parametric Excitation System, (A Disc Supported by an Asymmetric Flexible Shaft in Asymmetric*

Bearings)", Memoirs of the Faculty of Engineering, Kobe University, No. 24 (1978-3), pp. 31-43.

54) A. A. Müller, "*Einflüsse von Unsymmetrien auf das Bewegungsverhalten von Rotoren*", VDI-Z, Bd. **123**, Nr. 1/2 (1981-1), S. 22-30

55) L. Y. Banaf and F. M. Dimentberg, "*Flexural Vibrations of a Rotating Shaft Carrying a Component in Which the Values of the Principal Central Mass Moment of Inertia Are Unequal*", Izvest. A. N. SSSR, Otd. Tekh. Nauk, Vol. **6** (1960), pp. 91-97.

56) P. J. Brosens and S. H. Crandall, "*Whirling of Unsymmetrical Rotors*", J. Appl. Mech., Trans. ASME, Vol. **28**, No. 3 (1961-9), pp. 355-362.

57) T. Yamamoto and H. Ōta, "*On the Vibrations of the Shaft Carrying an Unsymmetrical Rotating Body*", Bulletin of JSME, Vol. **6**, No. 21 (1963-2), pp. 29-36.

58) S. Aiba, "*On the Vibration and Critical Speeds of an Asymmetrical Rotating Shaft*", Reports of the Faculty of Engineering, Yamanashi University, No. 13 (1962-12), pp. 30-43.

59) T. Yamamoto and H. Ōta, "*On the Unstable Vibrations of a Shaft Carrying an Unsymmetrical Rotor*", J. Appl. Mech., Trans. ASME, Vol. **31**, No. 3 (1964-9), pp. 515-522.

60) S. Aiba, "*The Effect of Gyroscopic Moment and Distributed Mass on the Vibration of a Rotating Shaft with a Rotor*", Bulletin of JSME, Vol. **16**, No. 100 (1973-10), pp. 1550-1561.

61) T. Yamamoto and H. Ōta, "*Unstable Vibrations of the Shaft Carrying an Unsymmetrical Rotating Body*" Bulletin of JSME, Vol. **6**, No. 23 (1963-8), pp. 404-411.

62) G. M. L. Gladwell and C. W. Stammers, "*Prediction of the Unstable Regions of a Reciprocal System Governed by a Set of Linear Equations With Periodic Coefficients*", J. Sound Vib., Vol. **8**, No. 3 (1968), pp. 457-468.

63) T. Yamamoto and K. Yasuda, "*Unstable Vibrations of an Unsymmetrical Rotor Supported by Flexible Bearing Pedestals*", Bulletin of JSME, Vol. **15**, No. 87 (1972-9), pp. 1063-1073.

64) O. N. Romaniv, "*Flexural Vibration of a Shaft With a Disc Having Unequal Equational Moments of Inertia*", Izvest. A. N. SSSR, Otd. Tekh. Nauk, Vol. **6** (1960), pp. 98-104.

65) S. H. Crandall and P. J. Brosens, "*On the Stability of Rotation of a Rotor With Rotationally Unsymmetric Inertia and Stiffness Properties*", J. Appl. Mech., Trans ASME, Vol. **28**, No. 4 (1961-12), pp. 567-570.

66) R. C. Arnold and E. E. Haft, "*Stability of an Unsymmetrical Rotating Cantilever Shaft Carrying an Unsymmetrical Rotor*", J. Eng. Ind., Trans. ASME, Vol. **94**, No. 1 (1972-2), pp. 243-249.

67) K. Okugawa, *Daisugaku*, Kyoritsu Shuppan, (1956).

68) T. Yamamoto and H. Ōta, "*The Damping Effect on Unstable Whirlings of a Shaft Carrying an Unsymmetrical Rotor*", Memoirs of the Faculty of Engineering, Nagoya University, Vol. **19**, No. 2 (1967-11), pp. 197-217.

69) H. Ōta and K. Kōno, "*On Various Vibrations of a Shaft Carrying an Unsymmetrical Rotor*", Jour. of Japan Soc. of Mech. Engrs., Vol. **72**, No. 610 (1969-11), pp. 1537-1546.

70) H. Ōta and K. Mizutani, "*Influence of Unequal Pedestal Stiffness on the Instability Regions of a Rotating Asymmetric Shaft*", J. Appl. Mech., Trans. ASME, Vol. **45**, No. 2 (1978-6), pp. 400-408.

71) H. Ōta, K. Mizutani and M. Miwa, "*Influence of Unequal Pedestal Stiffness on the Instability Regions of a Rotating Asymmetric Shaft,* (2nd Report, *Inclinational Vibrations with Effects of Gyroscopic Action*)", Bulletin of JSME, Vol. **23**, No. 183 (1980-9), pp. 1514-1521.

72) H. Ōta and K. Mizutani, "*Influence of Unequal Pedestal Stiffness on the Instability Regions of a Rotating Asymmetric Shaft,* (3rd Report, *Mechanism for Occurrence of Two Types of Unstable Vibrations*)", Bulletin of JSME, Vol. **24** No. 190 (1981-4), pp. 700-707.

73) H. Ōta and K. Mizutani, "*On the Occurrence of Unstable Vibrations of a Shaft Having Either Asymmetrical Stiffness or Asymmetrical Rotor, Supported by Asymmetrically Flexible Pedestals*", 2nd Int. Conf. on Vibrations in Rotating Machinery (Cambridge),

(1980-9), pp. 181–186.

74) H. Ōta and K. Mizutani, *"Influence of Unequal Pedestal Stiffness on the Instability Regions of an Asymmetrical Rotor"*, Bulletin of JSME, Vol. **24**, No. 198 (1981–12), pp. 2133–2140.

75) H. Ōta and K. Mizutani, *"On the Shaft End Torque and the Unstable Vibrations of an Asymmetrical Shaft Carrying an Asymmetrical Rotor"*, Bulletin of JSME, Vol. **25**, No. 208 (1982–10), pp. 1574–1581.

76) H. Ōta, K. Mizutani and Y. Nakatsugawa, *"On the Shaft End Torque and the Forced Vibrations of an Asymmetrical Shaft Carrying an Asymmetrical Rotor"*, Trans. of Japan Soc. of Mech. Engrs., Vol. **49**, No. 440, C (1983–4).